




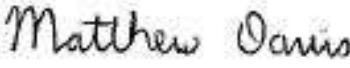
Central Waitemata Harbour Contaminant Study

Harbour Sediments

December

TR 2008/034

Technical Report, first edition.

Reviewed by:	Approved for ARC publication by:
	
Name: Hayden Easton	Name: Matthew Davis
Position: Team Leader Stormwater Action Team	Position: Group Manager Partnerships & Community Programmes
Organisation: Auckland Regional Council	Organisation: Auckland Regional Council
Date: 12 December 2009	Date: 18 December 2009

Recommended Citation:

SWALES, A.; STEPHENS, S.; HEWITT, J.; OVENDEN, R.; HAILES, S.; LOHRER, D.; HERMANSPHAN, N.; HART, C.; BUDD, R.; WADHWA, S. AND OKEY, M.J., 2008. Central Waitemata Harbour Contaminant Study. Harbour Sediments. Prepared by NIWA Ltd for Auckland Regional Council. Auckland Regional Council Technical Report 2008/034.

© 2008 Auckland Regional Council

This publication is provided strictly subject to Auckland Regional Council's (ARC) copyright and other intellectual property rights (if any) in the publication. Users of the publication may only access, reproduce and use the publication, in a secure digital medium or hard copy, for responsible genuine non-commercial purposes relating to personal, public service or educational purposes, provided that the publication is only ever accurately reproduced and proper attribution of its source, publication date and authorship is attached to any use or reproduction. This publication must not be used in any way for any commercial purpose without the prior written consent of ARC. ARC does not give any warranty whatsoever, including without limitation, as to the availability, accuracy, completeness, currency or reliability of the information or data (including third party data) made available via the publication and expressly disclaim (to the maximum extent permitted in law) all liability for any damage or loss resulting from your use of, or reliance on the publication or the information and data provided via the publication. The publication and information and data contained within it are provided on an "as is" basis.

Central Waitemata Harbour Contaminant Study. Harbour Sediments

A. Swales
S. Stephens
J. Hewitt
R. Ovenden
S. Hailes
D. Lohrer
N. Hermansphan¹
C. Hart
R. Budd
S. Wadhwa
M.J. Okey¹

(1) National Radiation Laboratory

Prepared for
Auckland Regional Council

NIWA Client Report: HAM2007-001
June 2007

NIWA Project: ARC07239 and ARC07243

National Institute of Water & Atmospheric Research Ltd
Gate 10, Silverdale Road, Hamilton
P O Box 11115, Hamilton, New Zealand
Phone: 07 856 7026 Fax: 07 856 0151
www.niwa.co.nz

Preface

The Waitemata Harbour is comprised of tidal creeks, embayments and the central basin. The harbour receives sediment and stormwater chemical contaminant run-off from urban and rural land from a number of subcatchments, which can adversely affect the ecology. An earlier study examined long-term accumulation of sediment and stormwater chemical contaminants in the Upper Waitemata Harbour. However, previously little was known about the existing and long-term accumulation of sediment and stormwater chemical contaminants in the central harbour. The Central Waitemata Harbour Contaminant Study was commissioned to improve understanding of these issues. This study is part of the 10-year Stormwater Action Plan to increase knowledge and improve stormwater management outcomes in the region. The work was undertaken by the National Institute of Water and Atmospheric Research (NIWA).

The scope of the study entailed:

- 1) field investigation,
- 2) development of a suite of computer models for
 - a. urban and rural catchment sediment and chemical contaminant loads,
 - b. harbour hydrodynamics and
 - c. harbour sediment and contaminant dispersion and accumulation,
- 3) application of the suite of computer models to project the likely fate of sediment, copper and zinc discharged into the central harbour over the 100-year period 2001 to 2100, and
- 4) conversion of the suite of computer models into a desktop tool that can be readily used to further assess the effects of different stormwater management interventions on sediment and stormwater chemical contaminant accumulation in the central harbour over the 100-year period.

The study is limited to assessment of long-term accumulation of sediment, copper and zinc in large-scale harbour depositional zones. The potential for adverse ecological effects from copper and zinc in the harbour sediments was assessed against sediment quality guidelines for chemical contaminants.

The study and tools developed address large-scale and long timeframes and consequently cannot be used to assess changes and impacts from small subcatchments or landuse developments, for example. Furthermore, the study does not assess ecological effects of discrete storm events or long-term chronic or sub-lethal ecological effects arising from the cocktail of urban contaminants and sediment.

The range of factors and contaminants influencing the ecology means that adverse ecological effects may occur at levels below contaminant guideline values for individual chemical contaminants (i.e., additive effects due to exposure to multiple contaminants may be occurring).

Existing data and data collected for the study were used to calibrate the individual computer models. The combined suite of models was calibrated against historic sedimentation and copper and zinc accumulation rates, derived from sediment cores collected from the harbour.

Four scenarios were modelled: a baseline scenario and three general stormwater management intervention scenarios.

The baseline scenario assumed current projections (at the time of the study) of

- future population growth,
- future landuse changes,
- expected changes in building roof materials,
- projected vehicle use, and
- existing stormwater treatment.

The three general stormwater management intervention scenarios evaluated were:

- 1) source control of zinc by painting existing unpainted and poorly painted galvanised steel industrial building roofs;
- 2) additional stormwater treatment, including:
 - raingardens on roads carrying more than 20,000 vehicles per day and on paved industrial sites,
 - silt fences and hay bales for residential infill building sites and
 - pond / wetland trains treating twenty per cent of catchment area; and
- 3) combinations of the two previous scenarios.

International Peer Review Panel

The study was subject to internal officer and international peer review. The review was undertaken in stages during the study, which allowed incorporation of feedback and completion of a robust study. The review found:

- a state-of-the-art study on par with similar international studies,
- uncertainties that remain about the sediment and contaminant dynamics within tidal creeks / estuaries, and
- inherent uncertainties when projecting out 100 years.

Key Findings of the Study

Several key findings can be ascertained from the results and consideration of the study within the context of the wider Stormwater Action Plan aim to improve stormwater outcomes:

- Henderson Creek (which drains the largest subcatchment and with the largest urban area, as well as substantial areas of rural land) contributes the largest loads of sediment, copper and zinc to the Central Waitemata Harbour. The second largest loads come from the Upper Waitemata Harbour.
- Substantial proportions of the subcatchment sediment, copper and zinc loads are accumulating in the Henderson, Whau, Meola and Motions tidal creeks and in the Shoal Bay, Hobson Bay and Waterview embayments.
- Central Waitemata Harbour bed sediment concentrations of copper and zinc are not expected to reach toxic levels based on current assumptions of future trends in urban landuse and activities.
- Zinc source control targeting industrial building roofs produced limited reduction of zinc accumulation rates in the harbour because industrial areas cover only a small proportion of the catchment area and most unpainted galvanised steel roofs are expected to be replaced with other materials within the next 25 to 50 years.
- Given that the modelling approach used large-scale depositional zones and long timeframes, differences can be expected from the modelling projections and stormwater management interventions contained within these reports versus consideration of smaller depositional areas and local interventions. (For example, whereas the study addresses the Whau River as a whole, differences exist within parts of the Whau River that may merit a different magnitude or type of intervention than may be inferred from considering the Whau River and its long-term contaminant trends as a whole.) As a consequence, these local situations may merit further investigation and assessment to determine the best manner in which to intervene and make improvements in the short and long terms.

Research and Investigation Questions

From consideration of the study and results, the following issues have been identified that require further research and investigation:

- Sediment and chemical contaminant dynamics within tidal creeks.
- The magnitude and particular locations of stormwater management interventions required to arrest sediment, copper and zinc accumulation in tidal creeks and embayments, including possible remediation / restoration opportunities.
- The fate of other contaminants derived from urban sources.
- The chronic / sub-lethal effects of marine animal exposure to the cocktail of urban contaminants and other stressors such sediment deposition, changing sediment particle size distribution and elevated suspended sediment loads.
- Ecosystem health and connectivity issues between tidal creeks and the central basin of the harbour, and the wider Hauraki Gulf.

Technical reports

The study has produced a series of technical reports:

Technical Report TR2008/032
Central Waitemata Harbour Contaminant Study. Landuse Scenarios.

Technical Report TR2008/033
Central Waitemata Harbour Contaminant Study. Background Metal Concentrations in Soils: Methods and Results.

Technical Report TR2008/034
Central Waitemata Harbour Contaminant Study. Harbour Sediments.

Technical Report TR2008/035
Central Waitemata Harbour Contaminant Study. Trace Metal Concentrations in Harbour Sediments.

Technical Report TR2008/036
Central Waitemata Harbour Contaminant Study. Hydrodynamics and Sediment Transport Fieldwork.

Technical Report TR2008/037
Central Waitemata Harbour Contaminant Study. Harbour Hydrodynamics, Wave and Sediment Transport Model Implementation and Calibration.

Technical Report TR2008/038
Central Waitemata Harbour Contaminant Study. Development of the Contaminant Load Model.

Technical Report TR2008/039
Central Waitemata Harbour Contaminant Study. Predictions of Stormwater Contaminant Loads.

Technical Report TR2008/040
Central Waitemata Harbour Contaminant Study. GLEAMS Model Structure, Setup and Data Requirements.

Technical Report TR2008/041
Central Waitemata Harbour Contaminant Study. GLEAMS Model Results for Rural and Earthworks Sediment Loads.

Technical Report TR2008/042
Central Waitemata Harbour Contaminant Study. USC-3 Model Description, Implementation and Calibration.

Technical Report TR2008/043
Central Waitemata Harbour Contaminant Study. Predictions of Sediment, Zinc and Copper Accumulation under Future Development Scenario 1.

Technical Report TR2008/044
Central Waitemata Harbour Contaminant Study. Predictions of Sediment, Zinc and Copper Accumulation under Future Development Scenarios 2, 3 and 4.

Technical Report TR2009/109
Central Waitemata Harbour Contaminant Study. Rainfall Analysis.

Contents

1	Executive Summary	1
2	Introduction	3
2.1	Study aims	3
2.2	Model suite	3
2.3	Work plan	4
2.4	This report	4
2.5	Background	5
3	Methodology	8
3.1	Suspended sediment characteristics	8
3.1.1	Particle size distribution	9
3.1.2	Fall speed	11
3.2	Surface and subsurface sediments	14
3.2.1	Definition of the surface layer	15
3.2.2	Particle size analysis	16
3.2.3	Spatial distribution of sediments	16
3.2.4	Sediment bulk density	16
3.3	Sediment cores	16
3.3.1	X-radiographs	18
3.4	Sediment mixing	18
3.4.1	Mixing information from radioisotope profiles	20
3.4.2	Effects of benthic communities on bioturbation	22
4	Results	25
4.1	Suspended sediments	25
4.1.1	Particle size	25
4.1.2	Fall speed	35
4.2	Surface sediments	37
4.2.1	Particle size	37
4.2.2	Sediment bulk density	41
4.3	Sub-surface sediments: sedimentation	43

4.3.1	⁷ Be Profiles	43
4.3.2	²¹⁰ Pb and ¹³⁷ Cs profiles	45
4.3.3	Bioturbation	61
5	Synthesis: Recent Sedimentation and Mixing	69
5.1	Recent sedimentation in the Central Waitemata Harbour	69
5.1.1	Comparison of ¹³⁷ Cs and ²¹⁰ Pb sediment accumulation rates	69
5.1.2	²¹⁰ Pb and ¹³⁷ Cs budgets and implications for fine sediment fate	70
5.1.3	Comparison with previous studies	76
5.2	Sediment mixing	77
6	Acknowledgements	78
7	References	79
8	Appendix 1: Location of Surface-sediment Samples and Dating Cores	83
9	Appendix 2: Spatial Distribution of Sediments – Geostatistics	87
10	Appendix 3: Dating of Estuarine Sediments	89
10.1	¹³⁷ Cs dating	89
10.2	²¹⁰ Pb dating	90
10.3	Sediment accumulation rates (SAR)	91
10.4	SAR derived from ²¹⁰ Pb dating	92
11	Appendix 4: Dating of Estuarine Sediments	94
11.1	Usefulness of the Haywood et al. (1999) CWH habitat map	94

Reviewed by:



S. Nodder, NIWA

Approved for release by:



M. Green, NIWA

1 Executive Summary

The overall aim of the Central Waitemata Harbour (CWH) Contaminant Study is to model contaminant accumulation (sediment, zinc, copper) within the harbour for the purposes of, amongst other things, identifying significant contaminant sources, and testing efficacy of stormwater treatment and industrial roof contaminant source control. The objective is to predict (using models) contaminant build up and movement in the CWH.

Herein we report on physical characteristics of the suspended sediments discharged to the CWH from the Whau River and Henderson Creek, physical characteristics of surface sediments of the CWH, sediment accumulation rates, and mixing of sediment deposits by physical and biological processes.

Data are interpreted to provide an improved understanding of sediment processes relating to the dispersal, deposition and post-depositional mixing of sediments and contaminants associated with stormwater discharges into the CWH. Inputs to the Urban Stormwater Contaminant (USC) model are to be constructed from the data presented herein.

Particle size distributions and fall speeds of suspended sediments were measured on one ebb tide at the mouth of the Whau River and on one ebb tide at the mouth of Henderson Creek. Suspended sediments discharged to the CWH from the Whau River and Henderson Creek are mainly composed of mineral clays, silts and sand-sized flocs composed of smaller constituent particles. Fine sand is also present in suspension. The composition of the suspension is likely to vary depending on freshwater discharge. Fall speed of suspended particles greater than 3.5 μm and less than 100 μm was generally substantially less than the fall speed of same-sized solid inorganic particles. This implies that these particles are low-density aggregates of smaller constituent particles.

Surface sediments were sampled to 3 cm depth at 138 sites in the CWH and Shoal Bay. Maps showing distribution of mean and median particle diameter, sorting, mud content, and percentage of various size fractions are presented. The mud content of surface sediments is less than 16 per cent over much of the CWH and Shoal Bay. The finest size fractions are found on the intertidal flats near tidal creek outlets and at the northern tip of Te Tokaroa Reef. The dry bulk density and water content of surface sediments range between 0.7 to 2.6 g cm^{-3} and 23 to 69 per cent by weight, respectively.

Subsurface sediments were sampled to 0.5 m depth at 21 intertidal and subtidal sites. Time-averaged sediment accumulation rates (SAR) over the last 50 years were determined at 13 of the core sites from ^{210}Pb and ^{137}Cs concentration profiles. Sediment-mixing depths were determined from ^7Be and ^{210}Pb concentration profiles, x-ray images of sediment cores, and sampling and analysis of benthic-community structure.

Sediments deposited in the CWH and Shoal Bay over the last 50 years are mainly composed of muddy sands often containing buried cockle-shell layers between 0–15 cm depth. Particle-size data for three cores show that the mud content (5–25 per cent by volume) of sediment deposits has not substantially changed over the last 50 years.

Intertidal and subtidal flats are accumulating sediment at similar rates: 3.2 mm yr⁻¹ for intertidal flats (range: 0.7–6.8 mm yr⁻¹) and 3.3 mm yr⁻¹ for subtidal areas (range: 2.2–5.3 mm yr⁻¹). SAR is more variable at intertidal sites. Fine sediments are also accumulating in the tidal creeks (Henderson Creek 2.6–5.1 mm yr⁻¹) and in mangrove habitats that fringe the CWH, as observed in other Auckland estuaries. It is likely that sediment trapping in tidal creeks, including the Whau and Henderson, is less effective than in the past because of reduced accommodation space.

Surface sediments are well mixed to 1–5 cm depth and to ≥ 3 cm depth in 60 per cent of cases. A feature of the CWH is that the surface sediment layer is uniformly mixed, and this mixing is occurring over 100 days or less. The maximum residence time of sediments within the surface mixed layer (SML) varies between four and 14 years. Sediments are eventually removed from the SML by burial.

Bioturbation depths exceed 10 cm at most sites, but have varied over the past six years. Bioturbation depths in intertidal habitats are greater than in subtidal habitats. The bioturbation index was 120–970 at sites in the central basin and 2300–5600 at intertidal sites ringing the subtidal basin. The substantially lower values for the index in the subtidal sites reflect lower densities and sizes of animals.

X-radiographs typically do not preserve evidence of animal burrows or physical bedding below the SML. The fact that there are few traces of animal burrows in the x-radiographs does not preclude sediment mixing by feeding activities or animal movement. However, the intensity of sediment mixing below the SML is relatively low.

A conceptual model of fine sediment dispersal and fate in the CWH over the past 50 years is presented. Fine sediment is delivered to the tidal creeks fringing the CWH. The Whau River and Henderson Creek have substantially infilled with fine sediment. The sediment that does escape the tidal creeks is widely dispersed. Shoal Bay and the central basin of the Central Waitemata Harbour are long-term sinks for fine sediments. Intertidal flats and shallow subtidal flats provide temporary sinks for fine sediments.

2 Introduction

Modelling and empirical data indicate that stormwater contaminants are rapidly accumulating in the highly urbanised side branches of the Central Waitemata Harbour (CWH). However, there is no clear understanding of the fate of contaminants exported from these side branches into the main body of the harbour, or that of contaminants discharged directly into the harbour.

In response to this need, the Auckland Regional Council contracted NIWA to conduct the Central Waitemata Harbour Contaminant Study. The study began in September 2005 and is scheduled to run for three years. The main aim of the CWH study is to model contaminant (zinc, copper) and sediment accumulation within the CWH for the purposes of, amongst other things, identifying significant contaminant sources, and testing efficacy of stormwater treatment and industrial roof contaminant source control.

2.1 Study aims

The study aims to:

- predict contaminant loads based on past, present and future land use and population growth for each sub-catchment discharging into the CWH, allowing for stormwater treatment and industrial roof contaminant source control;
- predict dispersal and accumulation (or loss) of sediment and stormwater contaminants in the CWH;
- calibrate and validate the dispersal/accumulation model;
- apply the various models to predict catchment contaminant loads and accumulation of copper, zinc and sediment in the CWH under specific scenarios that depict various combinations of projected land use/population growth, stormwater treatment efficiency, and industrial roof contaminant source control;
- determine from the model predictions the relative contributions of sediment and contaminant from individual sub-catchments and local authorities;
- provide an assessment of the environmental consequences of model outputs;
- provide technical reports on each component of the work; and
- provide a desktop application suitable.

2.2 Model suite

The study centres on the application of three models that are linked to each other in a single suite:

- The GLEAMS sediment-generation model, which predicts sediment erosion from the land and transport down the stream channel network. Predictions of sediment

supply are necessary because, ultimately, sediment eroded from the land dilutes the concentration of contaminants in the bed sediments of the harbour, making them less harmful to biota¹.

- The CLM contaminant/sediment-generation model, which predicts sediment and contaminant concentrations (including zinc, copper) in stormwater at a point source, in urban streams, or at end-of-pipe where stormwater discharges into the receiving environment.
- The USC-3 (Urban Stormwater Contaminant) contaminant/sediment accumulation model, which predicts sedimentation and accumulation of contaminants (including zinc, copper) in the bed sediments of the estuary. Underlying the USC-3 model is yet another model: an estuarine sediment-transport model, which simulates the dispersal of contaminants/sediments by physical processes such as tidal currents and waves.

2.3 Work plan

There are eight modules in the work plan:

- Module 1 – Implementation of the sediment-generation model.
- Module 2 – Implementation of the contaminant/sediment-generation model.
- Module 3 – Implementation of the contaminant/sediment-accumulation model.
- Module 4 – Calibration and validation of the model suite.
- Module 5 – Depiction of development scenarios, including stormwater treatment and Industrial roof contaminant source control, as required.
- Module 6 – Execution of the model suite to produce predictions of contaminant build-up in bed sediments of the CWH.
- Module 7 – Evaluation of predictions with management.

This may lead to reconsideration of Module 5, and subsequent re-running of Module 6 until an acceptable development scenario can be found.

- Module 8 – Development of desktop application.

2.4 This report

Herein we report on:

- Particle size and fall speed of suspended sediments discharged to the CWH from the Whau River and Henderson Creek.
- Physical characteristics of the surface sediments of the CWH. This includes particle size and bulk density.

¹ We use the term “contaminant” herein to mean chemical contaminants such as zinc and copper, and we refer to “sediments” separately.

- Sediment accumulation rates determined from radioisotope profiles measured in sediment cores.
- Mixing of sediment deposits by physical and biological processes. This draws on radioisotope profiles, x-ray images of sediment cores, and sampling and analysis of benthic-community structure at intertidal and subtidal sites.

Data are interpreted to provide an improved understanding of the dispersal, deposition and post-depositional mixing of sediments and contaminants associated with stormwater discharges into the CWH.

Inputs to the Urban Stormwater Contaminant model (USC-3) are to be constructed from the data presented herein.

2.5 Background

Tidal creeks fringing the CWH have largely infilled with sediments. Consequently, there is limited accommodation space for fine sediments to accumulate, and tidal creeks are likely to be exporting fine sediments and associated urban stormwater contaminants (eg, Cu, Zn) into the main body of the harbour (Figure 1).

Figure 1

Fine sediment plumes discharging from the Whau River, Henderson Creek and Waterview Creek, 7 October 2002. The Whau River outlet is at the right-hand side of the image. (Image courtesy: NASA ISS005-16874, International Space Station.)



The CWH covers 50 km² between the Upper Harbour Bridge at Whenuapai and the Auckland Harbour Bridge (Figure 2). The central basin of the CWH covers ~4 km² of subtidal flat between 0 and 5 m below chart datum. The central basin is bounded to the west by the Te-Atatu and Whau intertidal flats and to the north and east, respectively, by the main channel and Te Tokaroa (Meola) Reef.

Figure 2

Map showing the Upper Waitemata Harbour (UWH), Central Waitemata Harbour (CWH) and Shoal Bay. The CWH and Shoal Bay are the focus of the present study. Extent of intertidal flat and mangrove habitats is also shown. Water depths (m) are relative to chart datum (CD).



The Waitemata Harbour is a drowned-valley estuary. It is the largest estuary on the east coast of the Auckland region, with a surface area of some 80 km² and a tidal prism of about 216 million m³. The CWH remains substantially subtidal despite the sediment deposition that has occurred over the last several thousand years. Infilling is most advanced in the tidal creeks. The central basin (Figure 2, 0–5 m below chart datum) is flanked by extensive intertidal flats east of Te Atatu Peninsula and Pollen Island. Te Tokaroa (Meola) Reef extends some 2 km from the shore and largely constrains tidal flows into and out of the CWH to the main tidal channel. Field

measurements show that fine sediments in both intertidal and subtidal areas are mainly resuspended by waves (Oldman et al. 2008).

The CWH receives run-off from a 205 km² land catchment, 50 per cent of which discharges to the Harbour via Henderson Creek. The Henderson Creek sub-catchment drains the eastern Waitakere Ranges, with landcover consisting of regenerating native conifer–hardwood forest dominated by kauri, rata, toatoa and rimu. The lower flanks of the ranges include low-density urban land use. Large-scale catchment deforestation began in the late 1840s and was largely complete by the late 1860s. Establishment of pasture involved scrub clearance by fire, which was often uncontrolled, and it is likely that soil erosion increased during this period. Viticulture and orcharding were established in the lower catchment in the 1890s, when Henderson Township was expanding. Farming had virtually ceased by the 1920s due to soil infertility. Large-scale urbanisation at Henderson, Massey and Te Atatu began in the 1960s following construction of the Northwestern Motorway (Denyer et al. 1993, Swales et al. 2002a).

Auckland City developed from the 1840s onwards and land fringing the southern shore of the CWH at Avondale, Point Chevalier and Herne Bay had been urbanised by the early 1900s. On the North Shore, settlements developed at Birkenhead, Northcote, Takapuna and Devonport from the mid-1800s were serviced by ferries. However, most of the North Shore remained rural (pasture and native scrub). Large-scale urbanisation followed the construction of the Auckland Harbour Bridge in the early 1950s. For example, the Hellyers Creek catchment was completely urbanised by the early 1970s (Williamson and Morrissey 2000).

3 Methodology

3.1 Suspended sediment characteristics

Particle-size distribution (PSD) and fall speed are first-order controls on the attachment of heavy metals to sediment particles and on the dispersal and settling of suspended sediments delivered by tidal creeks to the CWH. In this section, we present the methods used to characterise PSD and fall speed of suspended sediments in ebb-tidal flows from the Whau River and Henderson Creek, the catchments of which account for 67 per cent of the land catchment draining to the CWH.

Cohesive clays, fine silts and organic substances discharged in stormwater into tidal creeks flocculate upon mixing with saline estuarine water. Flocculation is the process of aggregation of particles to form larger flocs or clumps. The formation, growth and decay of flocs are influenced by flow conditions, such as the degree of turbulence, suspended-sediment concentration, water salinity and temperature. These may all vary during the course of a storm and/or over a tidal cycle.

We used a Sequoia Laser In Situ Scattering and Transmissometry (LISST) instrument to measure PSD and fall speed. The LISST uses a laser to make measurements. Particles scatter the laser light at different angles depending on their size, with the largest particles scattering light at the smallest angles. Scattered light is measured by an array of 32 annular detector rings of decreasing diameter, with particle size measured at 32 log-spaced intervals in the range 2.7–462 μm . This technique is relatively insensitive to particle composition so that light diffraction is primarily the result of particle size. The LISST employs a 10 mW diode laser, which produces a 670 nm light source. Agrawal and Pottsmith (2000) provided a technical description of the LISST.

The LISST has several limitations that are relevant to the present study.

Firstly, there is a maximum suspended-sediment concentration (SSC) at which the instrument will function and this varies with particle size. For fine sediments, the maximum SSC is $\sim 160 \text{ mg l}^{-1}$ when the LISST is fitted with a transmission path reduction device (PRD). The maximum SSC for sand particles will be higher than for fine sediments because there are fewer sand particles in suspension per unit SSC. As SSC increases above the maximum operational value, multiple-scattering of laser light occurs, which leads to underestimation of the PSD. Typical background SSC in Auckland estuaries is in the range 10–50 mg l^{-1} , which does not present a problem, but SSC during storms may be an order of magnitude higher, thus exceeding the maximum operational value.

Secondly, minute changes in water density due to salinity variations may affect measurements. As a precaution, we discard from any further analysis as a matter of routine all information on particles/flocs greater than 128 μm diameter

Before and after each deployment, the background or zero-scatter (ZSCAT) response in optically clear water was measured. The ZSCAT response in each size range was similar to the factory-calibrated value. Higher values indicate that the transmitter/detector windows are dirty and/or the water is not clear and/or the laser-beam is out of alignment.

The ZSCAT data are used to process the raw data into a particle-volume concentration ($\text{cm}^3 \text{ l}^{-1}$) for each size class. The volume concentration is based on the assumption that particles are spherical, which is reasonable for silt-sand sized particles.

Volume concentration is converted to a mass concentration (mg l^{-1}) by assuming a particle density of 2.65 g cm^{-3} (equivalent to quartz). By comparison, biogenic particles and flocs have effective densities of $\sim 1 \text{ g cm}^{-3}$. Suspended sediments measured in the present study were mainly composed of inorganic material, so the mass concentration estimates are probably reasonable.

3.1.1 Particle size distribution

Particle size measurements were made during a deployment of the LISST at the mouth of the Whau River (Figure 3) and at the mouth of Henderson Creek (Figure 4). During both deployments, the LISST was mounted near the bed in the tidal channel, and measurements were made for six hours over an ebbing tide. Measurements were made in the Whau River on 31 May 2006 and in Henderson Creek on 1 June 2006. Weather during both deployments was fine with a light southeast wind. Stormwater discharges at the time were zero.

Water samples collected at 0.3 m and 1 m above the bed during early May 2006 showed SSC during ebbing tides was in the range $10\text{--}160 \text{ mg l}^{-1}$, which is within the operating range of the LISST.

Figure 3

Site of LISST deployment on 31 May 2006 near the mouth of the Whau River ($35^{\circ}51.101'S$, $174^{\circ}39.710'E$) and $\sim 300 \text{ m}$ seaward of the Northwestern Motorway bridge.



Figure 4

Site of LISST deployment at Henderson Creek, Luckens Point (36°49.110'S, 174°38.700'E) on 1 June 2006.



The LISST was mounted horizontally on a purpose-built frame with the measurement cell oriented horizontally into the flow at 0.64 m above the bed (Figure 5). This enabled free flow through the measurement cell. The LISST was programmed for continuous sampling with three samples measured and averaged at two-second intervals.

A submersible pump was mounted at the same elevation above the bed but at the opposite end of the LISST to collect duplicate water samples at 15 minute intervals during the ebb tide. The water samples were subsequently analysed for SSC and PSD using a Galai particle-sizing instrument. SSC was determined by filtering the water samples through pre-dried and pre-weighed Whatman 1.2 mm glass-fibre filters and dried at 105°C for 24 hours. The volatile (organic) suspended solids (VSS) component was determined from loss on ignition at 400°C. The average flow speed in the hose was maintained at $\sim 1 \text{ m s}^{-1}$ so that larger sand particles with much higher fall speeds than clays and silts would be sampled.

Figure 5

LISST mounted on the frame with water pump inlet (blue) and Acoustic Doppler Current Profiler (bottom) before deployment at the mouth of the Whau River, 31 May 2006.



A sediment trap was also mounted on the frame with its orifice 57 cm above the bed to provide a time-integrated suspended-sediment sample. The sediment trap was constructed from 45 cm long, 5 cm internal diameter PVC tube. The 9:1 aspect ratio is intended to minimise particle resuspension within the trap.

LISST data were analysed to determine time-averaged PSD at 1, 2, 5, 10 and 15 minute intervals.

3.1.2 Fall speed

The LISST can be configured to measure fall speeds of suspended particles and flocs by the addition of a vertical settling tube (ST) (Figure 6). Fall speed is measured in eight size increments between 3.5 and 360 μm diameter. Measurements are made as 83 transmission scans at log-spaced time increments between 1 second and 22 hours after water-sample capture.

The suspension is drawn into the settling column through round ports at the top of the column by a propeller mounted below the optical-transmission path. (The sampling ports are 0.9 m above the bed with the LISST mounted on the instrument frame.) The ports close immediately after sampling and seal the interior of the column from the surrounding water.

Figure 6

LISST with the settling column attached. The sample inlet ports can be seen at the top of the settling column.



The LISST was initially deployed in the channel at the mouth of the Whau River (Whau #6 port channel marker: 36°51.083'S 174°39.799'E) and at the mouth of Henderson Creek (Luckens Point: 36°49.110'S, 174°38.700'E) on one occasion each during the period 25–26 September 2006. In both cases a sample was captured by the LISST for fall-speed analysis ~2 hours after predicted high water. This time was chosen to allow time for water from the tidal creek to reach the creek mouth. A SCUBA diver collected duplicate 1 litre water samples for constituent particle size and SSC determination. An RBR Model XR-620 conductivity-temperature-depth (CTD) profiler was mounted on the frame, with sensors 0.5 m above the bed. Raw data were used to determine water

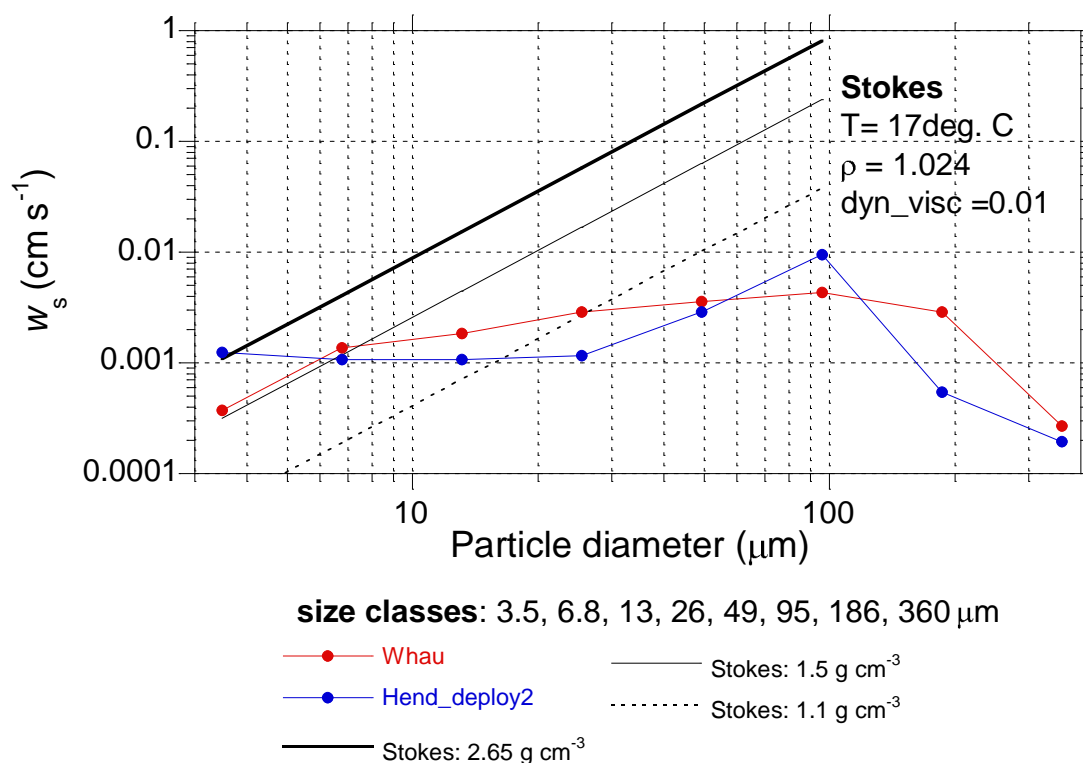
salinity and density based on the UNESCO 1980 International Seawater State Equations, commonly referred to as the Practical Salinity Scale.

The measured fall speeds were unrealistically low and uniform across size-classes (Figure 7). As a check we repeated the measurements at Henderson Creek on 27 September 2006, with similar results.

Figure 7 also compares the measured fall speeds with theoretical values predicted by Stokes Law for the settling of solitary spheres over a range of particle densities from 1.1 g cm^{-3} (organic particles) to 2.65 g cm^{-3} (quartz). Stokes Law is applicable to settling at low Reynolds numbers which, for quartz particles, equates to a spherical diameter less than $100 \mu\text{m}$. Stokes estimates were based on fluid density of 1.024 g cm^{-3} and dynamic viscosity of $0.01 \text{ g cm}^{-1} \text{ s}^{-1}$. Figure 7 shows that the measured fall speeds diverged markedly from the envelope of Stokes values for particles sizes greater than $13 \mu\text{m}$.

Figure 7

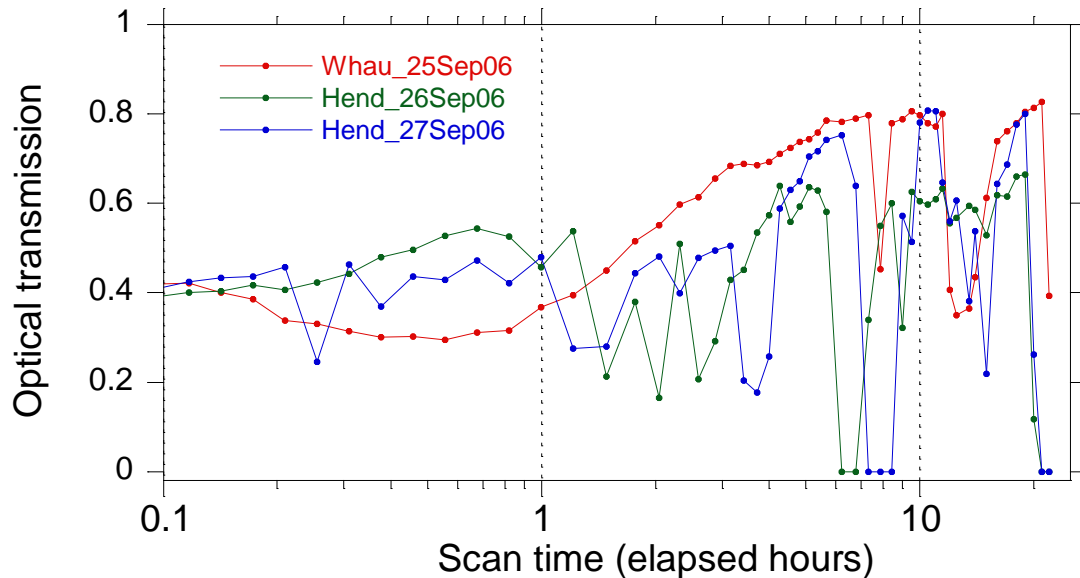
Fall speed of suspended sediments on the ebb tides of 25–27 September, Whau River and Henderson Creek, measured by the LISST. Fall speed predicted by Stokes equation is also shown.



The optical transmission time series at both sites showed intermittent abrupt drops to values close to zero (Figure 8), which is not realistic, and which could be the reason the fall speeds are not sensible. Consultation with Sequoia suggested that the seals on the LISST settling column could be at fault, which we confirmed with laboratory tests. We were not able to rectify the problem with the settling column so that it could be used in the field to make in situ measurements.

Figure 8

Optical transmission record, Whau River and Henderson Creek, 25–27 September 2006.

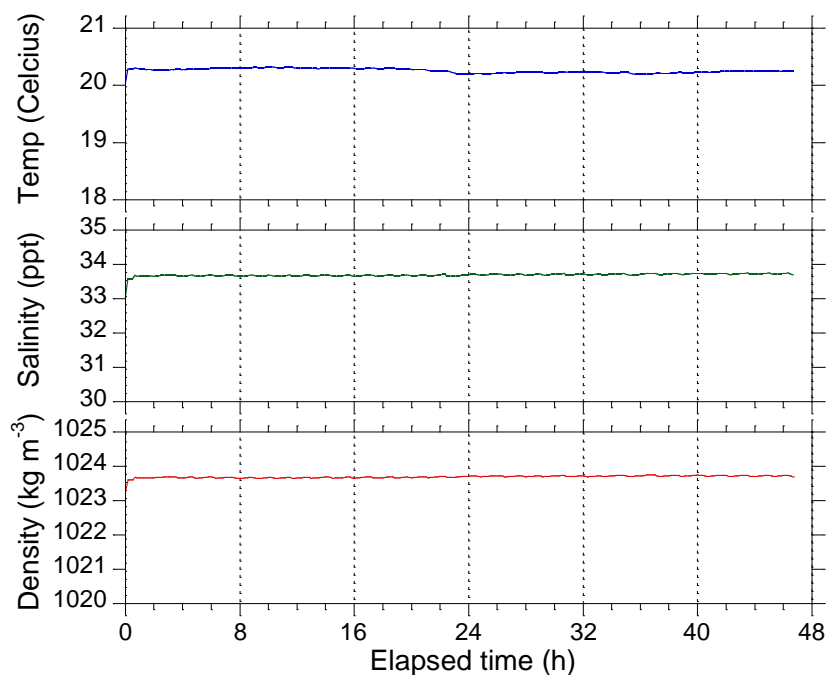


We resorted to measuring particle fall speed with the LISST in a laboratory tank housed in a constant-temperature room. Fall speed so determined cannot be considered to be an in situ value.

For the analysis, a peristaltic pump was used to collect one 300 litre water sample at each site at 0.9 m above the bed. Samples were obtained on 9–10 November 2006. The samples were refrigerated immediately on return to NIWA, Hamilton, and the measurements were conducted during 16–20 November 2006. Each water sample was allowed to equilibrate with the air temperature (20 °C) for 24 hours, and then the sample was homogenised using pumps for one-hour before measurement began. Figure 9 shows that water temperature, salinity and density remained constant during the laboratory experiments.

Figure 9

Time series of water temperature, salinity and density during the fall speed measurements conducted with the LISST in controlled laboratory conditions (start time 0813 NZST, 18 November 2006).



3.2 Surface and subsurface sediments

Information on the physical characteristics of the CWH surface and subsurface sediments is required to set up and validate the USC model. Physical characteristics to be reported on include particle size, bulk density, total organic carbon (TOC) and copper (Cu), zinc (Zn) and iron (Fe) concentrations. TOC and heavy-metal concentrations were determined for the following particle-size fractions:

- Clay-fine silt (0–25 μm).
- Medium-coarse silt (25–62.5 μm).
- Fine sand (62.5–250 μm).

Surface sediments were sampled at 138 sites and particle size determined. Particle-size data were used to select a subset of 33 samples for heavy metal and TOC analyses of the silt and fine sand fractions, which are reported by Ahrens et al. (2008).

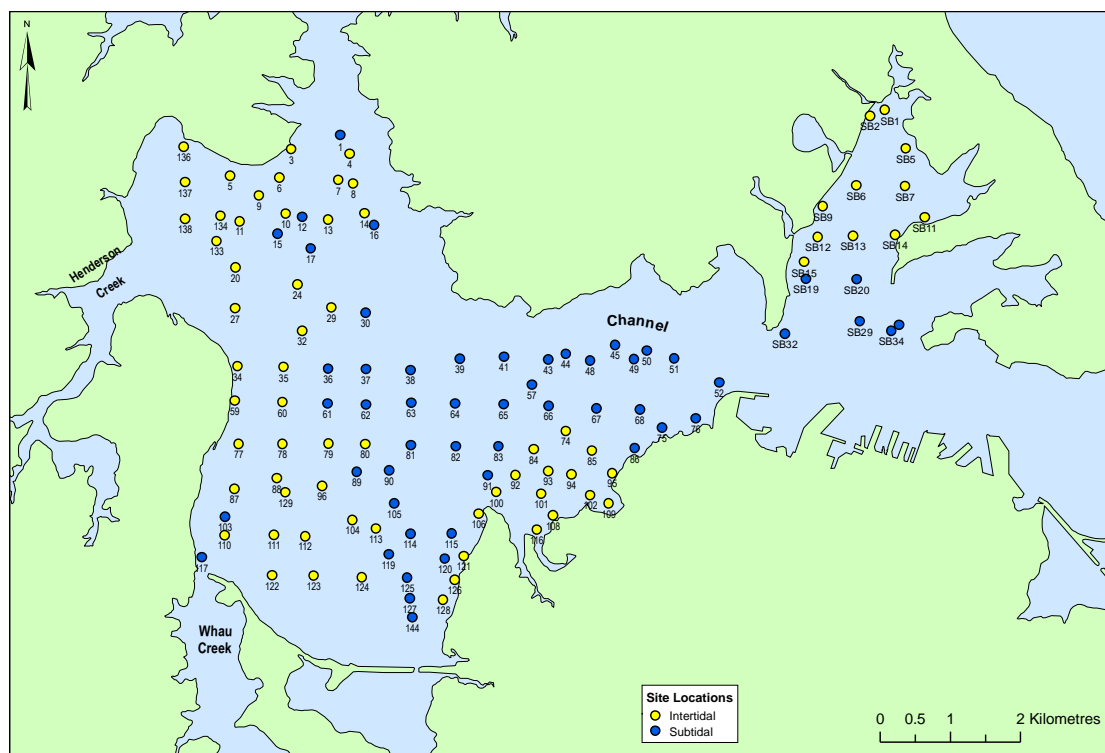
Subsurface sediments were sampled to 0.5 m depth in replicate cores at 21 sites. The cores were primarily acquired for the purposes of dating (Section 3.5.1), but three cores were also analysed for physical characteristics. These cores were from site SB-I1 (Shoal Bay intertidal), WT-S3 (CWH subtidal basin) and HN-I1 (Henderson Creek mouth intertidal).

Sampling was designed to identify spatial patterns/gradients in particle size. Duplicate sediment samples were collected on a semi-regular grid (~0.5 km spacing) during 19–

20 January and 20–21 March 2006 (Figure 10). SCUBA divers inserted 20 cm long by 5 cm diameter clear PVC push cores into the sediment to obtain a sample. The locations of the sampling sites are given in Appendix 1. One sample from each duplicate set was refrigerated and the other frozen immediately after collection and stored at NIWA Hamilton.

Figure 10

Location of surface sediment samples: subtidal sites are shown by blue symbols and intertidal sites by yellow symbols.



3.2.1 Definition of the surface layer

Definition of the surface layer was based on the vertical distribution of beryllium-7 (^7Be) in sediment cores collected at 21 sites for dating (Section 3.5.1). ^7Be is a short-lived radioisotope (half-life 53 days) that is particle reactive and concentrated in aquatic systems, which makes it an excellent tracer of sediment dispersal and reworking in fluvial and marine systems over seasonal timescales (Sommerfield et al. 1999). In the absence of vertical mixing, ^7Be should occur only in the top 1 mm or less of the sediment column, given sedimentation rates of 2–4 mm yr⁻¹ (Swales et al. 2002a). The maximum depth of ^7Be was 3 cm or more in 60 per cent of the cores collected in this study (depth range 1–5 cm), from which we define the surface layer as the top 3 cm of the sediment column.

3.2.2 Particle size analysis

The top 3 cm of each refrigerated core was removed and a sub-sample taken as a 1/8 vertical slice. Sub-samples were passed through a 2 mm sieve to remove shell fragments, and then homogenised in a 1 litre suspension. A 10 ml sub-sample was taken from each suspension with an auto-pipette.

Particle size distribution (PSD) in the 10 ml sub-sample was measured using a Galai CIS-100 time-of-transition (ToT) stream-scanning laser system. Samples were dispersed in an ultrasonic bath for 20 minutes before and then during analysis. The PSD was determined in the range 2–600 μm . When samples contained material over 600 μm diameter, the PSD was also determined in the 10–3600 μm size range. Typically 300,000 to 500,000 particles were counted per sample. Particle volumes were estimated from the measured particle diameters assuming spherical grains, and volume-based PSDs were constructed.

3.2.3 Spatial distribution of sediments

Geostatistical techniques were used to map the spatial distribution of particle-size parameters in the Central Waitemata Harbour, but there were insufficient data to do the same for Shoal Bay. Particle size parameters mapped included mean, median, standard deviation and the percentage of sediment by sample volume in the following size fractions: $\leq 25 \mu\text{m}$, $\leq 63 \mu\text{m}$, 25–63 μm , 63–125 μm , 125–250 μm . The geostatistical methods are described in Appendix 2.

3.2.4 Sediment bulk density

Sediment wet and dry bulk densities were determined for the 33 frozen samples selected for TOC and heavy metals analysis. The top 3 cm of each frozen sample was removed using a bandsaw. Frozen top water was removed and a 1/8 slice taken for bulk density analysis. The frozen wet weight of the slice was recorded. The sample was dried at 70°C for 24 hours and reweighed to obtain the dry-sample weight. The sediment bulk densities were calculated from these weights and the sample volume.

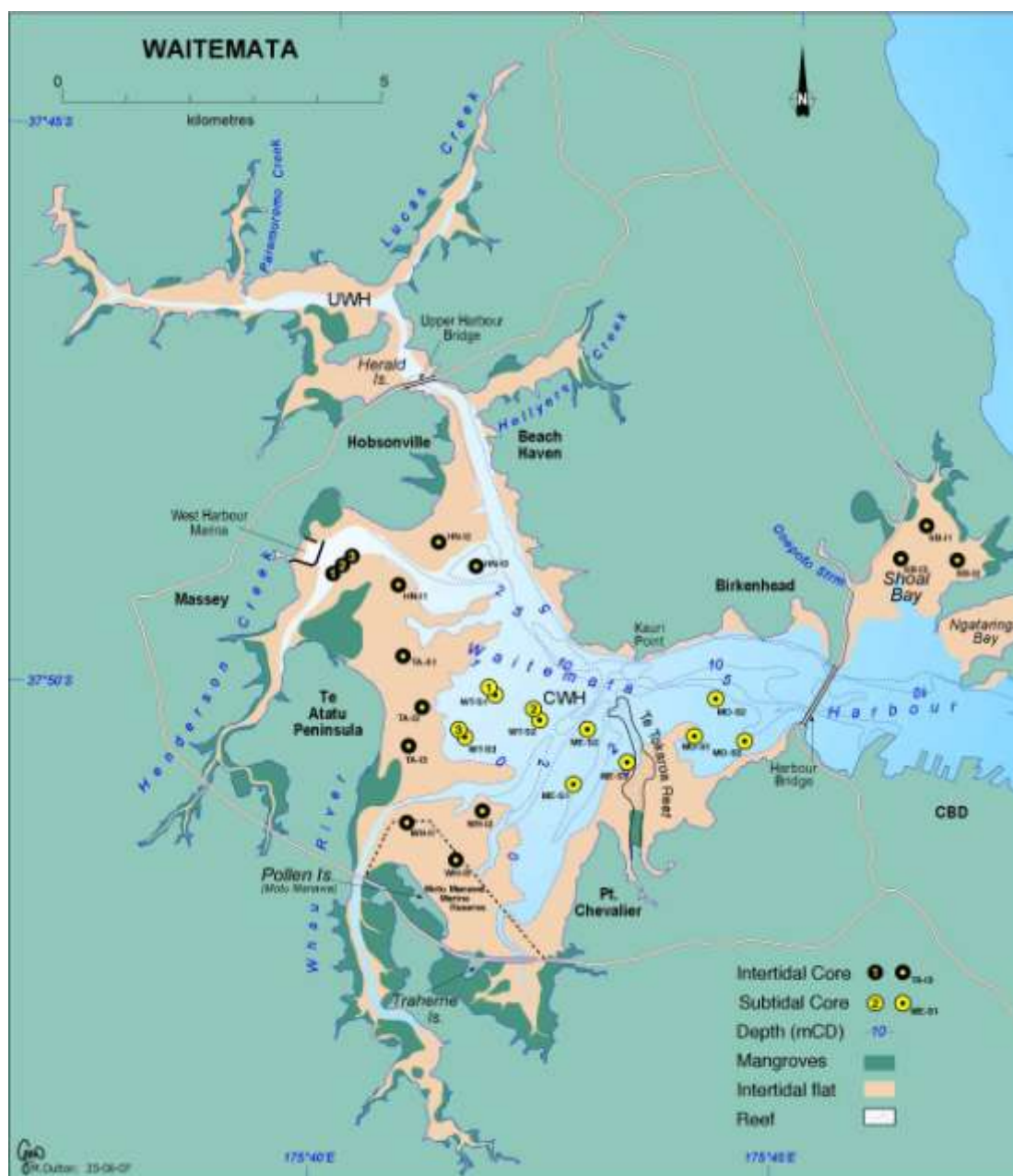
3.3 Sediment cores

Three replicate sediment cores were collected at 18 sites in the CWH and at three sites in Shoal Bay during February–March 2006 (Figure 11). Sediment cores were dated using radioisotope techniques. Radioisotopes, including caesium-137 (^{137}Cs , half-life ($t_{1/2}$) 30 years) and lead-210 (^{210}Pb , half-life 22.3 years), and plant pollen can be used to reconstruct the recent sedimentation history of an estuary. Heavy metal profiles in estuarine sediments have also been shown to provide useful additional information to identify the onset of urban development (eg, Valette-Silver 1993; Abraham and Parker 2002; Swales et al. 2002a, 2002b, 2005). Dating of estuarine sediments using several independent methods offsets the limitations of any one approach. This is important when interpreting cores from lakes, estuaries and the sea because of the potential confounding effects of physical and biological mixing (Robbins and Edgington 1975;

Olsen et al. 1981; Sharma et al. 1987; Alexander et al. 1993; Valette-Silver 1993; Benoit et al. 1999; Chagué-Goff et al. 2000).

Figure 11

Location of sediment cores collected for radioisotope dating. Cores labelled 1–3 were collected in January 2002 (Swales et al. 2002 ARC TP221).



Sediment accumulation rates (SAR) were estimated from ^{210}Pb and ^{137}Cs profiles measured in the sediment cores. Concentrations of the cosmogenic radioisotope beryllium-7 (^7Be , $t_{1/2}$ 53 days) were also measured in the core samples. ^7Be is particle reactive and tends to be concentrated in aquatic systems, making it a useful sediment tracer in fluvial-marine systems at seasonal timescales (Sommerfield et al. 1999). In the present study, ^7Be is used to provide information on the depth and intensity of

sediment mixing. The radioisotope-dating techniques used in the present study are described in Appendix 3.

Radioisotope activity concentrations expressed in International System of units of Becquerel (disintegration s^{-1}) per kilogram (Bq kg^{-1}) were determined by gamma-spectrometry. For simplicity, we will refer to the activity concentrations of ^{137}Cs and ^{210}Pb as concentrations. Dry samples (40–60 g) were counted for 23 hrs using a Canberra Model BE5030 hyper-pure germanium detector. The unsupported or excess ^{210}Pb concentration ($^{210}\text{Pb}_{\text{us}}$) was determined from the ^{226}Ra ($t_{1/2}$ 1622 yr) assay after a 30 day ingrowth period for ^{222}Rn ($t_{1/2}$ 3.8 days) gas in samples embedded in epoxy resin. Gamma spectra of ^{226}Ra , ^{210}Pb and ^{137}Cs were analysed using Genie2000 software.

The $^{210}\text{Pb}_{\text{us}}$ profiles in each core were used to determine: (1) time-averaged SAR from regression analysis of natural log-transformed data; (2) $^{210}\text{Pb}_{\text{us}}$ inventory (A , Bq cm^{-2}) and; (3) mean annual supply rate (P , $\text{Bq cm}^{-2} \text{ yr}^{-1}$) based on the ^{210}Pb decay co-efficient (k , 0.0311 yr^{-1}). These data were compared with the ^{210}Pb atmospheric flux ($0.005 \text{ Bq cm}^{-2} \text{ yr}^{-1}$) measured by NIWA at Auckland (Section 5). SAR were estimated from ^{137}Cs profiles based on the maximum depth of ^{137}Cs in each core and included corrections for sediment mixing indicated by ^7Be profiles. In NZ, ^{137}Cs deposition from the atmosphere was first detected in 1953 (Matthews 1989).

3.3.1 X-radiographs

Sediment cores were split and sectioned into 2 cm thick longitudinal slabs for x-ray imaging. The x-ray image (or x-radiograph) enables the fine-scale sedimentary fabric to be observed and interpreted. For example, density differences between thin laminae of silt and sand or burrows infilled with mud make these features clearly visible on x-ray images, whereas these features may not be visible to the naked eye.

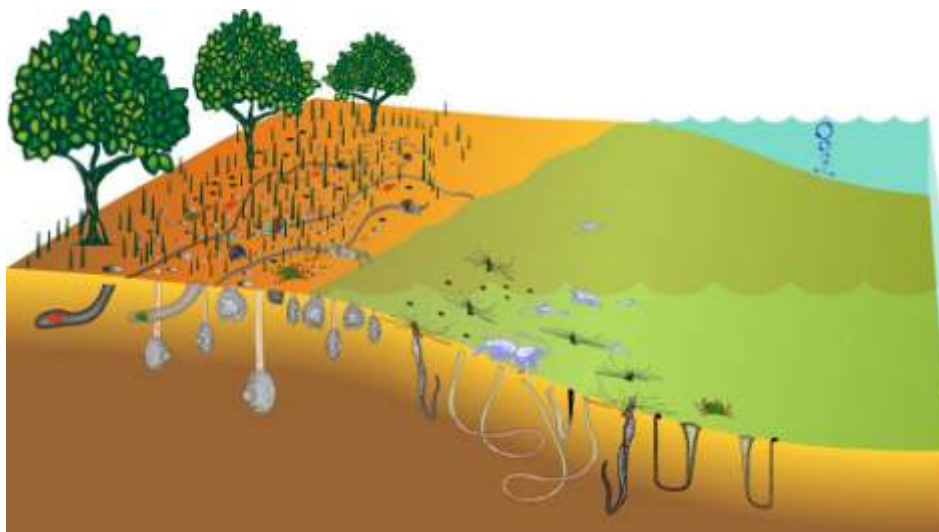
The sediment slabs were imaged using a Thales Flashscan 35 digital X-ray panel detector, illuminated by a Kramex PX15HF portable X-ray generator, at exposures of 60 kV and 15mA for three seconds. Images were stored as 16-bit grayscale and converted to 8-bit TIFF files for subsequent interpretation.

3.4 Sediment mixing

Biological and physical processes mix the upper sediment column both horizontally and vertically (Bromley 1996). Vertical mixing influences contaminant cycling as well as altering sediment profiles. Sediment bedding can be completely erased (Figure 12).

Figure 12

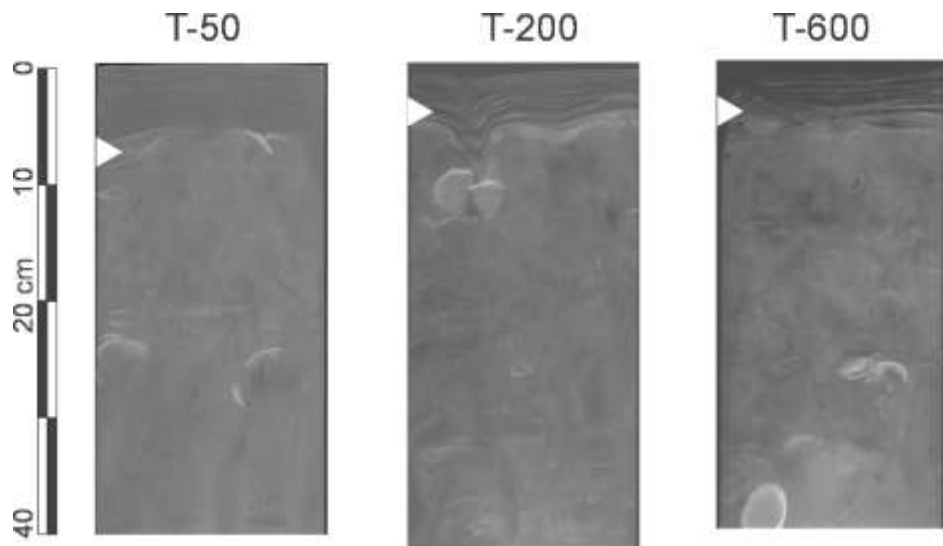
Biological and physical processes, such as the burrowing and feeding activities of animals and sediment resuspension by waves, mix near-surface sediments. The depth of the surface mixed layer (SML) is indicated by the yellow zone.



Diagnostic features of mixing by physical processes include fine-scale laminations in surface sediments, sharp basal contact with a higher density sediment corresponding to the ^7Be maximum depth, and an absence of animal traces (Figure 13). We expect physical mixing of sediments by waves to occur in the CWH, given its relatively large size and extensive intertidal and shallow subtidal areas.

Figure 13

X-radiographs of sediment cores taken from wave-exposed mudflats, Firth of Thames. These images show finely laminated bedding in low-density muds, absence of animal burrows, and traces indicative of resuspended-redeposited sediments. Bright shades indicate high-density and/or coarser sediment and dark shades low-density and/or finer sediment. The depth of the surface mixed layer is also shown by the maximum ^7Be penetration depth (indicated by the white triangles). (Images courtesy: Dr Sam Bentley, Earth Sciences Dept., Memorial University, Canada.)



Biological mixing or bioturbation of sediments results from the burrowing and feeding activities and movements of animals. Sediment is transported vertically both up and down by bioturbating organisms, which influence contaminant cycling within the sediment column. For example, less contaminated sediments deeper in the sediment column can be mixed with more contaminated surface sediments. As a result, contaminated surface sediments are diluted. Bioturbators that move on the surface or within the top 2 cm of the sediment column may also increase the potential for sediment resuspension, thus dispersing contaminated sediment.

The rate of bioturbation (sediment volume transported per unit time) is a function of the type of movements the resident animals make, their degree of mobility and their sizes. Animals bioturbate the sediment by creating and maintaining vertical burrows (eg, some crabs, polychaetes and amphipods), moving sediment up or down the sediment column while feeding and excreting (eg, deposit-feeding bivalves such as the wedge shell *Macomona liliana*), moving through the sediment in their search for food (eg, urchins and many deposit-feeding polychaetes), and moving across the sediment surface (eg, grazers such as many of the gastropods).

3.4.1 Mixing information from radioisotope profiles

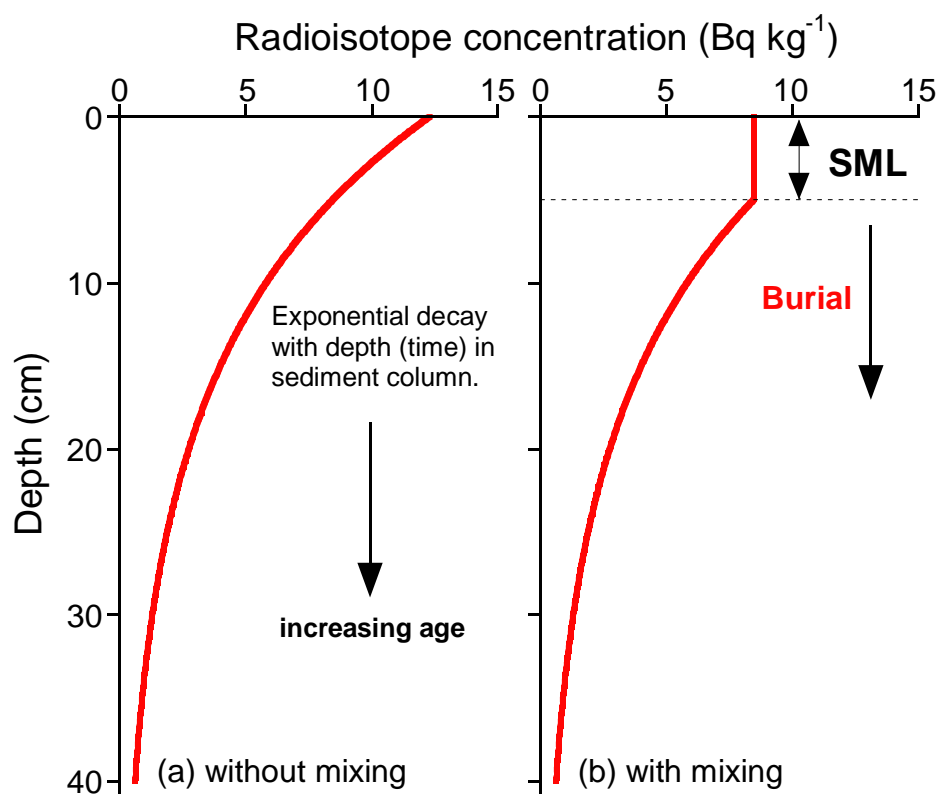
Depth profiles of naturally occurring radisotopes including ^7Be ($1/2$ -life 53 days) and ^{210}Pb (half-life 22.3 years) can provide information about the depth, rate and intensity of sediment mixing (Appendix 3). In the absence of sediment mixing and under a constant sedimentation rate, ^7Be and ^{210}Pb will decline exponentially with depth in

the sediment column (Figure 14a). By contrast, in sediments subject to intense mixing there is typically a surface mixed layer (SML) in which radioisotope concentrations are uniform. Beneath the SML, radioisotope concentration in buried sediments not subject to intense mixing declines exponentially with depth (Figure 14b).

Mathematical models have been proposed to take into account the effects of bioturbation on ^{210}Pb concentration profiles (eg, Guinasso and Schink 1975). For instance, biological mixing has been modelled as a one-dimensional particle-diffusion process (Goldberg and Kide, 1962). The assumption is usually made that the mixing intensity (ie, diffusion coefficient) and mixing depth (ie, SML) are fixed in time. More recent models have used sediment mixing coefficients that vary with depth in the sediment column (Fuller et al. 1999). The validity of this assumption usually cannot be tested, but changes in bioturbation depth and/or mixing rate could be expected to follow changes in benthic community structure.

Figure 14

Examples of idealised radioisotope profiles in estuarine sediments under a constant sedimentation rate and (a) without and (b) with vertical mixing due to physical and/or biological processes. Radioisotope concentrations are uniform within the surface-mixed layer (SML). As sediments are removed from the SML by burial, radioisotope concentration decays according to its decay constant.



3.4.2 Effects of benthic communities on bioturbation

3.4.2.1 Bioturbation index

To estimate the degree of bioturbation, a per capita bioturbation index was created by ranking different species of animals in relation to three categories thought to influence bioturbation. The bioturbation index provides a relative measure of the degree of bioturbation by a community of animals at a particular site. The three categories (Table 1) used to develop the index were based on animal size, behaviour and mobility.

Bioturbation potential for a single “average” individual of a given species² was calculated by multiplying the ranks of each category together. These species-specific values were then applied to a site in accordance with the species present and their relative abundances.

3.4.2.2 Bioturbation depth

Knowledge of animal burrowing behaviour was also used to estimate the likely depth of bioturbation. Some species live on the sediment surface (eg, the gastropod *Cominella glandiformis*), while others live deep within the sediment column (eg, adult *Macomona liliana*, which live ~10 cm below the sediment surface but feed on surface deposits using a long siphon). A large number of species, particularly those that are small, live in the top 2 cm of the sediment column, while others live throughout the sediment.

Depth of bioturbation at a site was derived by calculating the 50th percentile from the frequency of occurrence of animals observed at a site in each of three depth categories (0–2 cm, 2–10 cm and over 10 cm).

Table 1

Variables affecting the bioturbation index and their ranking in the index calculation and depth range.

Variable affecting bioturbation	Ranking
Burrowing	0 – organisms that live on the sediment surface and thought to make a minimal contribution to bioturbation. 1 – organism does not form a burrow and does not move sediment. 2 – organism does not form a burrow but may live close to or on the sediment surface and disturb the sediment surface. 3 – organism forms a burrow but does not move sediment actively. 4 – organism forms a burrow and maintains the burrow and does transport/move sediment, but not actively. 5 – organism is an active burrower and maintains its burrow; transports material from depth to the sediment/water interface and vice versa.
Mobility	1 – organism is reasonably sedentary and may live in a tube.

² Bivalves *Austrovenus stutchburyi* and *Macomona liliana* were sorted into three size classes: small <5 mm, medium 5–20 mm, and larger than 20 mm.

Variable affecting bioturbation	Ranking
	2 – organism moves in response to environmental cues (eg, tides) but remains sedentary for most of the time. 3 – organism is motile. 4 – organism is highly motile and actively moves through the sediment most of the time.
Size (average size of the organism)	1-2 – organism <5 mm. 3-4 – organism between 5 and 20 mm. 5-6 – organism between 20 and 30 mm. 7-8 – organism between 30 and 50 mm. 9-10 – organism >50 mm.
Range of movement (vertical mixing potential)	1 – lives in the top 2 cm of the sediment column. 2 – lives within the top 2–10 cm of the sediment column. 3 – lives >10 cm below the sediment surface.

3.4.2.3 Site comparisons

The bioturbation index and mixing depth based on benthic community structure were estimated for five intertidal sites where cores for dating were also collected (Figure 11). The five sites selected were:

- near the Henderson Creek mouth (sites HN-I2 and HN-I3);
- upper intertidal flats flanking the Te Atatu Peninsula (sites TA- I1 and TA-I2); and
- lower intertidal flats northeast of Pollen Island near Whau River (site WH-I2).

Three replicate macrofauna cores were collected from each site using a 13 cm diameter, 15 cm long corer. Samples were sieved on a 0.5 mm mesh.

Sediment-mixing depths were estimated from both radioisotope profiles and benthic community data. Sediment-mixing depths estimated from radioisotope profiles were based on SML thickness. The presence of laminated sediments in the SML is diagnostic of physical mixing only. The absence of laminated sediments is indicative of biological and/or physical mixing. For the latter case it is not usually possible to separate the effects of bioturbation from physical mixing based.

Although no subtidal sites were sampled in 2006, benthic-community data were available for subtidal sites WT-S1 – WT-S3 in the central basin. Samples were collected at these sites in January 2002 as part of the “Evidence for the physical effects of catchment sediments preserved in estuarine sediments” study for ARC (Swales et al. 2002a; Lundquist et al. 2003).

An attempt was made to use benthic community data drawn from a habitat map of the Central Waitemata Harbour prepared by Haywood et al. (1999). However, the descriptions index therein (refer to Appendix 4) did not generally match well with animals contributing to the bioturbation.

Data from the Central Waitemata Harbour benthic-macrofaunal monitoring programme were also used. These data were collected at five sites, bi-monthly from October 2000, and were used to address the following questions:

- Are bioturbation indices for any given site likely to be constant over time or do they exhibit seasonal or multi-year cycles?

- Do changes in community structure affect bioturbation rates and depths?

4 Results

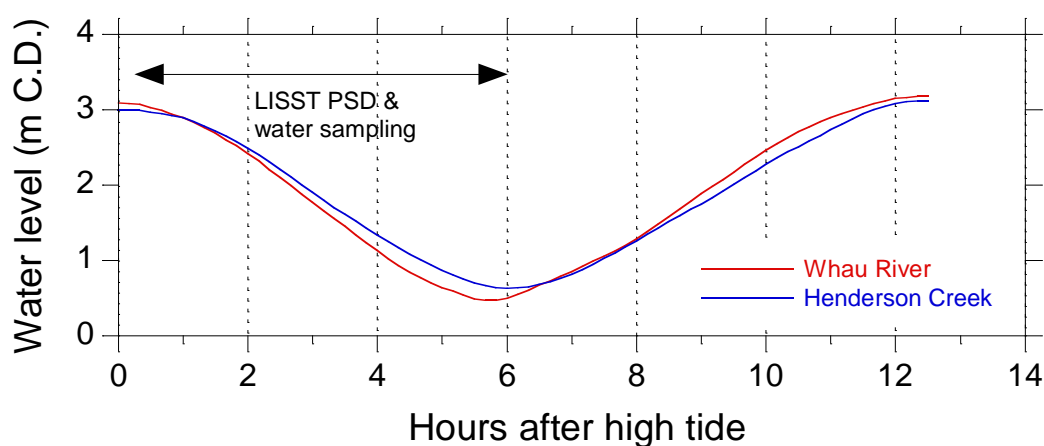
4.1 Suspended sediments

4.1.1 Particle size

Suspended sediment concentrations (SSCs) and particle size distributions (PSDs) were measured during an ebb tide at the mouth of the Whau River and Henderson Creek on 31 May and 1 June 2006, respectively. Figure 15 shows water levels during the measurement periods.

Figure 15

Water levels relative to chart datum recorded near the Whau River sampling site (31 May 2006) and near the Henderson Creek sampling site (1 June 2006).



SSC was lower and showed less variation ($7\text{--}14\text{ mg l}^{-1}$) in the Whau River compared to Henderson Creek ($11\text{--}25\text{ mg l}^{-1}$) (Figure 16a). Volatile (organic) suspended solids accounted for 5 per cent or less of the Whau River suspended sediment and 6–13 per cent of the Henderson Creek suspended sediment.

Particles in the Whau River were smaller than particles in Henderson Creek (Figures 16b and c). Median particle diameter was $5\text{--}15\text{ }\mu\text{m}$ for the Whau River and $7\text{--}20\text{ }\mu\text{m}$ for Henderson Creek. At both sites the largest particles were encountered at mid-ebb tide (ie, 3.5 hours after high tide), which coincided with maximum ebb-current speeds.

Figure 16

Characteristics of suspended sediments in water samples taken 1 m above the bed under low freshwater inflow. (a) Total suspended sediment concentration. Particle size statistics (mean, median and standard deviation): (b) Whau River, (c) Henderson Creek. Water levels (m above chart datum) are shown as dashed lines.

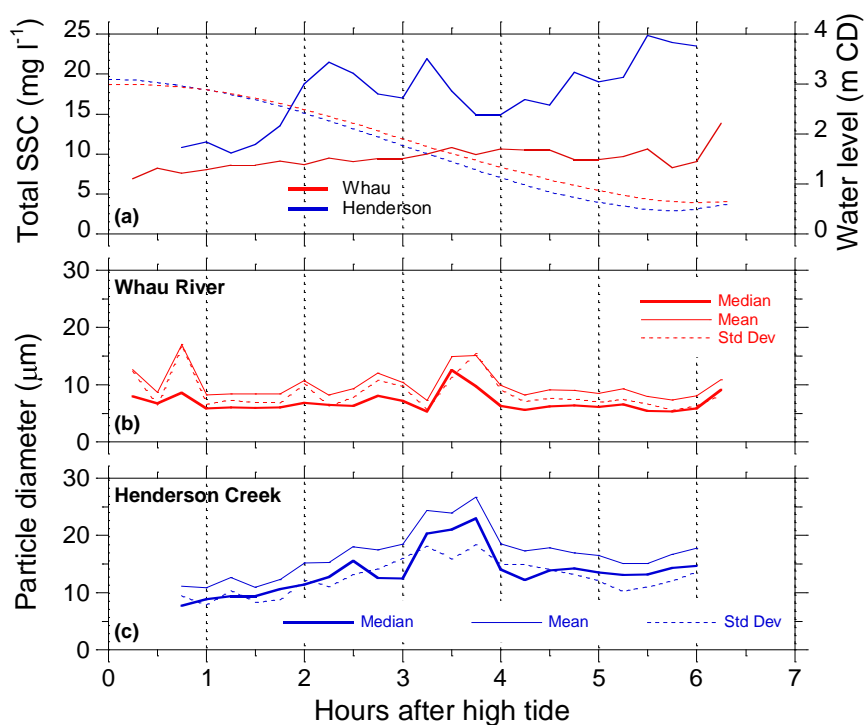


Figure 17 shows examples of PSDs for Henderson Creek suspended sediments, derived from the LISST data.

Table 2 summarises the PSDs measured with the LISST. The clay content of the Whau River suspension (5 per cent) was two-fold higher than in Henderson Creek. The silt fraction was similar at both sites. The percentage of particles in the very fine sand fraction was 30 per cent for the Whau River and 40 per cent for Henderson Creek.

Figure 17

Henderson Creek (1 June 2006) time-averaged particle size distributions (range 0–128 μm), where time averaging is over 5 minute intervals. Elapsed time after high tide: (a) 5–45 minutes, (b) 50–90 minutes, (c) 95–135 minutes, (d) 140–180 and (e) 180–225 minutes.

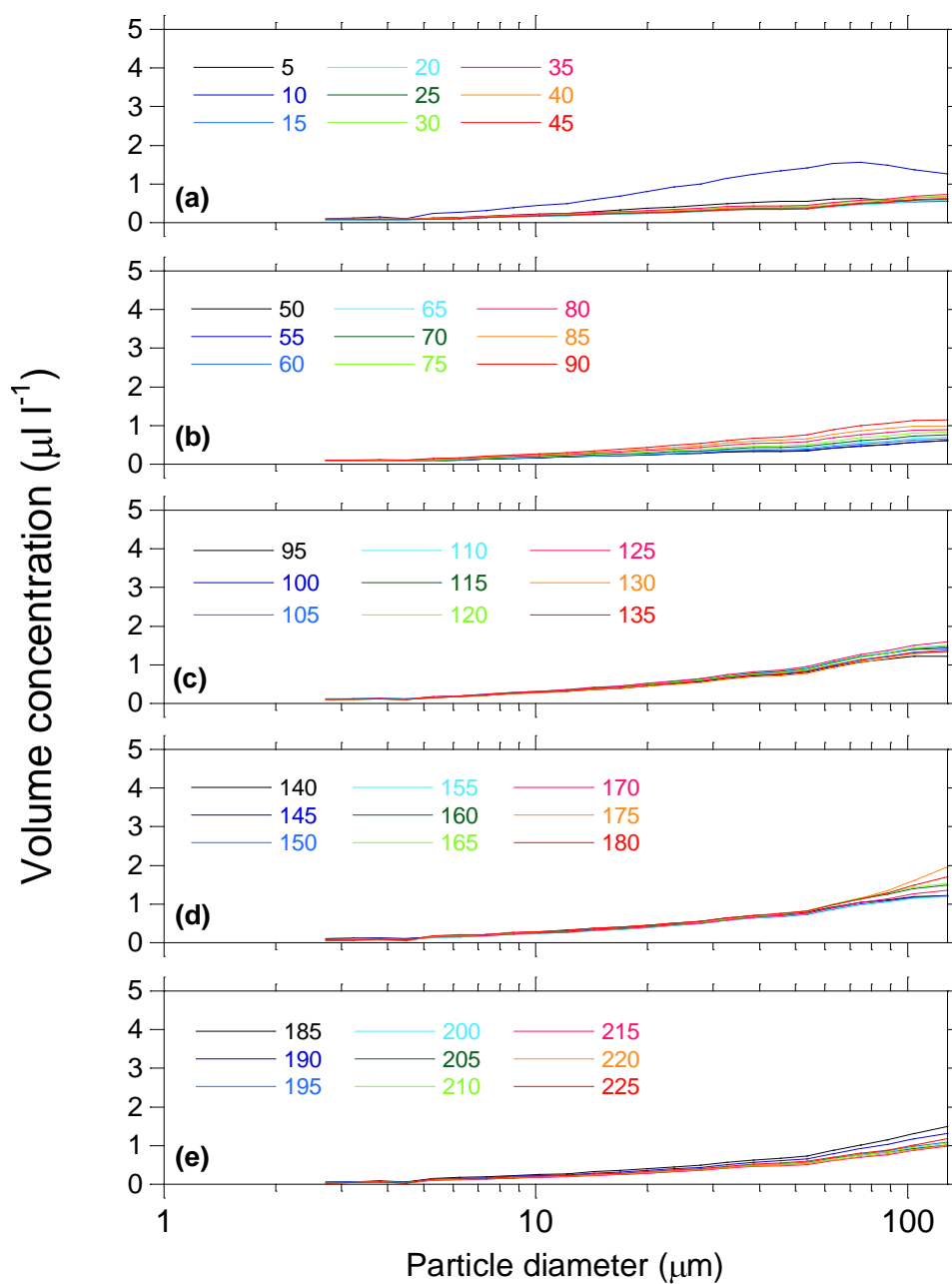


Table 2

Particle size distributions for the Whau River (W, $n = 10,042$) and Henderson Creek (H, $n = 10,088$). The distributions are expressed as the per cent of the total particle volume $\leq 128 \mu\text{m}$ in the following classes: clay ($\leq 3.8 \mu\text{m}$), very fine silt ($4.5\text{--}7.4 \mu\text{m}$), fine silt ($8.7\text{--}16.8 \mu\text{m}$), medium silt ($19.9\text{--}32.7 \mu\text{m}$), coarse silt ($38.5\text{--}63.3 \mu\text{m}$), very fine sand ($74.7\text{--}128 \mu\text{m}$). *sd* is the standard deviation.

	Clay		VF Silt		F Silt		M Silt		C Silt		VF Sand	
	W	H	W	H	W	H	W	H	W	H	W	H
Mean	5	2	7	5	16	12	18	16	23	24	30	40
Median	5	2	7	5	16	12	18	16	23	24	30	40
sd	0.9	1.2	0.8	0.9	2	2	2	3	2	3	5	8
Min.	0	0	4	0	7	1	7	1	0	3	0	2
Max.	10	6	17	14	69	45	37	36	31	33	67	92

Figures 18 and 19 show time series of cumulative particle volume. At the Whau River, variability reduces over the ebb tide and is highest for the ≤ 23.5 to $\leq 63.3 \mu\text{m}$ fractions. At Henderson Creek, variability increases during the ebb tide, and the volume in each fraction $\leq 104 \mu\text{m}$ reduces over time.

Figures 20 and 21 present time series of particle volume. At the Whau River, the $\leq 12 \mu\text{m}$ fraction and the $63\text{--}104 \mu\text{m}$ fraction each account for 20–25 per cent of the total particle volume. The $104\text{--}128 \mu\text{m}$ fraction accounts for less than 10 per cent of the total particle volume. The size composition of the suspension does not substantially change over the tide.

At Henderson Creek, the $63\text{--}104 \mu\text{m}$ fraction also accounts for a large proportion (20–40 per cent) of the total particle volume. The $104\text{--}128 \mu\text{m}$ fraction accounts for less than 10 per cent of the total particle volume. In contrast to the Whau, the Henderson data indicate an increase in the proportion of sand-sized particles as the ebb tide proceeds.

Figure 18

Whau River (31 May 2006) time series of cumulative particle volume as a percentage of total particle volume $\leq 128 \mu\text{m}$ in the following size classes: (a) $\leq 12 \mu\text{m}$; (b) $\leq 23.5 \mu\text{m}$; (c) $\leq 23.5 \mu\text{m}$; (d) $\leq 38.5 \mu\text{m}$; (e) $\leq 63.3 \mu\text{m}$; (f) (c) $\leq 104 \mu\text{m}$. Data are time-averaged at 1, 2, 5, 10 and 15 minute intervals.

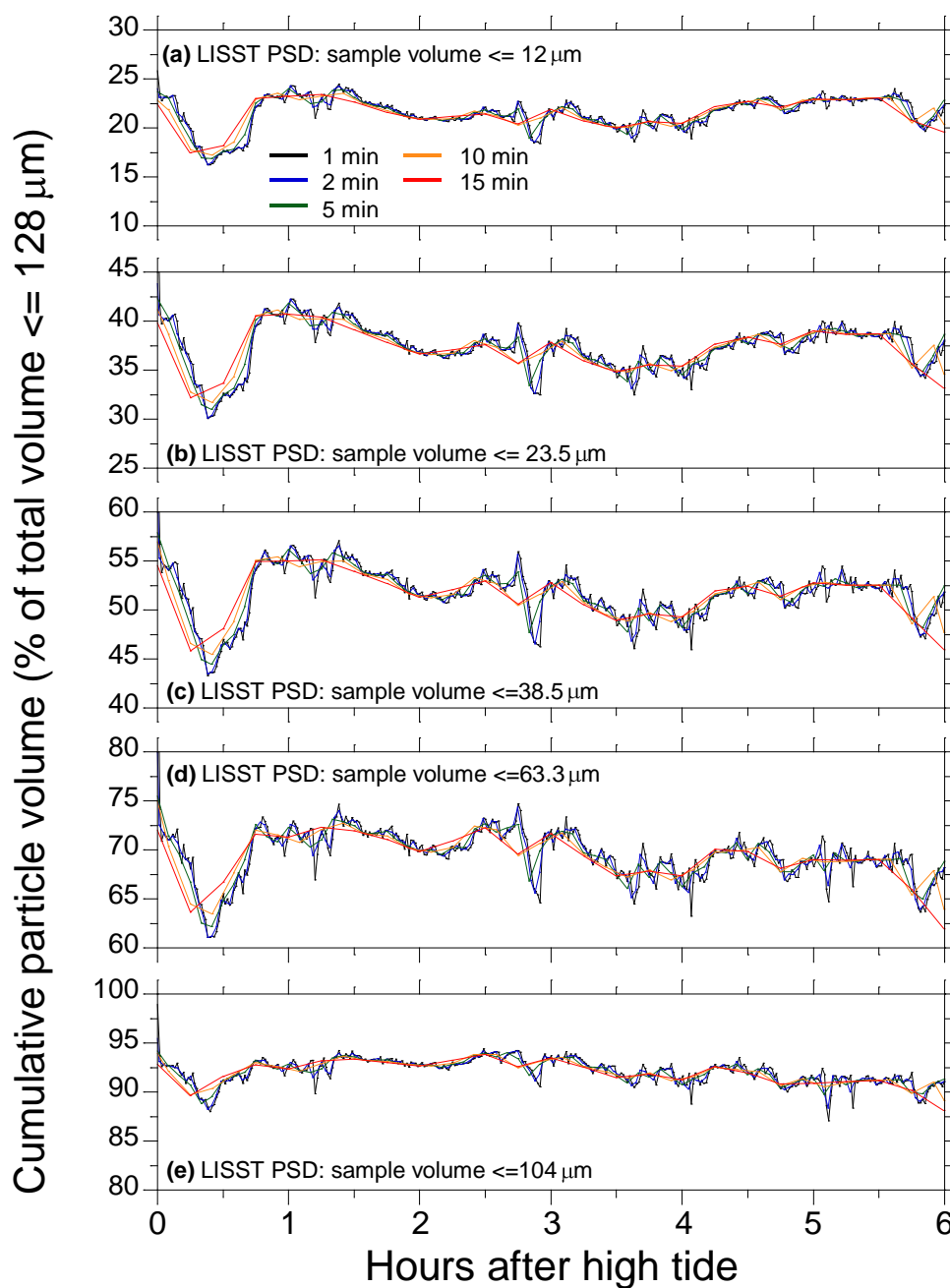


Figure 19

Henderson Creek (1 June 2006) time series of cumulative particle volume as a percentage of total particle volume $\leq 128 \mu\text{m}$ in the following size classes: (a) $\leq 12 \mu\text{m}$, (b) $\leq 23.5 \mu\text{m}$; (c) $\leq 23.5 \mu\text{m}$; (d) $\leq 38.5 \mu\text{m}$; (e) $\leq 63.3 \mu\text{m}$; (f) (c) $\leq 104 \mu\text{m}$. Data are time-averaged at 1, 2, 5, 10 and 15 minute intervals.

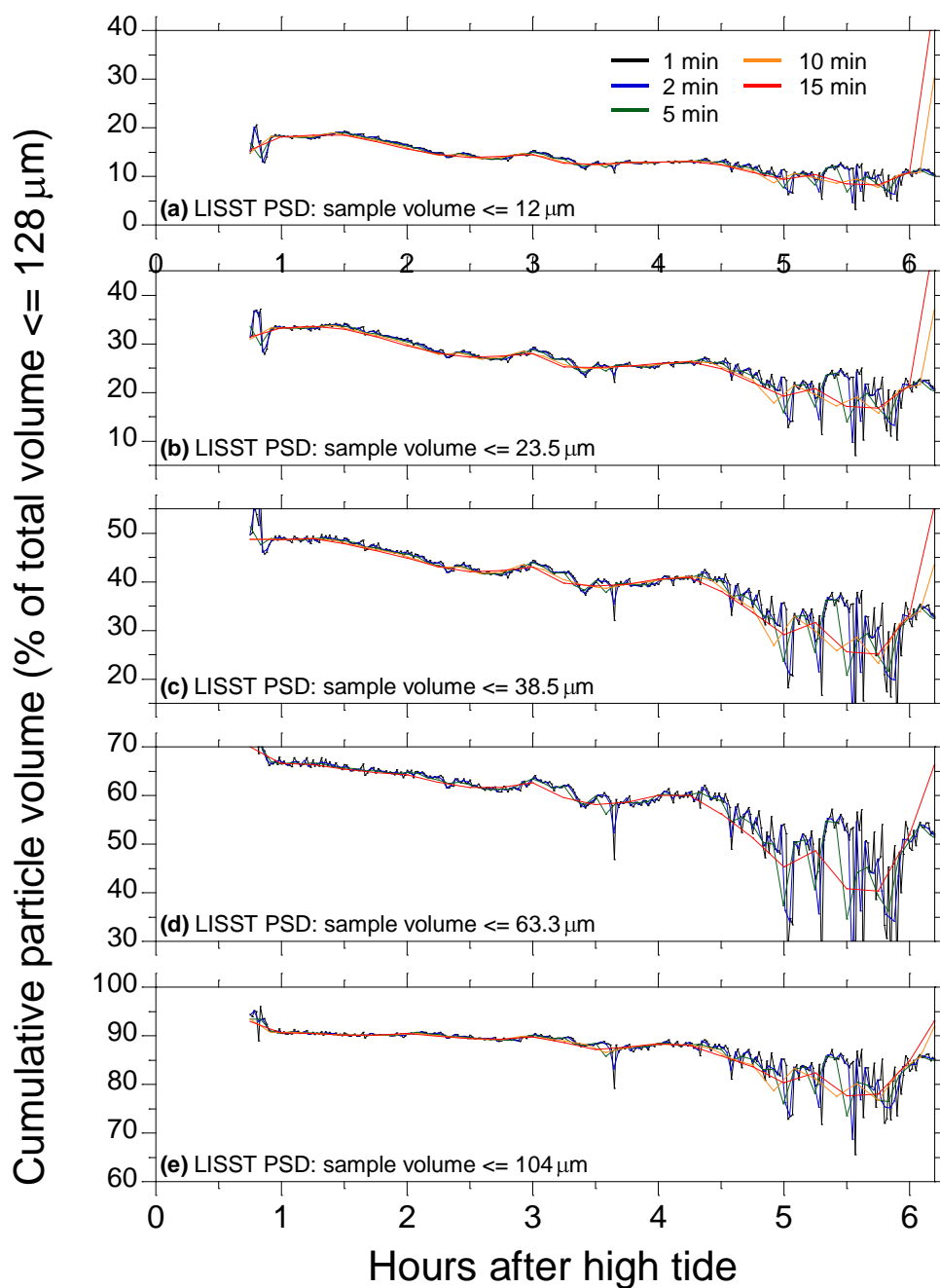


Figure 20

Whau River (31 May 2006) time series of particle volume as a percentage of total particle volume $\leq 128 \mu\text{m}$ for the following size fractions: $\leq 12 \mu\text{m}$, $12\text{--}23.5 \mu\text{m}$, $23.5\text{--}38.5 \mu\text{m}$, $38.5\text{--}63.3 \mu\text{m}$, $63.3\text{--}104 \mu\text{m}$ and $104\text{--}128 \mu\text{m}$. Time averaging at (a) 1 minute, (b) 2 minute, (c) 5 minute, (d) 10 minute and (e) 15 minute intervals.

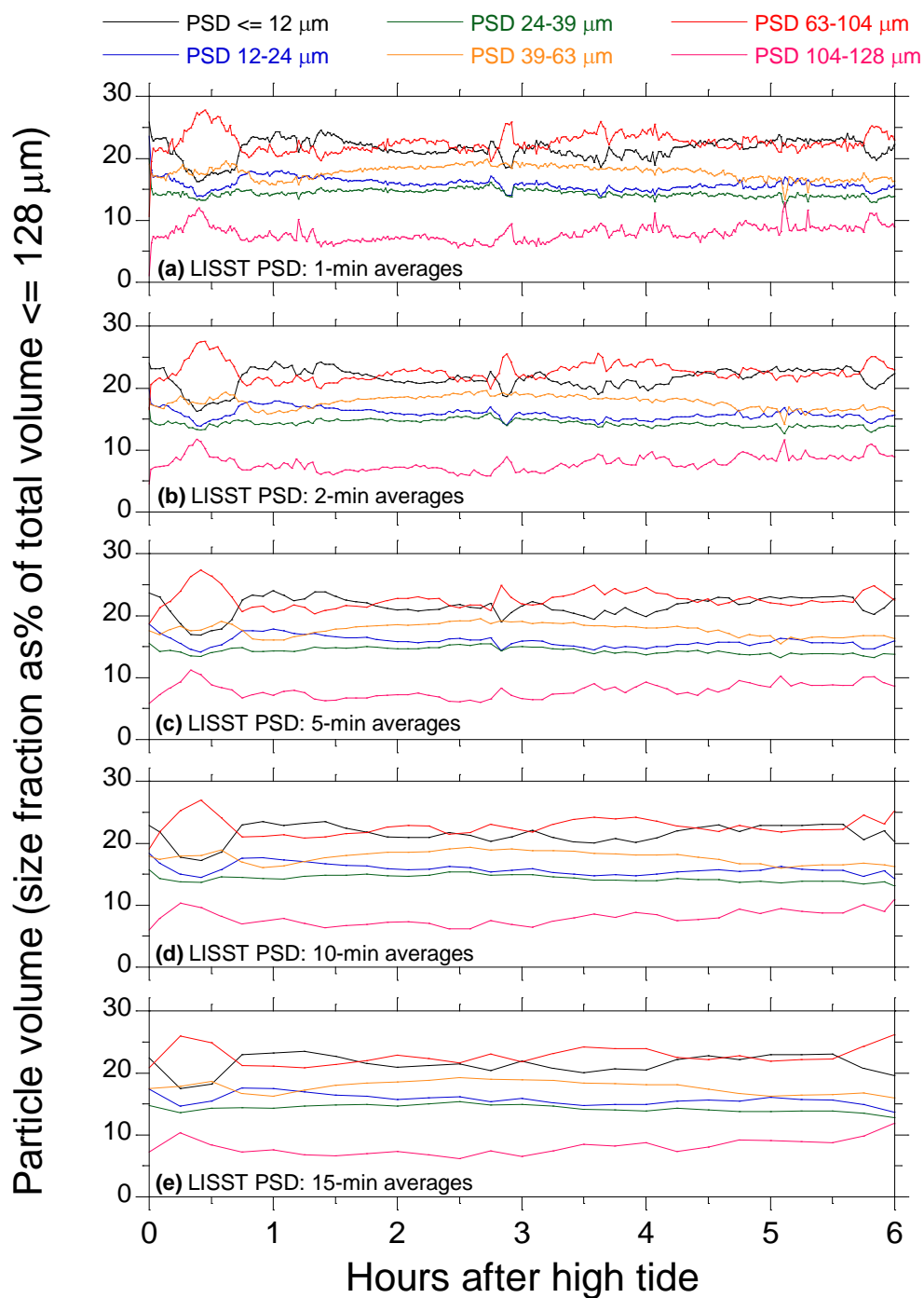
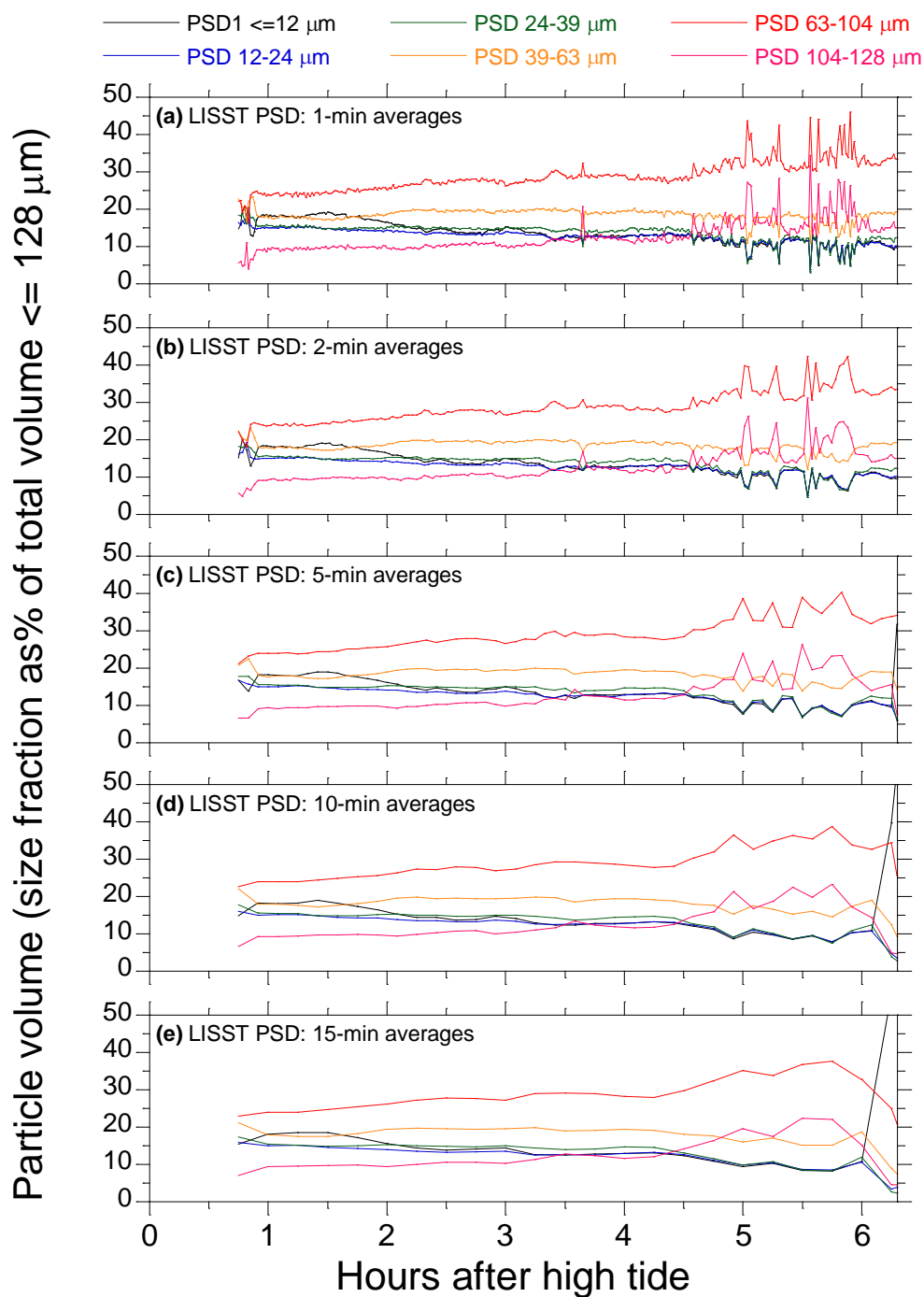


Figure 21

Henderson Creek (1 June 2006) time series of particle volume as a percentage of total particle volume $\leq 128 \mu\text{m}$ for the following size fractions: $\leq 12 \mu\text{m}$, $12\text{--}23.5 \mu\text{m}$, $23.5\text{--}38.5 \mu\text{m}$, $38.5\text{--}63.3 \mu\text{m}$, $63.3\text{--}104 \mu\text{m}$ and $104\text{--}128 \mu\text{m}$. Time averaging at (a) 1 minute, (b) 2 minute, (c) 5 minute, (d) 10 minute and (e) 15 minute intervals.

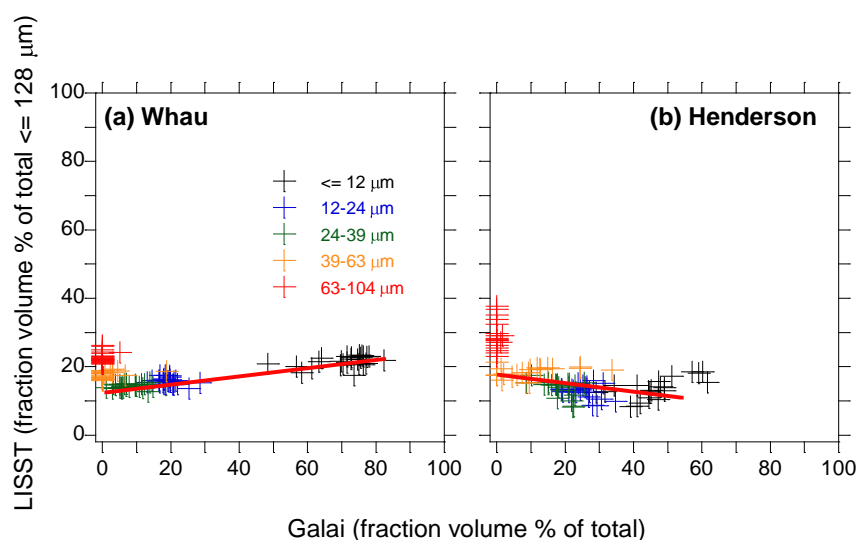


In Figure 22 the LISST data are compared with the Galai analysis of suspended particles captured in the water samples taken at 15 minute intervals. The Galai measurements were made in a laboratory on samples that had been largely

disaggregated using ultra-sound, whereas the LISST measured in situ particle sizes, which may also include particle aggregates or flocs composed of constituent particles. This is a key difference between the Galai and LISST measurements. The Galai data show that constituent particle diameters were less than 63 μm for most of the time.

Figure 22

PSD of disaggregated particles measured in the laboratory by the Galai versus PSD of suspended sediments measured in situ by the LISST: (a) Whau River; (b) Henderson Creek.



Galai data from the Whau River indicate that particles less than 24 μm account for 50–85 per cent of the total particle volume compared with 17–23 per cent from the LISST data. The 63–104 μm size fraction accounts for 21–26 per cent of the total particle volume derived from the LISST data, whereas this size fraction is absent from the Galai data.

Galai data from Henderson Creek indicate that the suspension is graded by particle size such that the volume contribution of each size fraction increases with decreasing particle size. By comparison, the LISST data indicate that volume contribution increases with increasing particle size.

There are several possible explanations for the absence of constituent particles greater than 63 μm diameter in the Galai data at both sites:

1. the Galai and LISST measure particle size using different methods and therefore produce different results;
2. the pumped samples, collected over ~30 seconds, did not adequately sample the less numerous large sand-sized particles that were detected by the LISST; and
3. particle aggregates were present in the suspension and measured by the LISST but were not detected by the Galai in the laboratory because the samples were disaggregated before analysis.

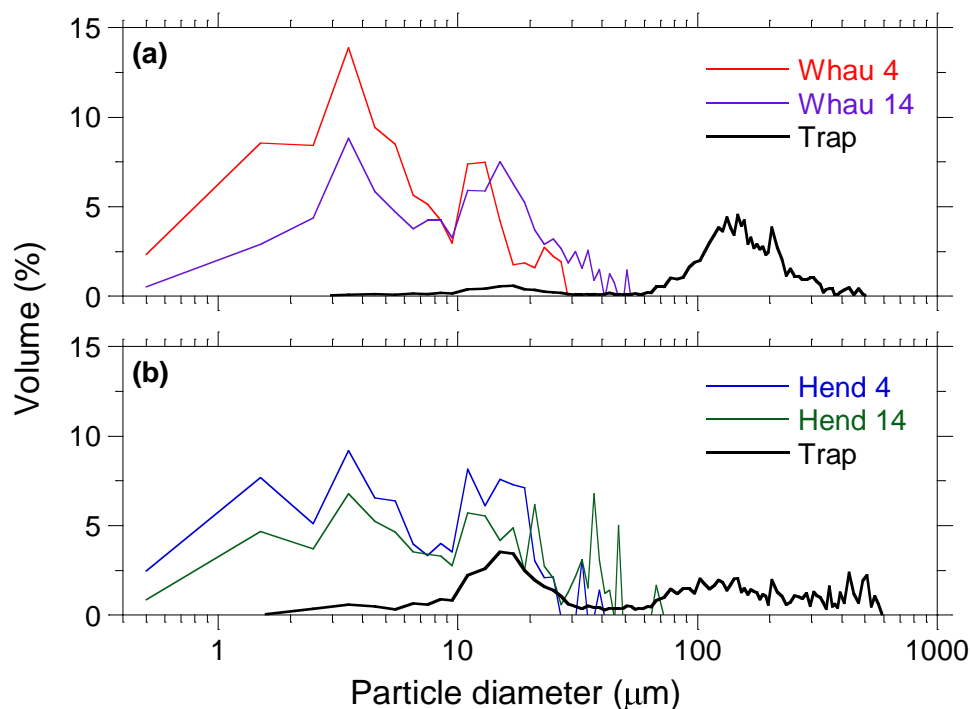
The first explanation is unlikely based on direct comparisons between the LISST and Galai using standards composed of glass spheres and natural sands.

The second explanation is a possibility. Figure 23 compares the PSD, measured by the Galai, of sediment trap samples and water samples collected one-hour after high tide and at peak-ebb tide. The trap was deployed on the LISST frame at both sites and sampled the suspension at 0.57 m above the bed for six hours during the ebb tide. The Henderson and Whau trap samples were composed of 70 per cent and 95 per cent sand ($> 63 \mu\text{m}$), respectively, but the pumped water samples contained no sand particles. (It is actually likely that the proportion of sand in the trap samples is higher than in the suspension, because of trap bias.)

The third explanation is the most feasible. It is likely that particle aggregates or flocs greater than $63 \mu\text{m}$ diameter and composed of smaller constituent particles were the main component of the sand-sized objects in the suspension, for the following reasons. Firstly, the fall speeds of sand-sized particles in water samples collected from the Whau and Henderson sites are an order of magnitude lower than for same-size quartz sand. This is consistent with the behaviour of flocs composed of smaller constituent particles. Secondly, conditions were suitable for flocculation. Flocs form due to the electrostatic attraction between cohesive clay, fine silt and physical binding with organic particles. Collision frequency is an important factor and this process is primarily controlled by differential settling rates, fluid shear and SSC. Salinity also influences flocculation and is largely complete when salinity is ≤ 3 parts per thousand (Dyer, 1986). Salinity measurements made by a sensor attached to the LISST during the fall speed measurements showed that salinities were greater than 20 parts per thousand at both sites.

Figure 23

PSDs for sediment trap and selected water samples, measured by the Galai. (a) Whau River, (b) Henderson Creek.



4.1.2 Fall speed

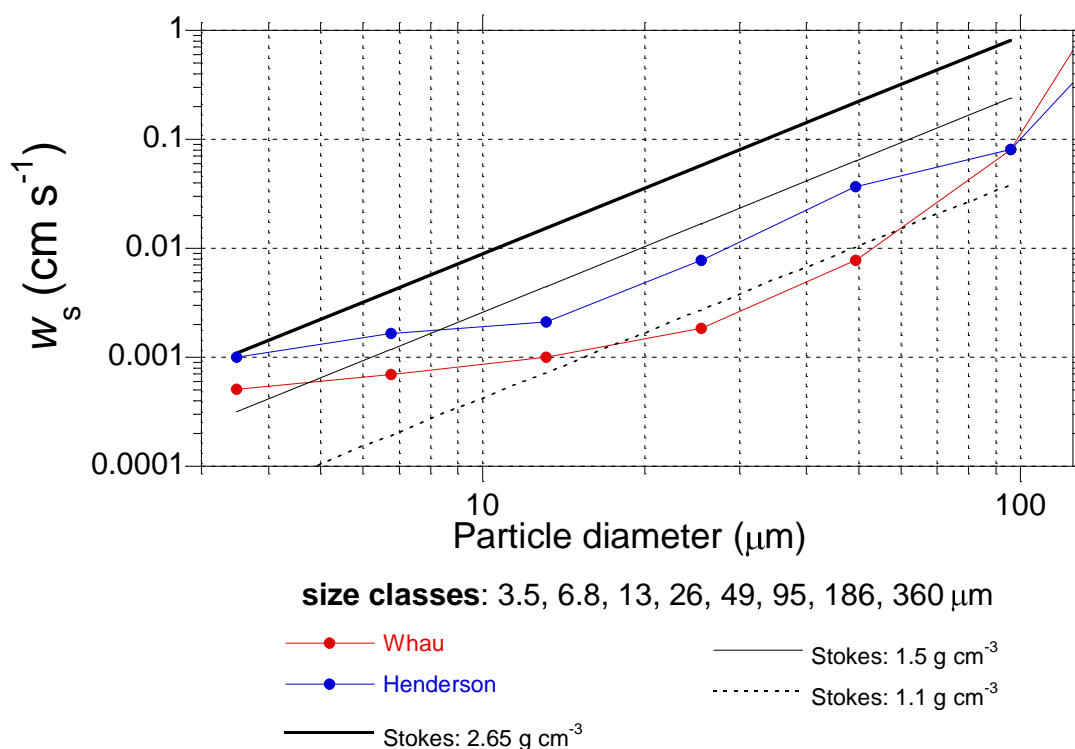
The results of the laboratory fall speed measurements are plotted in Figure 24, which shows the following:

- For particles/flocs less than 50 μm , fall speed of Henderson Creek suspended sediments is 2–5 times higher than fall speed of Whau River suspended sediments.
- For particle/flocs less than 100 μm , fall speeds measured in the laboratory experiments are consistent with the Stokes predictions for particle densities of 1–2.65 g cm^{-3} .
- The smallest measured particles/flocs (3.5 μm) had fall speeds most similar to Stokes predictions with particle density 2.56 g cm^{-3} . For larger particles/flocs, fall speeds are as much as 30 times lower than Stokes predictions with particle density 2.65 g cm^{-3} .
- For particles/flocs less than 13 μm , the rate of increase in fall speed with increase in particle size is less than predicted by Stokes.
- For particles/flocs greater than 13 and less than 95 μm , the rate of increase in fall speed with increase in particle size is similar to that predicted by Stokes Law.
- Fall speeds in this study that are lower than Stokes predictions are consistent with reduced floc densities due to fluid trapping between particles (eg, Hill et al. 1998; Khelifa and Hill 2006) rather than settling retardation due to shape effects on form drag. This is because shape effects are less pronounced at low Reynold numbers ($\text{Re} < 1$), and Reynolds numbers in the laboratory tank were less than 0.08 for particles/flocs $\leq 96 \mu\text{m}$ diameter.

The results of the laboratory fall speed experiments are summarised in Table 3.

Figure 24

Fall speed of suspended sediments sampled from the Whau River and Henderson Creek (9 and 10 November 2006). Fall speeds were measured using the LISST in a laboratory tank at 20 °C. Water temperatures at the field sites averaged 19.5 °C (range: 16.7–20.6 °C) at the Whau River and 19.4 °C (range: 17.6–20.6 °C) at Henderson Creek. Fall speeds predicted by the Stokes equation for solitary spherical particles $\leq 100 \mu\text{m}$ diameter and densities of 1.1, 1.5 and 2.65 g cm^{-3} . Predictions based on a water temperature of 20 °C, density of 1.024 g cm^{-3} and dynamic viscosity of $0.01 \text{ g cm}^{-1} \text{ s}^{-1}$.

**Table 3**

Falls speeds (cm s^{-1}) measured by the LISST in a laboratory tank and comparison with Stokes predictions for spheres with densities of 2.65, 1.5 and 1.1 g cm^{-3} .

Size (μm)	Whau	Henderson	Average	Stokes 2.65	Stokes 1.5	Stokes 1.1
3.5	5E-04	0.001	8E-04	0.001	3E-04	5E-05
6.8	7E-04	0.002	0.001	0.004	0.001	2E-04
13.1	0.001	0.002	0.002	0.015	0.015	7E-04
25.5	0.002	0.008	0.005	0.058	0.017	0.003
49.4	0.008	0.037	0.022	0.216	0.063	0.010
95.8	0.080	0.080	0.080	0.814	0.238	0.038
185.8	15.47	2.68	Data unreliable	Data unreliable	Data unreliable	Data unreliable-
360.3	15.47	2.21	Data unreliable	Data unreliable	Data unreliable-	Data unreliable-

4.2 Surface sediments

4.2.1 Particle size

The output from the geostatistical analysis of the surface sediment samples is a series of contour maps of particle size summary statistics. Data have been extrapolated beyond the sampling areas to the Henderson Creek mouth and near the Northwest Motorway along the southern shore of the CWH. These areas, therefore, may not be well represented in the maps. For example, surface sediments deposited in the mangroves at the northern tip of Te Atatu Peninsula are likely to be mud.

The contour maps of median and mean particle diameter (Figures 25 and 26) show that the finest sediments, composed of silts and very fine sand ($\leq 100 \mu\text{m}$), occur on intertidal and subtidal flats of the Whau embayment. The surface sediments of the CWH central basin are mainly composed of very fine sand, whereas sediments east of Te Tokaroa (Meola) Reef are composed of fine sand. Surface sediments in Shoal Bay are generally finer than in the CWH and are composed of mud at the head of bay.

Figure 27 maps the standard deviation of the particle diameter as a percentage of the mean particle diameter, which is a measure of the degree of particle sorting. The most well sorted sediments (standard deviation = 30–40) occur on the Whau and Te Atatu intertidal flats adjacent to the Whau channel. Sediments in the Whau embayment and central basin are better sorted than sediments elsewhere in the CWH. The most poorly sorted sediments occur near the Whau Creek outlet, on the upper intertidal flats and near the northern tip of Te Tokaroa (Meola) Reef. Poorly sorted sediments also occur near the tidal creek outlets at the northern end of Shoal Bay.

The mud content of surface sediments is typically less than 16 per cent by volume over most of the CWH and Shoal Bay (Figure 28). Sediments in the Whau embayment contain greater than 16 per cent mud ($\leq 62.5 \mu\text{m}$ size fraction), with mud content increasing towards the Whau River mouth (> 64 per cent mud). Upper Shoal Bay is also a mud sink. Te Atatu and Meola–Motions intertidal flats flanking the main channel have the lowest mud content, being less than 2 per cent. Sediments of the central basin contain 8–16 per cent mud.

Clay and fine silt ($\leq 25 \mu\text{m}$) is mapped in Figure 29 and medium–coarse silt ($25\text{--}63 \mu\text{m}$) is mapped in Figure 30. These finest fractions are concentrated in the Whau embayment and Shoal Bay. The Te Atatu and Meola–Motions intertidal flats have the lowest amounts of these fractions.

Figure 31 maps the distribution of very fine sand ($62.5\text{--}125 \mu\text{m}$). The mid–lower intertidal flats seaward of Pollen Island and flanking the main channel near Hobsonville at the outlet to the Upper Harbour and near Henderson Creek have the highest amounts of very fine sand in the CWH. In Shoal Bay, very fine sand is most abundant in the centre of the bay.

Figure 25

Median particle diameter (microns) of surface sediments in the Central Waitemata Harbour and Shoal Bay, December 2005 – March 2006.

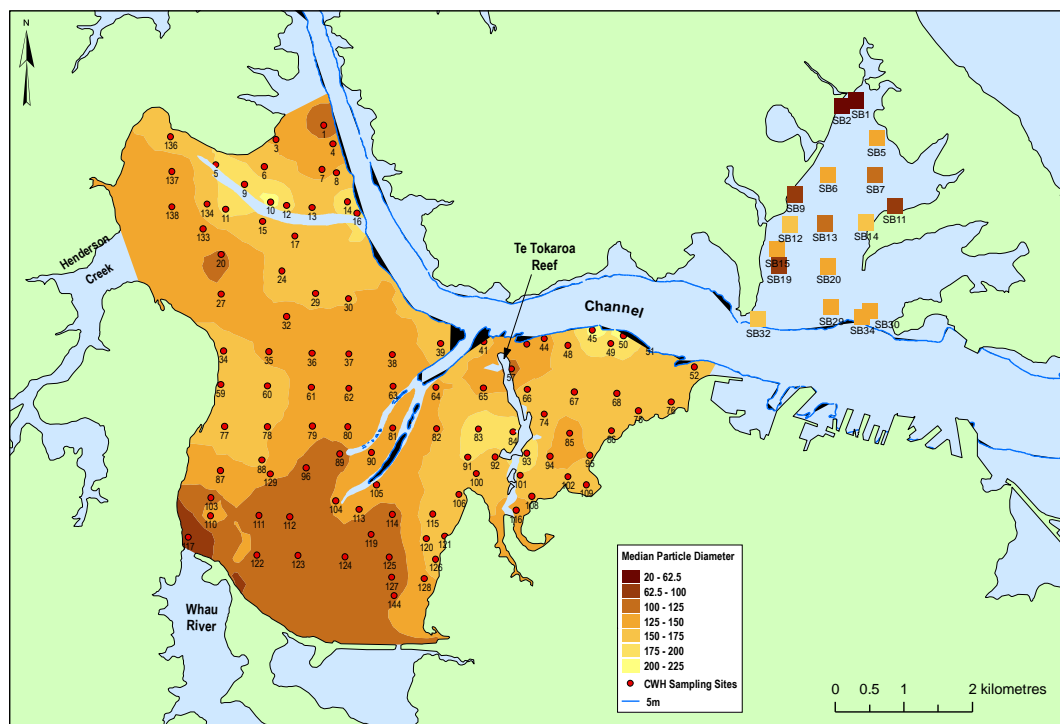


Figure 26

Mean particle diameter (microns) of surface sediments in the Central Waitemata Harbour and Shoal Bay, December 2005 – March 2006.

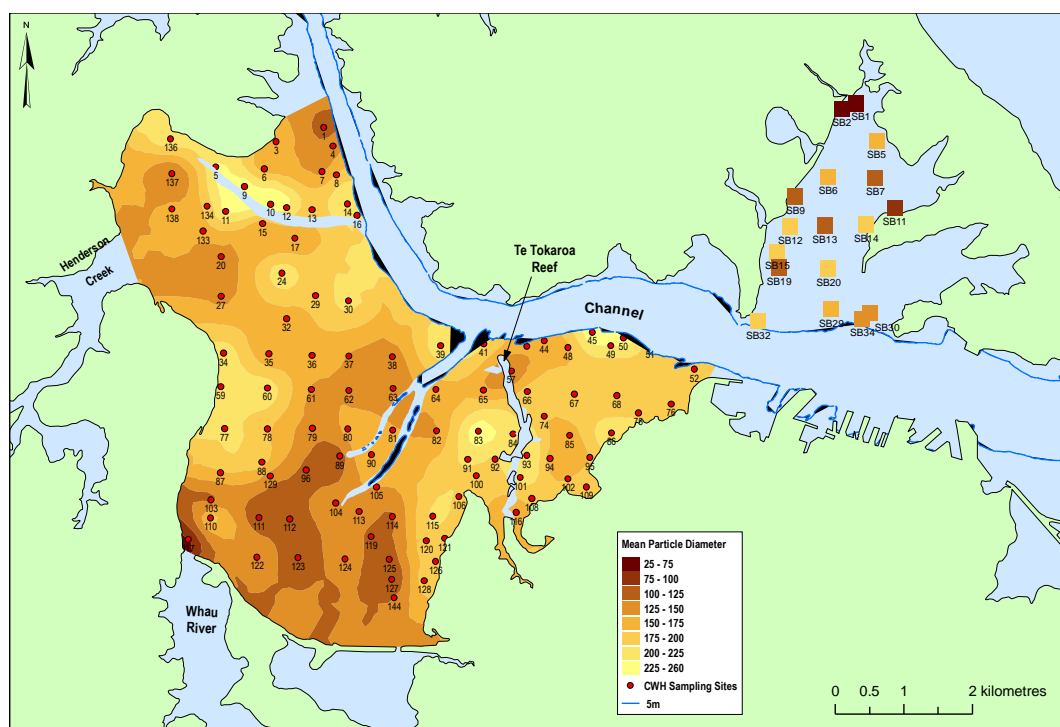


Figure 27

Standard deviation of particle diameter (as percentage of mean diameter) for surface sediments in the Central Waitemata Harbour and Shoal Bay, December 2005 – March 2006.

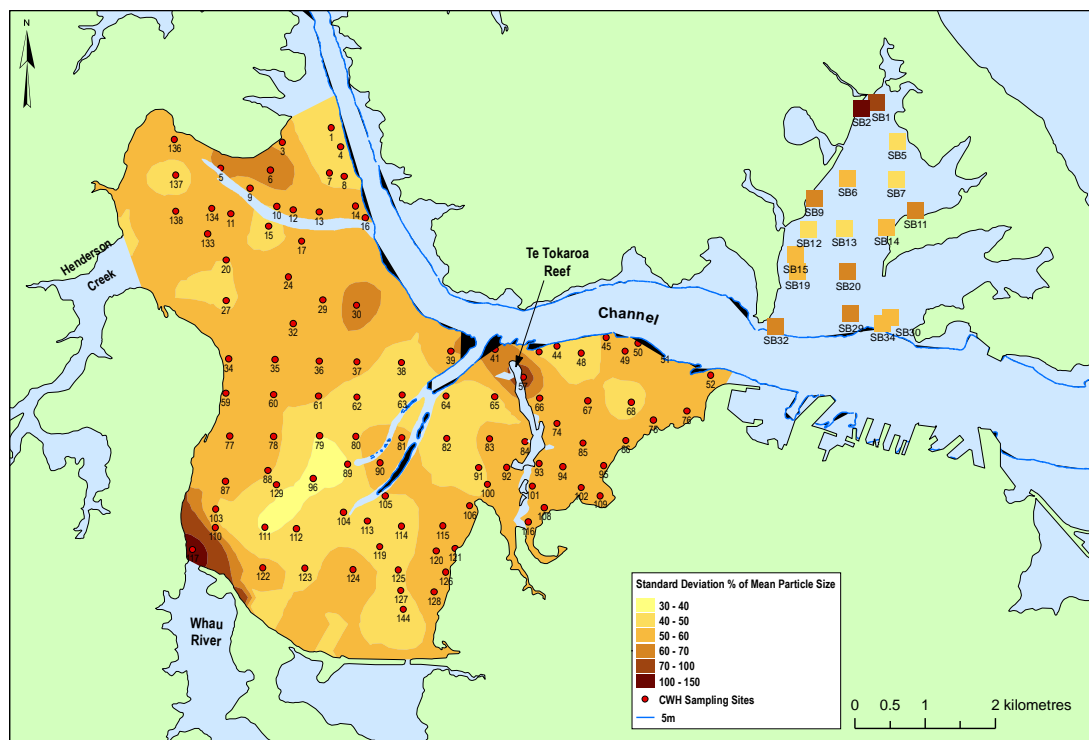


Figure 28

Mud content ($\leq 62.5 \mu\text{m}$ size fraction by percentage of volume) of surface sediments in the Central Waitemata Harbour and Shoal Bay, December 2005 – March 2006.

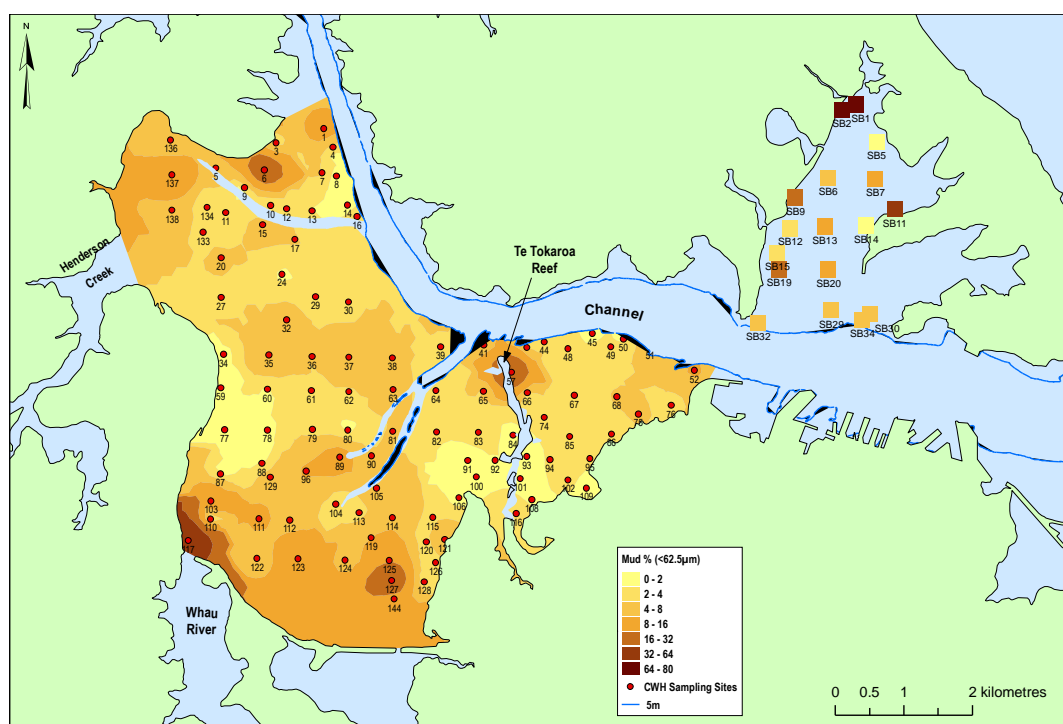


Figure 29

Clay and fine silt size fraction $\leq 25 \mu\text{m}$ (percentage of volume) of surface sediments in the Central Waitemata Harbour and Shoal Bay, December 2005 – March 2006.

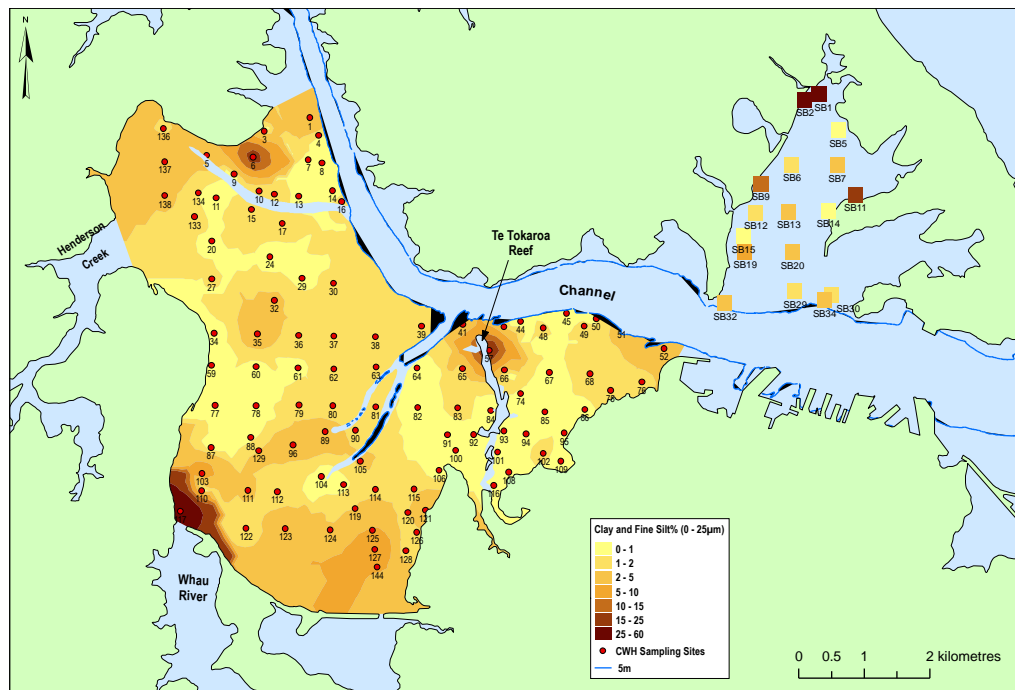


Figure 30

Medium-coarse silt size fraction $25-62.5 \mu\text{m}$ (percentage of volume) of surface sediments in the Central Waitemata Harbour and Shoal Bay, December 2005 – March 2006.

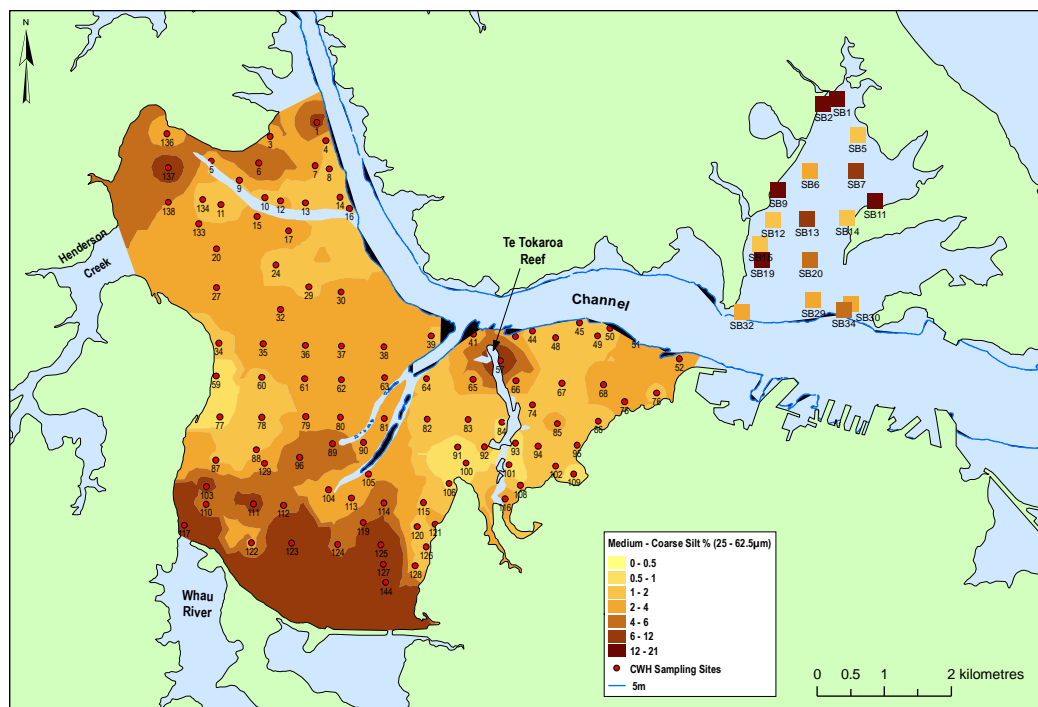
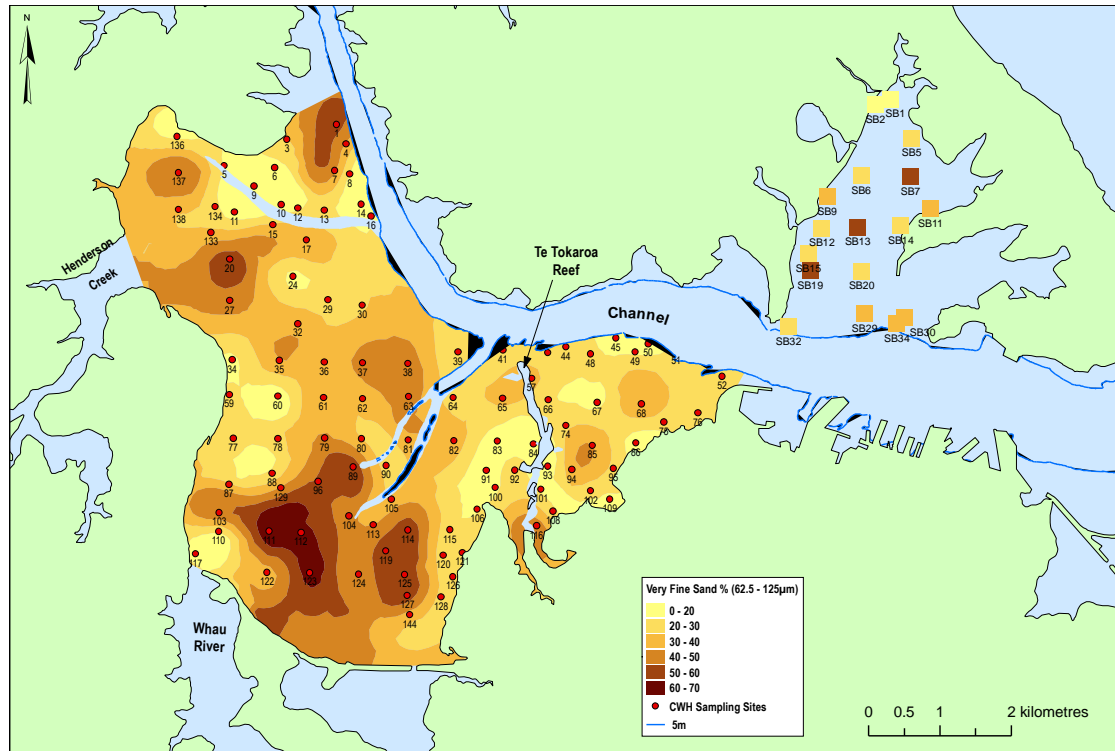


Figure 31

Very fine sand fraction 62.5–125 μm (percentage of volume) of surface sediments in the Central Waitemata Harbour and Shoal Bay, December 2005 – March 2006.



4.2.2 Sediment bulk density

The dry bulk density and water content of surface sediments in the CWH and Shoal Bay range between 0.7 to 2.6 g cm^{-3} (Figure 32) and 23 to 69 per cent by weight (Figure 33), respectively. Between-site differences primarily reflect the mud content of the sediments, with lowest dry bulk density and highest water contents occurring in muddy sediments near the Whau River mouth and in the upper reaches of Shoal Bay.

Figure 32

Dry bulk density (g cm^{-3}) of surface sediments in the CWH and Shoal Bay, December 2005 – March 2006.

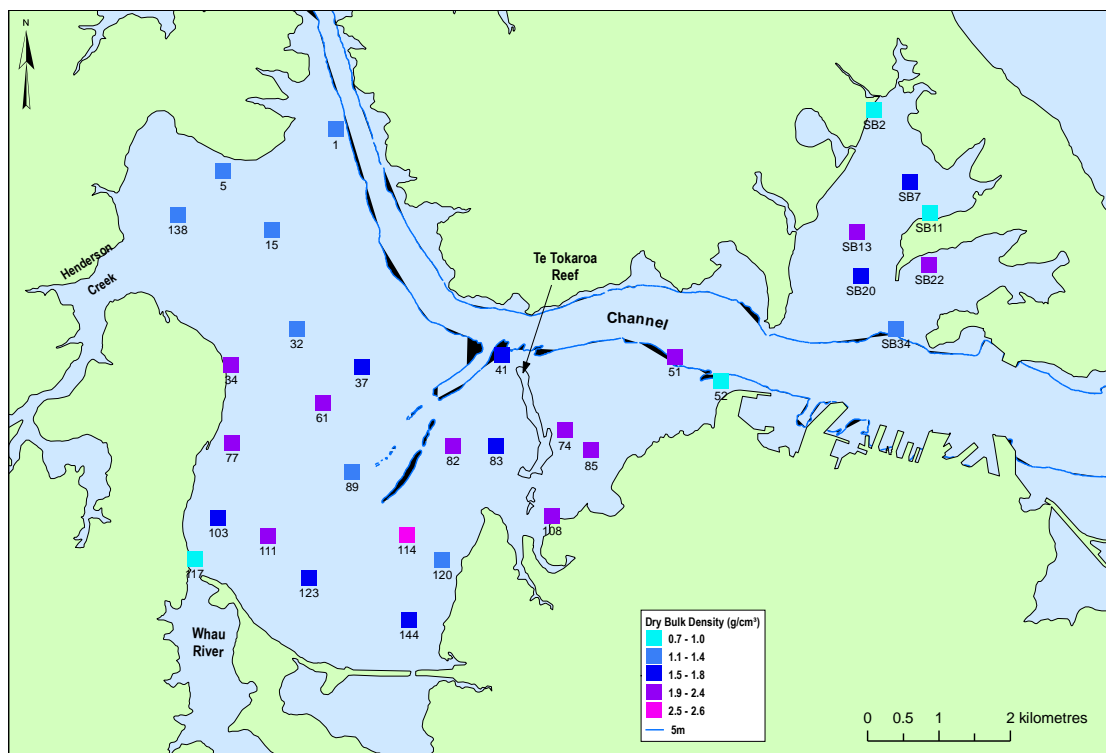
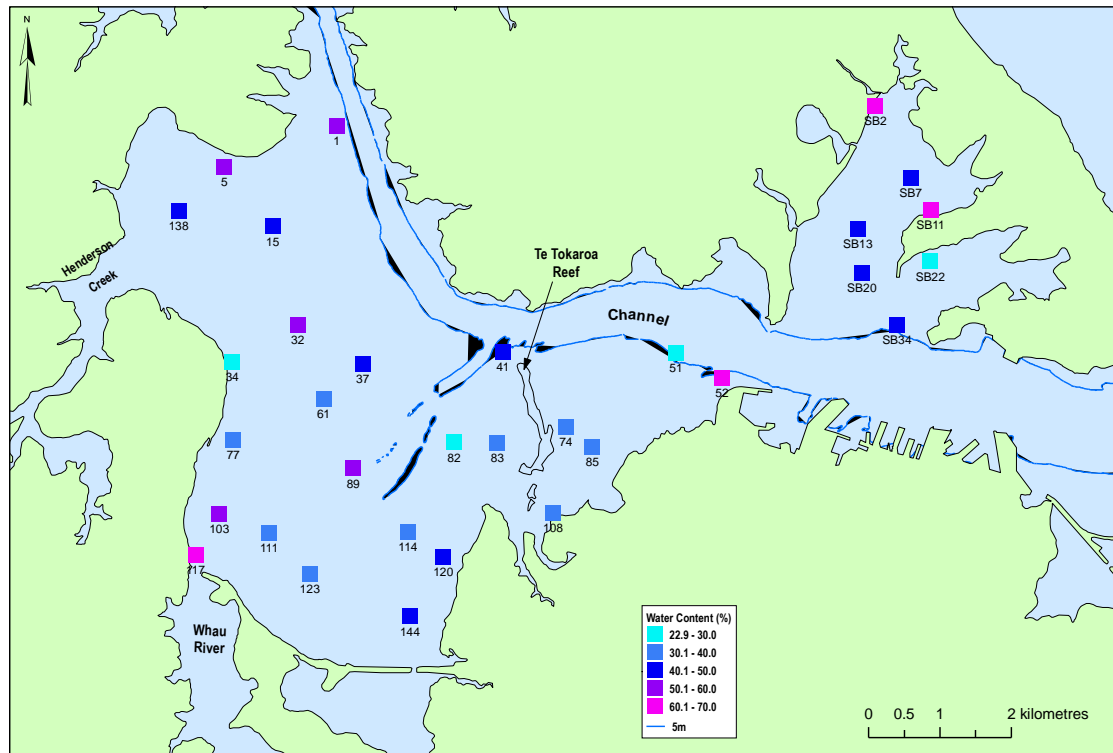


Figure 33

Water content (percentage of weight) of surface sediments in the CWH and Shoal Bay, December 2005 – March 2006.



4.3 Sub-surface sediments: sedimentation

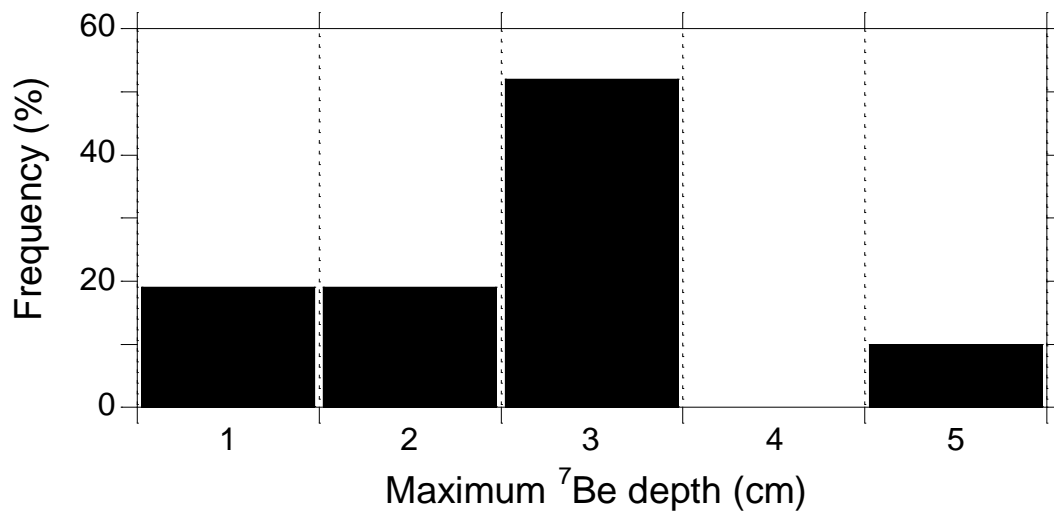
The radioisotope profiles provide information on sediment mixing and sediment accumulation rates (SAR).

4.3.1 ⁷Be Profiles

⁷Be data for the 21 sediment cores collected from the CWH and Shoal Bay showed that ⁷Be was present in the top 1–5 cm of the sediment column (Figure 34). Maximum ⁷Be penetration depths were 1–2 cm in 40 per cent of the cores, 3 cm in 50 per cent of the cores, and 5 cm in 10 per cent of the cores. (Note: the depth interval 3–4 cm was not sampled.) In the absence of sediment mixing, maximum ⁷Be penetration depth should be ≤ 1 mm given an SAR of less than 4 mm yr^{-1} . The presence of ⁷Be to 1–5 cm depth in the sediment column indicates that surface sediments are mixed over ≤ 100 days by physical and/or biological processes.

Figure 34

^7Be maximum penetration depths in 21 cores collected in the CWH and Shoal Bay. Note: the depth interval 3–4 cm was not sampled.

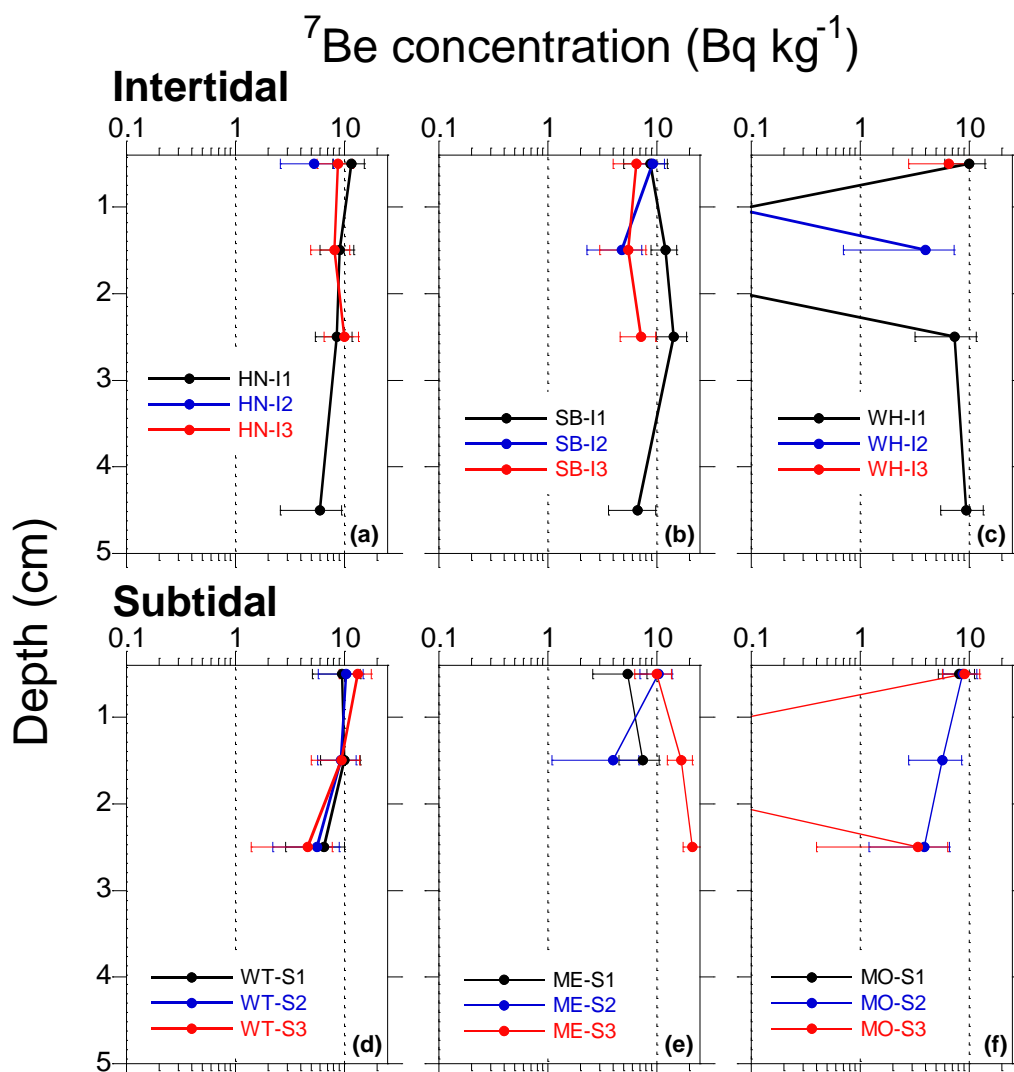


The ^7Be concentration profiles provide information about how vertical mixing in near-surface (≤ 5 cm) sediments varies with depth over timescales of less than ~ 100 days (Figure 35). The profiles are of two types: (1) well-mixed surface sediments, shown by homogenous ^7Be concentration (Figures 35a–b, d–e); and (2) complex profiles with intermittent ^7Be occurrence (Figures 35c and f). ^7Be concentrations at 0–1 cm depth average $\sim 10 \text{ Bq kg}^{-1}$ in most cores. Variations from this average may indicate accumulation of fine sediments in depositional environments (eg, core WT-S3) or winnowing in more energetic environments (eg, cores WH-I2 and HN-I2).

The three ^7Be profiles in the central basin of the CWH are very similar to each other (Figure 35d), which suggests homogeneous mixing conditions there.

Figure 35

^7Be concentration profiles in CWH and Shoal Bay intertidal (a–c) and subtidal (d–f) sediment cores. The 95 per cent confidence interval for ^7Be concentrations is also shown. Core sites: HN is Henderson Creek; SB is Shoal Bay; WH is Whau River; WT is central-harbour basin; ME is Meola; and MO is Motions. Refer to Figure 11 for core locations.



4.3.2 ^{210}Pb and ^{137}Cs profiles

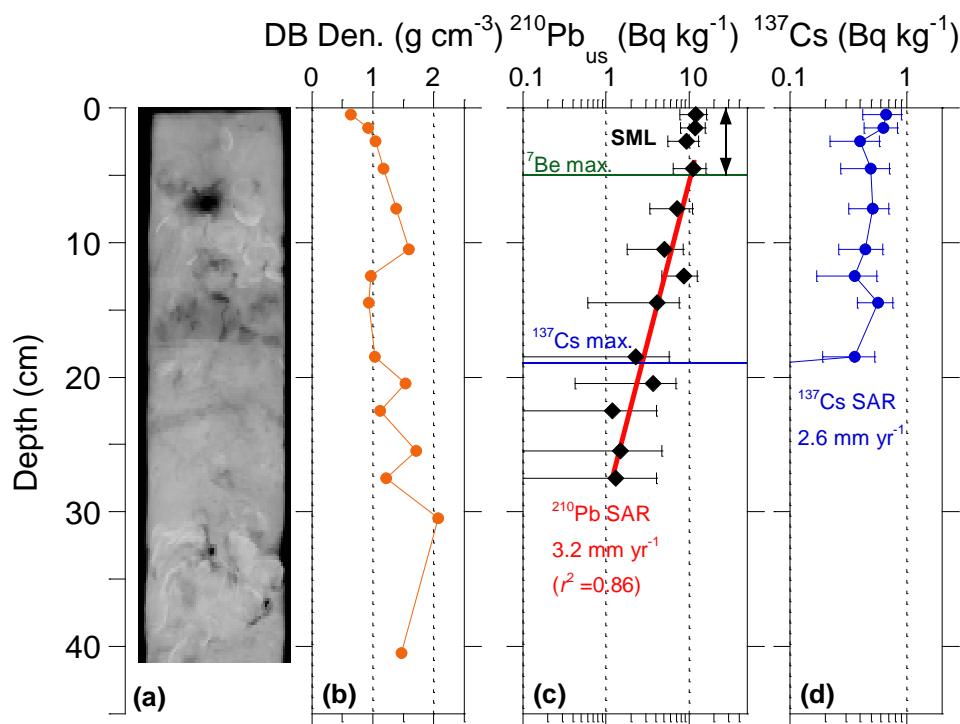
In this section we present interpretations of individual sediment cores based on x-radiographs, bulk density and radioisotope profiles from which time-averaged sediment accumulation rates (SAR) and mixing depths are derived. Unsupported ^{210}Pb concentration profiles provide the basis for estimating ^{210}Pb SAR (Appendix 3).

4.3.2.1 Henderson Creek (intertidal)

Core HN-I1, collected from intertidal flats at the outlet of Henderson Creek, is typical of intertidal sediments in the CWH, with poorly preserved bedding due to sediment mixing (Figure 36a).

Figure 36

Core HN-I1 (Henderson intertidal): (a) x-radiograph; (b) dry bulk sediment density; (c) unsupported ^{210}Pb concentration profile with 95 per cent confidence intervals, time-averaged sediment accumulation rate (SAR) and coefficient of determination (r^2) derived from fit to data (red line), maximum ^7Be depth and maximum ^{137}Cs depth; (d) ^{137}Cs concentration profile with 95 per cent confidence intervals and time-averaged SAR. **Note:** the ^{137}Cs SAR is calculated after subtraction of ^7Be mixing depth.



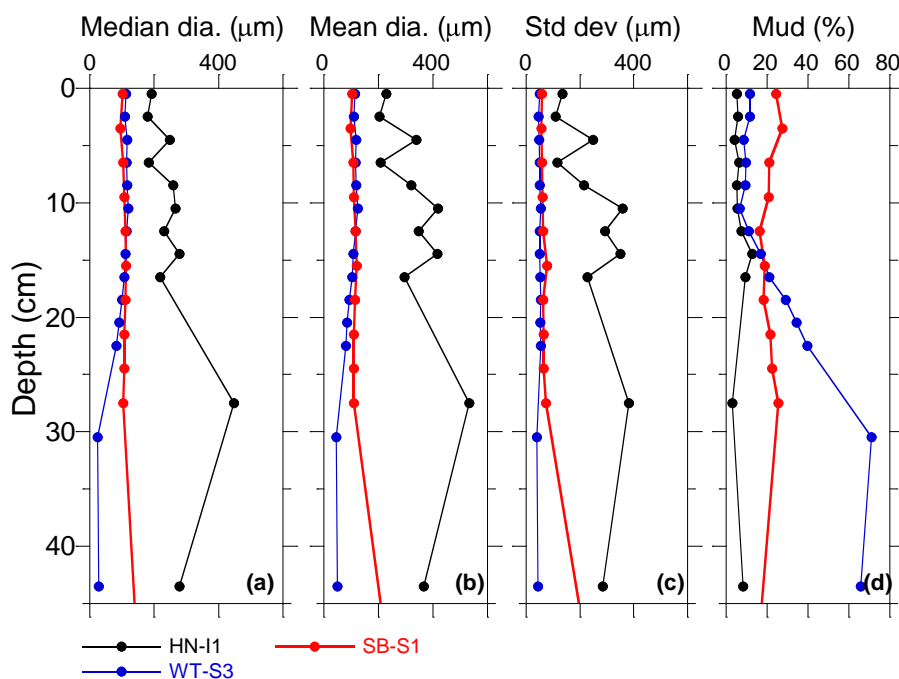
In this x-ray image high-density objects such as carbonate shells and sand appear white, and low-density and fine-grained muds appear in shades of grey. Very low-density organic material, such as peat or recent plant fragments, are almost black. The topmost 15 cm of the sediment column preserve neither sediment laminae nor animal burrows and traces. Disarticulated valves of *Nucula hartvigiana* are common in these sediments. This unit overlays a 5 cm thick wedge of lower density mud, which is also apparent in the vertical profile of sediment dry bulk density (DBD, Figure 36b). The Galai particle-size data for HN-I1 show substantial down-core variation in particle size and mud content (Figure 37). Below 20 cm depth, the core is characterised by muddy sand with some evidence of stratification. A layer of *Nucula* valves occurs below 30 cm depth.

The unsupported ^{210}Pb profile shows the effects of sediment mixing, with uniform ^{210}Pb concentrations (12 Bq kg^{-1}) in the top 5 cm of the profile. This surface mixed layer (SML) also coincides with the ^7Be maximum penetration depth (see Figure 36c). The ^{210}Pb SAR calculated for the accumulation zone below the SML is 3.2 mm yr^{-1} . Based on the rate of burial (from ^{210}Pb SAR) and ^7Be data, the maximum residence time of sediment in the SML is 16 years. The maximum ^{137}Cs penetration at 19 cm depth coincides with the top of the weakly stratified muddy-sand unit (Figure 36d). The ^{137}Cs SAR of 2.6 mm yr^{-1} is determined from the maximum penetration depth minus the depth of the ^7Be SML. This allows for the fact that ^{137}Cs is rapidly mixed within the

SML. In adopting this approach we make the assumption that the sediment mixing depth has been constant over time.

Figure 37

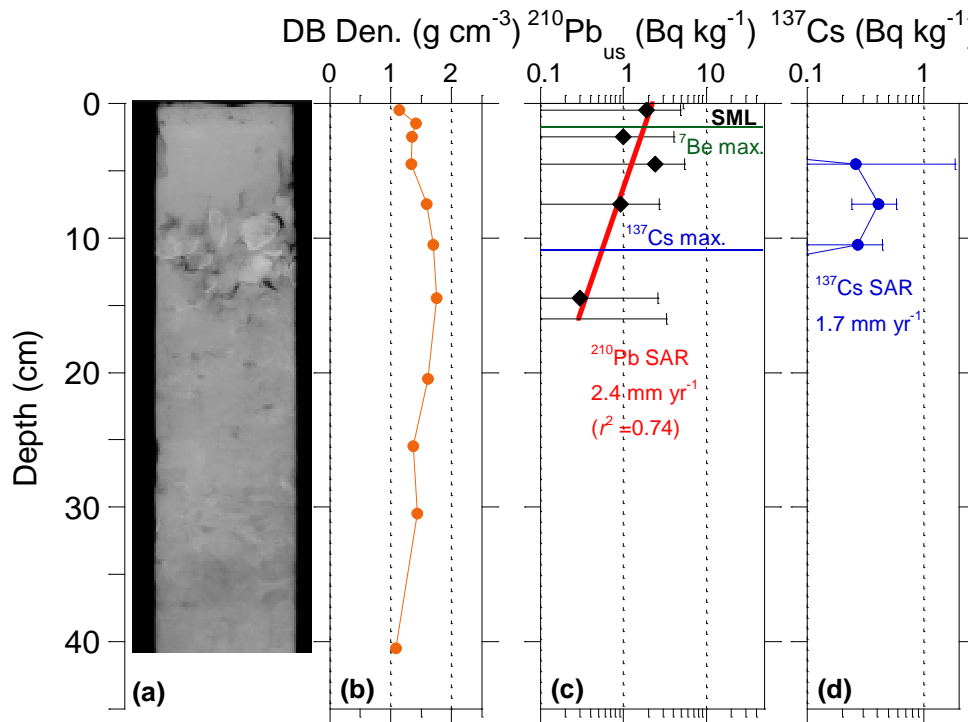
Galai particle-size statistics, cores HN-I1, WT-S3 and SB-S1: (a) median particle diameter; (b) mean particle diameter; (c) standard deviation particle diameter; (d) mud content.



Core HN-I2, collected from intertidal flats near the outlet of Henderson Creek, shows poorly preserved stratification of sediments. Homogeneous muddy sand occurs to 10 cm depth overlaying a 5 cm thick layer of disarticulated shell valves (Figure 38a). Sediments between 15 cm and 40 cm depth are composed of homogenous muddy sands, which is also indicated by the almost vertical DBD profile (Figure 4. 24b). ^{7}Be occurs to 2 cm depth (Figure 4. 34c). The ^{210}Pb concentration profile shows an exponential decay with depth from the surface and unsupported ^{210}Pb does not occur below 15 cm depth. The ^{210}Pb SAR is 2.4 mm yr^{-1} . Based on the rate of burial (ie, ^{210}Pb SAR) and ^{7}Be data, the maximum residence time of sediment in the SML is eight years. The ^{137}Cs concentration profile is atypical in that ^{137}Cs is below minimum detectable concentration in the top 5 cm of the sediment column. The ^{137}Cs SAR is 1.7 mm yr^{-1} .

Figure 38

Core HN-I2 (Henderson intertidal): (a) x-radiograph; (b) dry bulk sediment density; (c) unsupported ^{210}Pb concentration profile with 95 per cent confidence intervals, time-averaged sediment accumulation rate (SAR) and coefficient of determination (r^2) derived from fit to data (red line), maximum ^7Be depth and maximum ^{137}Cs depth; (d) ^{137}Cs concentration profile with 95 per cent confidence intervals and time-averaged SAR. **Note:** the ^{137}Cs SAR is calculated after subtraction of ^7Be mixing depth.



4.3.2.2 Te Atatu (intertidal)

Core TA-I1 was collected from the upper intertidal flats flanking the eastern shore of the Te Atatu Peninsula. The x-radiograph records an abrupt change from mud to sand at 16 cm depth (Figure 39a). The overlying muddy-sand unit is weakly stratified and contains occasional shell valves. There are few animal traces, such as infilled burrows, although this does not preclude sediment mixing by larger animals. The underlying mud unit contains evidence of animal burrows and traces. These sand and mud units are clearly identified by the sediment DBD profile (Figure 39b).

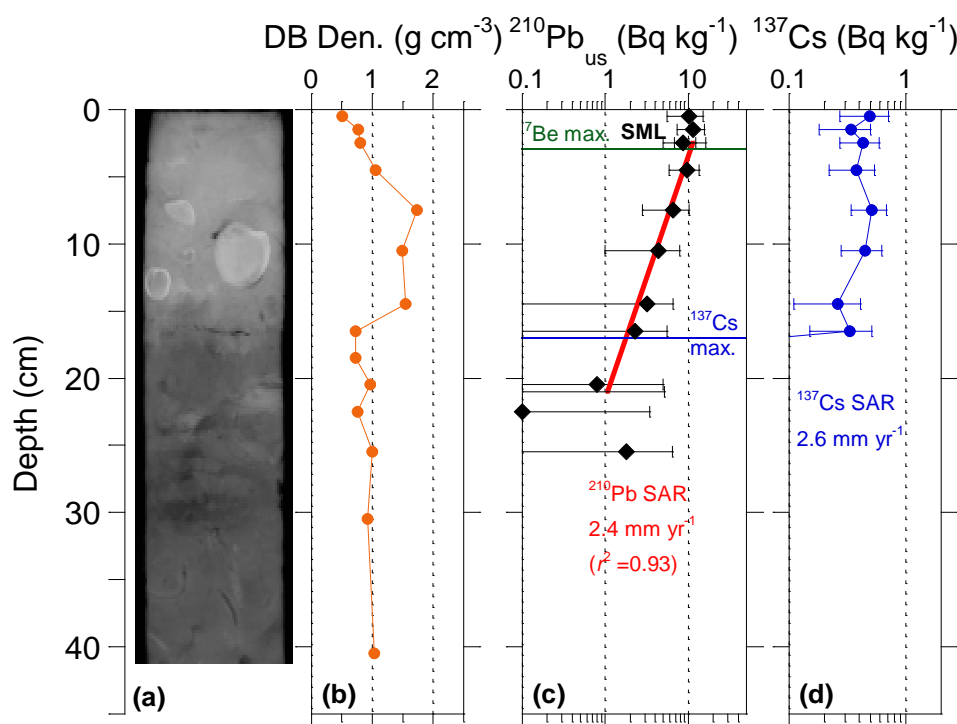
^7Be occurs to 3 cm depth (Figure 4. 25c). The ^{210}Pb concentration profile extends into the mud unit to 26 cm depth, with a calculated ^{210}Pb SAR of 2.4 mm yr^{-1} , which is similar to the ^{137}Cs SAR of 2.3 mm yr^{-1} . Based on the rate of burial and ^7Be data, the maximum residence time of sediment in the SML is 12 years.

Core TA-I2 was collected about 1 km south of TA-I2 on the upper intertidal flats flanking the Te Atatu Peninsula. The x-radiograph shows homogeneous muddy-sand occupying the top 30 cm of the sediment column. This unit overlays an old "peat" layer, with clear evidence of a large burrow infilled with sediment from the unit above. There are few traces of animal burrows in the overlying sand unit (Figure 40a). The

sediment DBD profile shows a linear increase to 1.6 g cm^{-3} at 10 cm depth (Figure 40b).

Figure 39

Core TA-I1 (Te Atatu Intertidal): (a) x-radiograph; (b) dry bulk sediment density; (c) unsupported ^{210}Pb concentration profile with 95 per cent confidence intervals, time-averaged sediment accumulation rate (SAR) and coefficient of determination (r^2) derived from fit to data (red line), maximum ^7Be depth and maximum ^{137}Cs depth; (d) ^{137}Cs concentration profile with 95 per cent confidence intervals and time-averaged SAR. **Note:** the ^{137}Cs SAR is calculated after subtraction of ^7Be mixing depth.

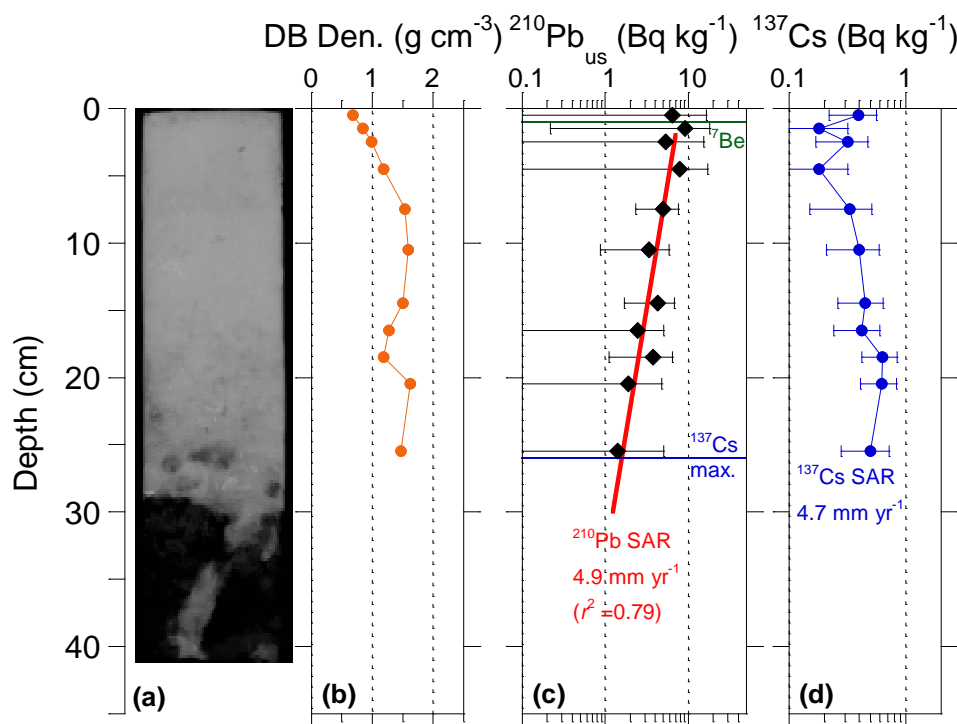


^7Be occurs to 2 cm depth (Figure 40c). The ^{210}Pb and ^{137}Cs concentration profiles extend to the sand–peat interface at ~30 cm depth, with calculated ^{210}Pb SAR and ^{137}Cs SAR of 4.9 mm yr^{-1} (Figure 40c). Based on the rate of burial and ^7Be data, the maximum residence time of sediment in the SML is six years.

The peat material from the base of core TA-I2 was submitted to Waikato University Radiocarbon Dating Laboratory (WURDL) for ^{14}C dating. The sample was initially washed in sodium hydroxide to remove humic acid, which is considered a contaminant given its potential post-depositional mobility (Dr Fiona Petchy, WURDL, pers. comm., Feb. 2007). The sample was found to consist mainly of humic acid and was not dated. Humic acid and other humic substances are major constituents of soil organic matter produced by the microbial degradation of lipids, proteins, carbohydrates and lignin. Thus, the peat is likely to have formed in a terrestrial or marsh environment that may not have existed for several thousand years. Sedimentation on this peat layer in the last ~50 years therefore represents either initial burial or one of a series of sedimentation and erosion cycles over a much longer period (Fig 4.26).

Figure 40

Core TA-I2 (Te Atatu intertidal): (a) x-radiograph; (b) dry bulk sediment density; (c) unsupported ^{210}Pb concentration profile with 95 per cent confidence intervals, time-averaged sediment accumulation rate (SAR) and coefficient of determination (r^2) derived from fit to data (red line), maximum ^7Be depth and maximum ^{137}Cs depth; (d) ^{137}Cs concentration profile with 95 per cent confidence intervals and time-averaged SAR. **Note:** the ^{137}Cs SAR is calculated after subtraction of ^7Be mixing depth.

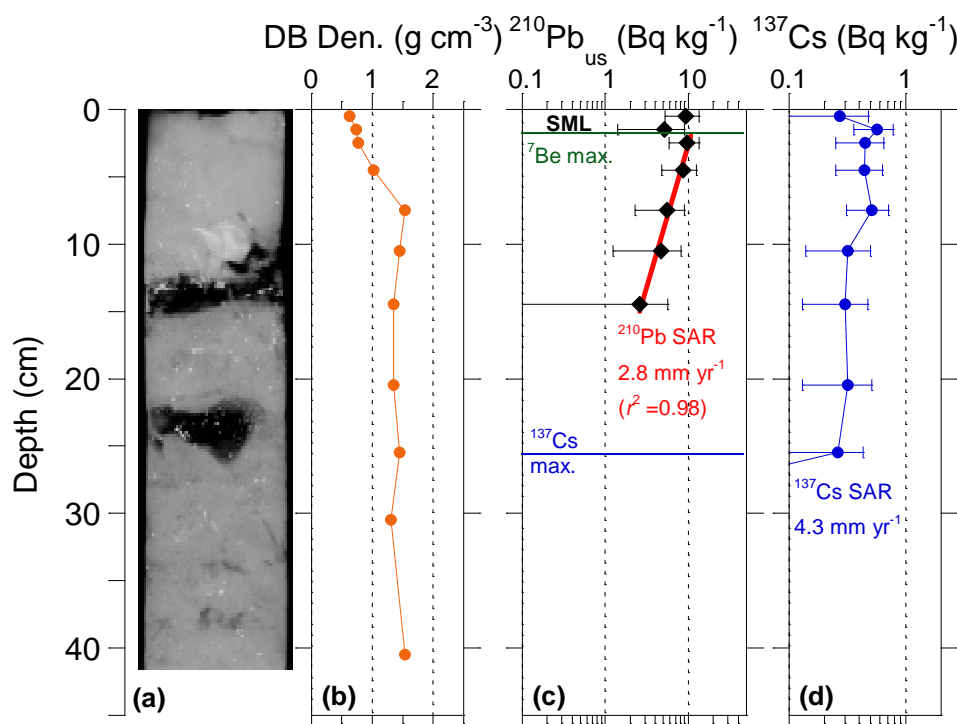


4.3.2.3 Waitemata Central Basin (subtidal)

Core WT-S1 was collected from the central basin of the CWH at one of three sites here (see Figure 11). The WT-series sites were originally sampled in January 2002 as part of a regional study of estuary sedimentation commissioned for the ARC (Swales et al. 2002a). The 2006 cores were collected within 16–34 m of the 2002 sites. The x-radiograph for WT-S1 indicates a muddy-sand substrate with large inclusions of wood at depths of 15 and 25 cm (Figure 41a). There are traces of mm-scale burrows infilled with mud at various depths in the core. The x-radiograph also clearly shows numerous high-density granules of unknown composition. Sediment DBD increases linearly from 0.5 to 1.5 g cm^{-3} within the top 8 cm of the core and is relatively uniform below this depth (Figure 4. 27b). The ^7Be and ^{210}Pb profiles indicate an SML of 3 cm (Figure 4. 27c).

Figure 41

Core WT-S1 (Waitemata Subtidal): (a) x-radiograph; (b) dry bulk sediment density; (c) unsupported ^{210}Pb concentration profile with 95 per cent confidence intervals, time-averaged sediment accumulation rate (SAR) and coefficient of determination (r^2) derived from fit to data (red line), maximum ^7Be depth and maximum ^{137}Cs depth; (d) ^{137}Cs concentration profile with 95 per cent confidence intervals and time-averaged SAR. **Note:** the ^{137}Cs SAR is calculated after subtraction of ^7Be mixing depth.

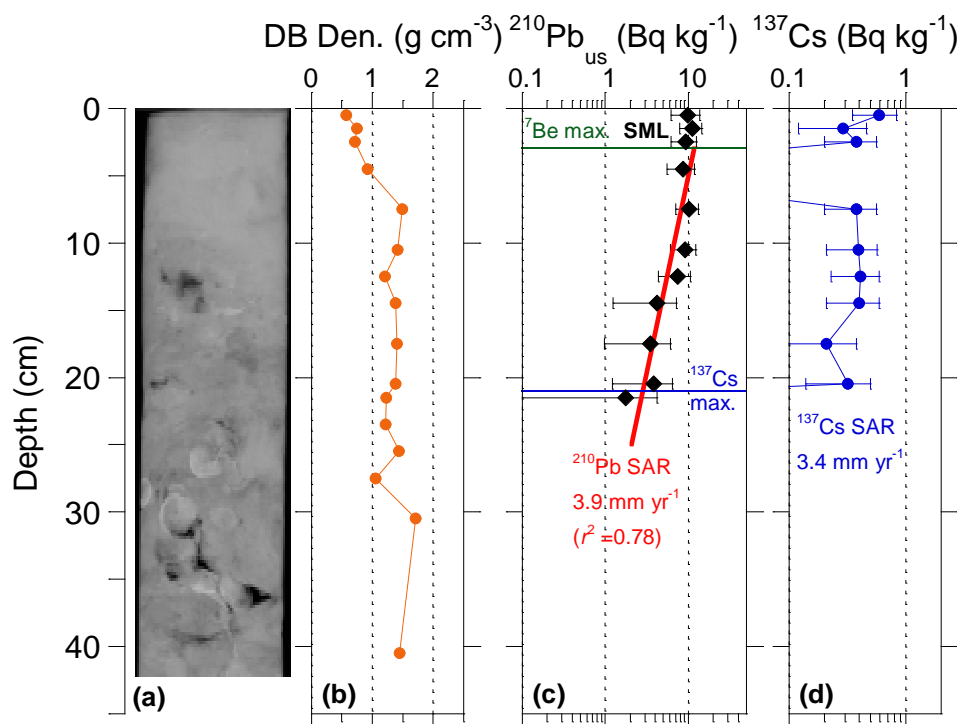


The ^{210}Pb concentration profile extends to 15 cm depth, with a calculated ^{210}Pb SAR of 2.8 mm yr^{-1} . By comparison, the ^{137}Cs profile extends to 25 cm depth and yields a ^{137}Cs SAR of 4.3 mm yr^{-1} (Figure 41d). Based on the rate of burial and ^7Be data, the maximum residence time of sediment in the SML is 11 years.

Core WT-S2 was collected $\sim 1 \text{ km}$ southeast of WT-S1. The x-radiograph for WT-S2 indicates a muddy-sand substrate with cockle shell valves common below 25 cm depth (Figure 42a). The top 10 cm of the core is a homogeneous muddy sand unit. There is some evidence of intact fine-scale laminations below 10 cm depth. Sediment DBD increases linearly from 0.5 to 1.5 g cm^{-3} within the top 8 cm of the core (Figure 42b). The ^7Be and ^{210}Pb profiles indicate an SML of 3 cm (Figure 42c).

Figure 42

Core WT-S2 (Waitemata subtidal): (a) x-radiograph; (b) dry bulk sediment density; (c) unsupported ^{210}Pb concentration profile with 95 per cent confidence intervals, time-averaged sediment accumulation rate (SAR) and coefficient of determination (r^2) derived from fit to data (red line), maximum ^7Be depth and maximum ^{137}Cs depth; (d) ^{137}Cs concentration profile with 95 per cent confidence intervals and time-averaged SAR. **Note:** the ^{137}Cs SAR is calculated after subtraction of ^7Be mixing depth.



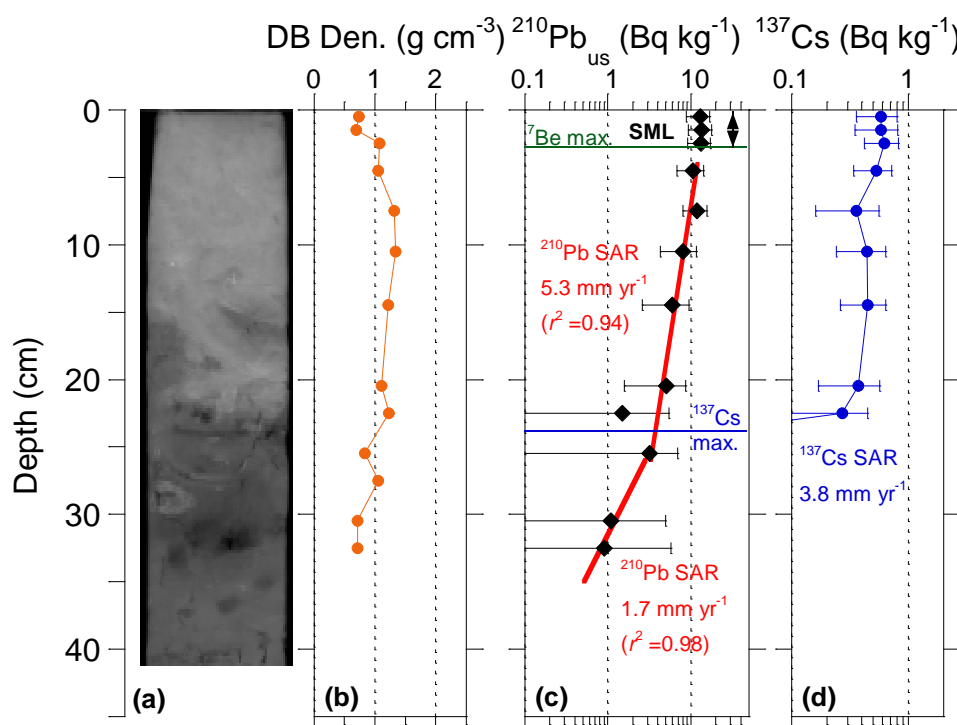
Unsupported ^{210}Pb and ^{137}Cs concentration profiles extend to 20 cm depth, with calculated ^{210}Pb and ^{137}Cs SAR of 3.9 mm yr⁻¹ and 3.4 mm yr⁻¹, respectively (Figures 42c and d). Based on the rate of burial and ^7Be data, the maximum residence time of sediment in the SML is eight years.

Core WT-S3 was collected ~1 km southwest of WT-S1. The x-radiograph for WT-S3 shows a 20 cm thick layer of muddy sand overlying low-density muds. Median particle diameter in the upper sand unit is ~100 μm and reduces to ~25 μm in the underlying mud unit, and the mud content increases from 10 per cent to 70 per cent (Figure 37). The mixing of these sediments at their interface between 15–25 cm depth can also be seen. The presence of millimetre-scale burrows indicates relatively intense mixing in the upper layer, which has erased most signs of bedding (Figure 43a). Apart from a low-density surface layer (0–2 cm, 0.7 g cm⁻³) sediment DBD is homogenous at ~1 g cm⁻³ (Figure 43b). The ^7Be and ^{210}Pb profiles indicate an SML of 3 cm (Figure 53c). The ^{210}Pb concentration profile displays a complex form with a change in slope at ~26 cm depth. This coincides with the change from mud to muddy-sand deposition over recent decades. The ^{210}Pb SAR in the older mud unit is 1.7 mm yr⁻¹, increasing to 5.3 mm yr⁻¹ in the overlying mud–sand unit.

The estimated age of sediments at 26 cm depth (at the ^{210}Pb profile inflection) is 49 years or about 1956 AD. This is similar to the the 1953 AD age for the maximum depth of ^{137}Cs occurrence at 23 cm depth.

Figure 43

Core WT-S3 (Waitemata subtidal): (a) x-radiograph; (b) dry bulk sediment density; (c) unsupported ^{210}Pb concentration profile with 95 per cent confidence intervals, time-averaged sediment accumulation rate (SAR) and coefficient of determination (r^2) derived from fit to data (red line), maximum ^7Be depth and maximum ^{137}Cs depth; (d) ^{137}Cs concentration profile with 95 per cent confidence intervals and time-averaged SAR. **Note:** the ^{137}Cs SAR is calculated after subtraction of ^7Be mixing depth.



^{137}Cs SAR averages 3.8 mm yr⁻¹ (Figure 43d). Based on the rate of burial and ^7Be data, the maximum residence time of sediment in the SML is six years.

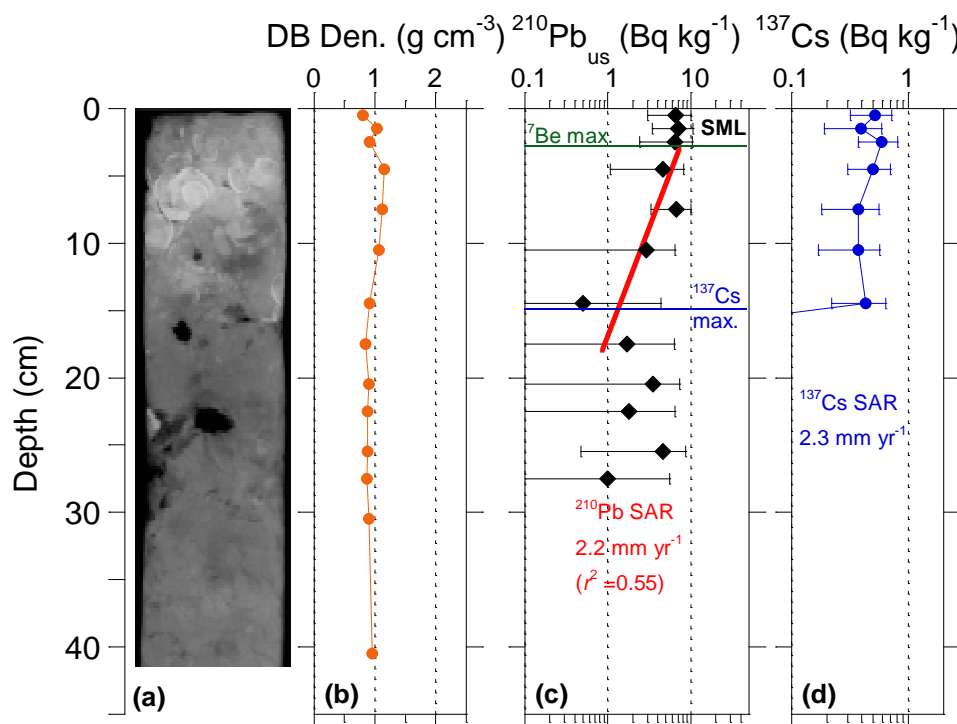
4.3.2.4 Whau (intertidal)

The Whau intertidal flats extend up to 2 km northeast from Pollen Island on the southwest shore of the CWH (see Figure 11). The intertidal flats are aligned with the prevailing southwest–northeast wind direction so that they are exposed to waves (Oldman et al. 2008).

Core WH-I1 came from the middle intertidal flat near the Whau River channel. The top 15 cm of the core is composed of muddy sand and shells and fragments of cockle (*Chione stutchburyi*). Below this unit, sediments are composed of a sandy mud that contains traces of millimetre-scale animal burrows that were probably formed by worms. Large wood fragments occur at 15 and 22 cm depth (Figure 44a).

Figure 44

Core WH-I1 (Whau intertidal): (a) x-radiograph; (b) dry bulk sediment density; (c) unsupported ^{210}Pb concentration profile with 95 per cent confidence intervals, time-averaged sediment accumulation rate (SAR) and coefficient of determination (r^2) derived from fit to data (red line), maximum ^7Be depth and maximum ^{137}Cs depth; (d) ^{137}Cs concentration profile with 95 per cent confidence intervals and time-averaged SAR. **Note:** the ^{137}Cs SAR is calculated after subtraction of ^7Be mixing depth.

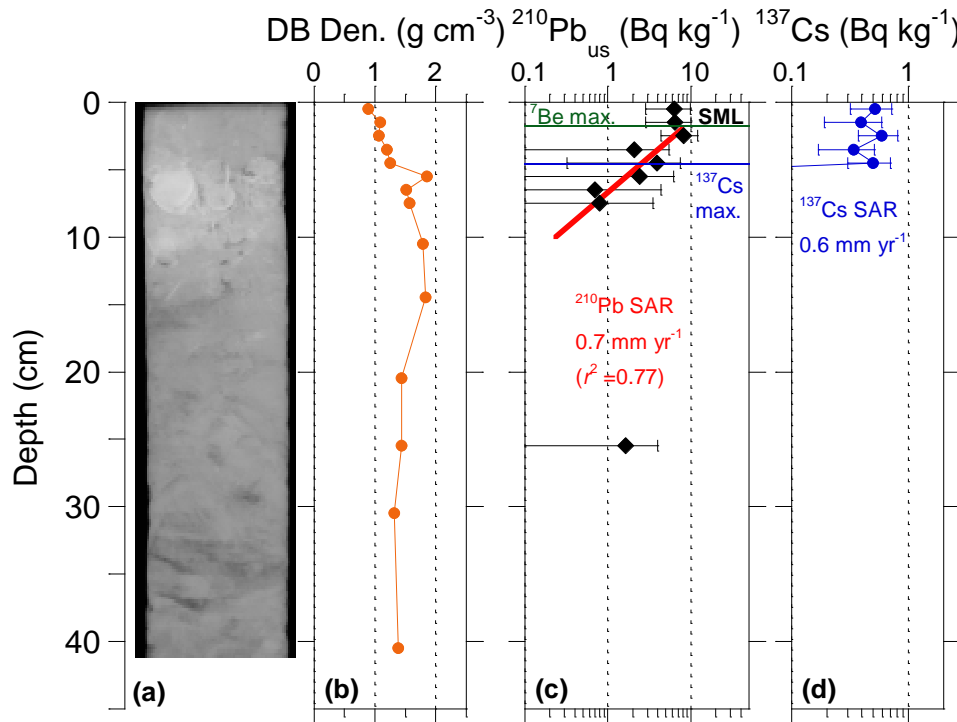


Sediment DBD shows little down-core variation, and averages 1 g cm⁻³ (Figure 44b). The ^7Be and ^{210}Pb profiles indicate an SML of 3 cm (Figure 44c). Unsupported ^{210}Pb is present to 28 cm depth, although the profile below 18 cm depth is relatively uniform, with ^{210}Pb concentrations of 1–3 Bq kg⁻¹. This may reflect mixing or, more likely, the large uncertainties in unsupported ^{210}Pb concentrations, which is indicated by the 95 per cent confidence intervals. The ^{210}Pb SAR calculated for the upper 20 cm of the profile is 2.2 mm yr⁻¹, which is in close agreement with the ^{137}Cs SAR of 2.3 mm yr⁻¹ (Figure 44d). Based on the rate of burial and ^7Be data, the maximum residence time of sediment in the SML is 14 years.

Core WH-I2 comes from the lower intertidal flat some 2 km northeast of Pollen Island and close to chart datum. The x-radiograph indicates that sediments deposited here are substantially sandier (Figure 45a) than previously described. The top 5 cm of the core is a homogenous slightly muddy sand. This unit overlays a 5 cm thick layer of cockle-shell valves. The slightly darker hue of the x-radiograph below 10 cm depth indicates that these sediments contain more mud, which is confirmed by the DBD profile (Figure 45b). Sediment DBD increases from 0.9 to 2 g cm⁻³ in the sand unit and is relatively uniform down core at 1.3 g cm⁻³ in the muddy sand below 20 cm depth.

Figure 45

Core WH-I2 (Whau intertidal): (a) x-radiograph; (b) dry bulk sediment density; (c) unsupported ^{210}Pb concentration profile with 95 per cent confidence intervals, time-averaged sediment accumulation rate (SAR) and coefficient of determination (r^2) derived from fit to data (red line), maximum ^7Be depth and maximum ^{137}Cs depth; (d) ^{137}Cs concentration profile with 95 per cent confidence intervals and time-averaged SAR. **Note:** the ^{137}Cs SAR is calculated after subtraction of ^7Be mixing depth.

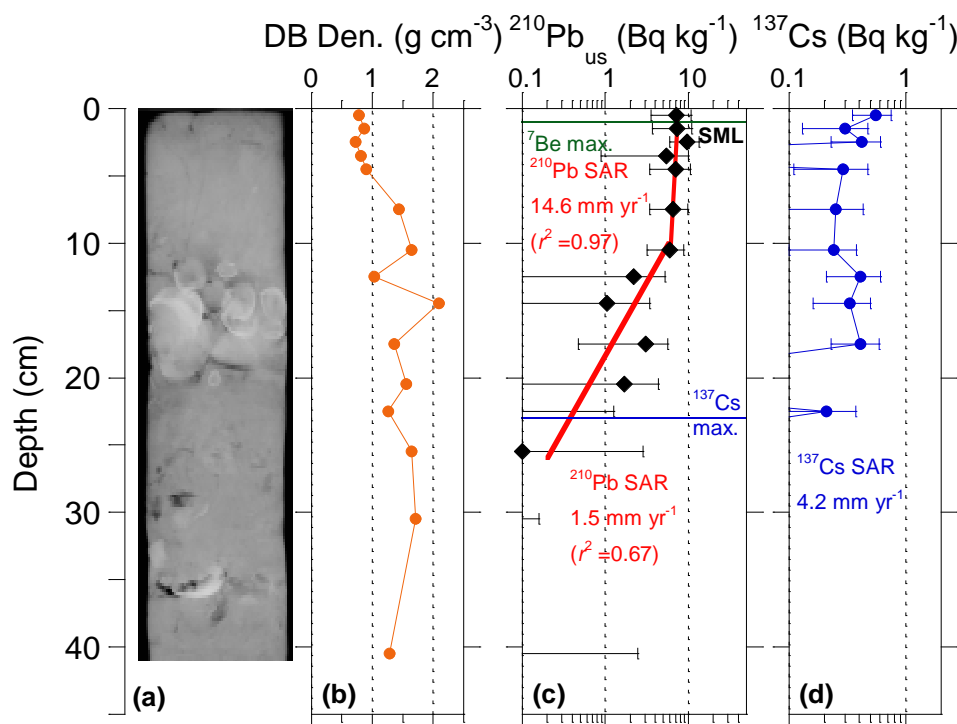


This lower muddy-sand unit preserves millimetre-scale laminations of the original deposits including evidence of cross bedding below 20 cm depth that may represent centimetre-scale ripples formed by waves. The ^7Be and ^{210}Pb profiles indicate an SML to 2 cm depth (Figure 45c). Unsupported ^{210}Pb is present to 10 cm depth, which coincides with the base of the shell layer. ^{137}Cs occurs to 5 cm depth, which coincides with the top of the shell layer (Figure 45d). ^{210}Pb and ^{137}Cs SAR average 0.7 mm yr^{-1} and 0.6 mm yr^{-1} , respectively. Based on the rate of burial and ^7Be data, the maximum residence time of sediment in the SML is 29 years. These data suggest that: (1) fine sediments are being winnowed from the lower intertidal flat; and (2) SAR on this intertidal flat is low in comparison to the rest of the CWH.

Core WH-I3 is located on the middle intertidal flat within the Motu Manawa Marine Reserve and 0.7 km northeast of Pollen Island. The x-radiograph indicates that sediments deposited here are composed of muddy sand (Figure 46a). Traces of mm-scale worm burrows filled with mud penetrate to 10 cm depth. Between 10 and 20 cm there is a shell-rich layer composed of cockle (*Chione stutchburyi*) valves and fragments. Below this unit, sediments are composed of a muddy sand with occasional cockle shell valves and fragments. In the topmost unit, sediment DBD increases from 0.8 to 1.5 g cm^{-3} , reaches 2 g cm^{-3} in the shell layer, and varies around 1.5 g cm^{-3} below 20 cm depth (Figure 46b).

Figure 46

Core WH-I3 (Whau intertidal): (a) x-radiograph; (b) dry bulk sediment density; (c) unsupported ^{210}Pb concentration profile with 95 per cent confidence intervals, time-averaged sediment accumulation rate (SAR) and coefficient of determination (r^2) derived from fit to data (red line), maximum ^7Be depth and maximum ^{137}Cs depth; (d) ^{137}Cs concentration profile with 95 per cent confidence intervals and time-averaged SAR. **Note:** the ^{137}Cs SAR is calculated after subtraction of ^7Be mixing depth.



The ^7Be and ^{210}Pb profiles indicate an SML of 1 cm (Figure 46c). Unsupported ^{210}Pb is present to 25 cm depth. The ^{210}Pb profile displays an abrupt change in slope at 10 cm depth, with an increase in SAR from 1.5 mm yr⁻¹ to 14.6 mm yr⁻¹ above this horizon. This change in SAR coincides with the top of the shell layer (Figure 4. 32c). ^{137}Cs occurs to 23 cm depth and yields a ^{137}Cs SAR of 4.2 mm yr⁻¹ (Figure 4. 32d).

This apparent increase in SAR indicated by the ^{210}Pb profile may indicate an increase in SAR or could result from sediment mixing. The shell acts as a physical barrier to benthic infauna, so that bioturbation should largely be restricted to the surface layer. Grading of estuarine sediments due to rapid bioturbation to produce buried layers of coarse material has been observed for lugworms. These animals can completely mix the top 10–30 cm of the sediment column in ≤ 100 days (Bromley 1996). In the present study, we would expect to see ^7Be below 1 cm depth in core WH-I3 if rapid and deep sediment mixing was occurring. The apparent increase in ^{210}Pb SAR could also result from sediment mixing over longer timescales. ^{210}Pb and ^{137}Cs SAR measured in the Whau WH-I1 and WH-I2 cores are comparable, but this is not the case for WH-I3. The estimated ^{210}Pb age of sediments at the maximum ^{137}Cs depth is 1911 AD, which is substantially older than the maximum possible ^{137}Cs age of 1953

AD. The poor agreement between the ^{210}Pb and ^{137}Cs dating indicates that the sedimentation chronology for WH-I3 is not reliable.

Based on the rate of burial using the ^{137}Cs SAR and ^7Be penetration depth, the maximum residence time of sediment in the SML is ~2 years.

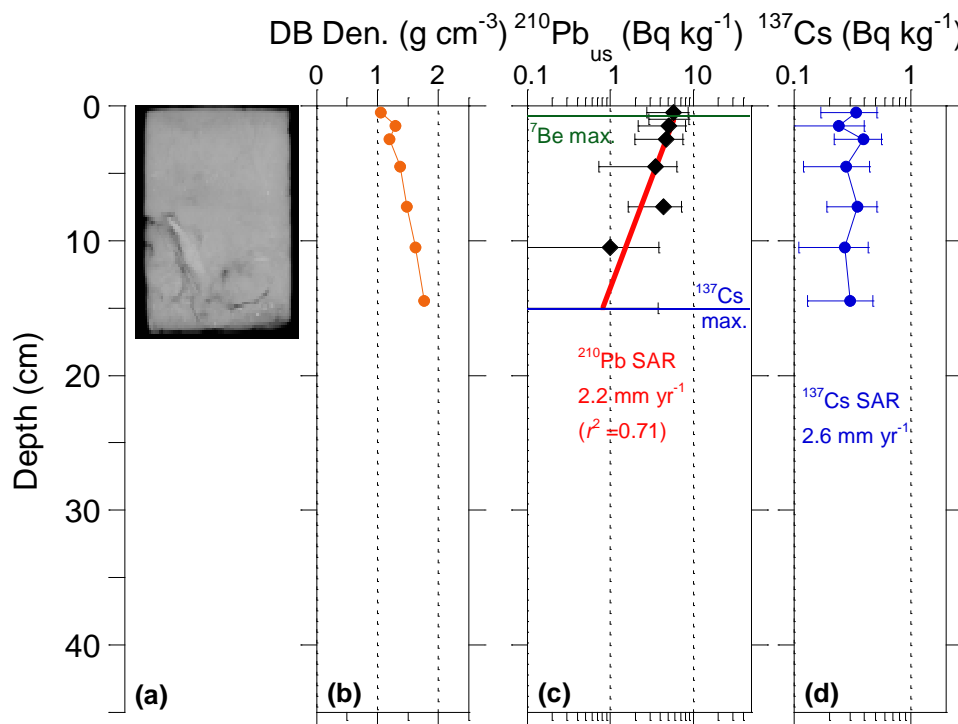
4.3.2.5 Motions (subtidal)

The Motions Creek (MO) cores were collected from a 2 km² subtidal flat that receives run-off from the Motions Creek catchment. The Motions subtidal flat is located between Te Tokaroa (Meola) Reef and the Auckland Harbour Bridge at 0–2 m below chart datum.

Core MO-S1 (Figure 47) was collected 2 km north of the Motions Creek outlet. The core is short because the sediments below 17 cm consisted of densely packed shell valves of cockle and scallop that could not be penetrated by the push core. The x-radiograph shows that these sediments contain numerous millimetre-scale, mud-filled burrows up to several cm long (Figure 47a). Sediment DBD increases linearly with depth from 1 to 1.9 g cm⁻³ (Figure 47b). The ^7Be profile indicates an SML to 1 cm depth (Figure 47c). Unsupported ^{210}Pb concentration decays exponentially with depth and is present to the base of the core. The ^{210}Pb SAR of 2.2 mm yr⁻¹ is similar to the ^{137}Cs SAR of 2.6 mm yr⁻¹. Based on the rate of burial and ^7Be data, the maximum residence time of sediment in the SML is five years.

Figure 47

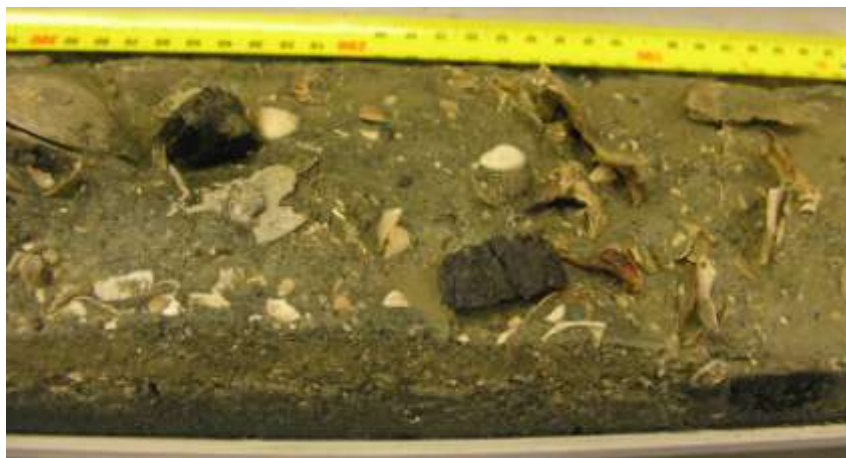
Core MO-S1 (Motions subtidal): (a) x-radiograph; (b) dry bulk sediment density; (c) unsupported ^{210}Pb concentration profile with 95 per cent confidence intervals, time-averaged sediment accumulation rate (SAR) and coefficient of determination (r^2) derived from fit to data (red line), maximum ^7Be depth and maximum ^{137}Cs depth; (d) ^{137}Cs concentration profile with 95 per cent confidence intervals and time-averaged SAR. **Note:** the ^{137}Cs SAR is calculated after subtraction of ^7Be mixing depth.



Core MO-S2 was collected 1 km north of MO-S2 and near the main tidal channel at 2 m below chart datum. An x-radiograph is not available for this core. The core log records a muddy sand with abundant shell and wood fragments (Figure 48). The top 15 cm of the core is composed of a muddy sand with numerous millimetre- to centimetre-scale shell fragments.

Figure 48

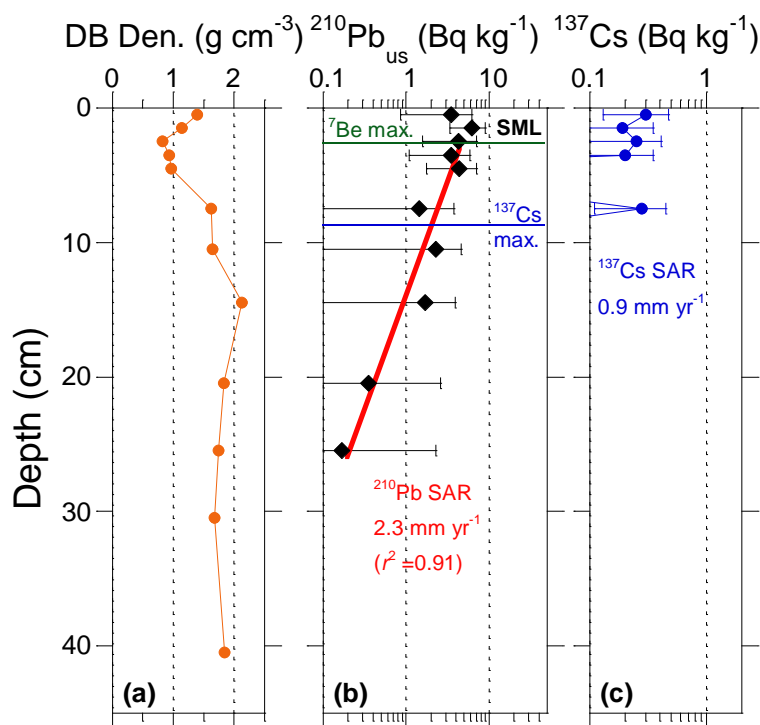
Core MO-S2: photograph taken during core logging. The top of the core is to the right-hand side. Note the abundant shell and wood fragments.



Below this surface layer, sediment is composed of a shell hash in a mud-sand matrix. Shells include those of horse mussel (*Atrina zelandica*), pipi (*Paphies australis*) and cockle. The sediment DBD profile reflects this composition and increases from 1 to 2 g cm⁻³ in the top 15 cm of the core (Figure 4.44a). The ⁷Be and ²¹⁰Pb profiles indicate an SML to 3 cm depth (Figure 49b). Unsupported ²¹⁰Pb concentration decays exponentially with depth and is present to 25 cm depth. The ²¹⁰Pb SAR is 2.3 mm yr⁻¹. The ¹³⁷Cs concentration profile extends to 8 cm depth, with ¹³⁷Cs absent between 4 cm and 6 cm depth (Figure 49). The ¹³⁷Cs SAR is 0.9 mm yr⁻¹. The ²¹⁰Pb SAR is likely to be the most reliable estimate of sedimentation at this site because of the intermittent occurrence of ¹³⁷Cs with depth. Based on the rate of burial and ⁷Be data, the maximum residence time of sediment in the SML is 13 years.

Figure 49

Core MO-S2 (Motions subtidal): (a) x-radiograph; (b) dry bulk sediment density; (c) unsupported ^{210}Pb concentration profile with 95 per cent confidence intervals, time-averaged sediment accumulation rate (SAR) and coefficient of determination (r^2) derived from fit to data (red line), maximum ^7Be depth and maximum ^{137}Cs depth; (d) ^{137}Cs concentration profile with 95 per cent confidence intervals and time-averaged SAR. **Note:** the ^{137}Cs SAR is calculated after subtraction of ^7Be mixing depth.



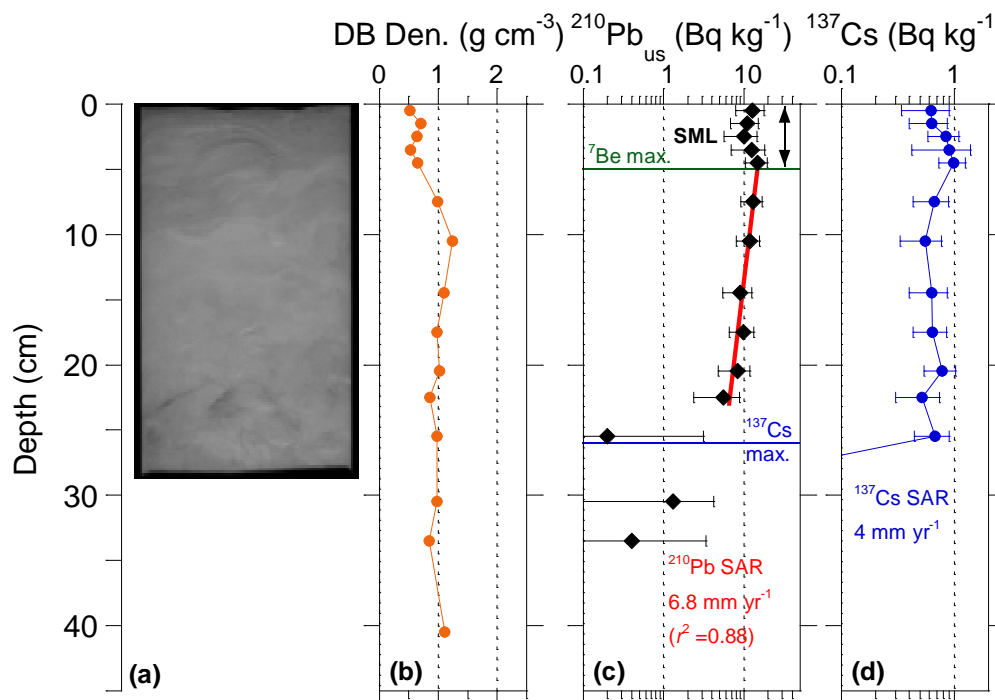
4.3.2.6 Shoal Bay (intertidal)

Shoal Bay is a 4 km² intertidal embayment on Auckland's North Shore (see Figure 11). Sediment cores were collected at three sites within the bay. Sediment profiles for **SB-I1**, located opposite the Tank Farm, are presented here. The x-radiograph shows a 10 cm deep surface layer of low-density laminated mud, consisting of millimetre-scale interlayered silts (Figure 50a). This type of bedding is similar to that observed in near-surface sediments of the Firth of Thames (see Figure 13) on wave-exposed intertidal flats. This laminated mud unit overlays a mixed muddy-sand unit. Laminae and traces of animal burrows are absent. Sediment DBD increases from 0.5 to 1.1 g cm⁻³ at the base of the mud unit and remains constant below 10 cm depth (Figure 50b). Median particle size increases from 100 μm at the surface to 140 μm at 45 cm depth. Mud content varies between 19 and 25 per cent (see Figure 37).

The ^7Be and ^{210}Pb profiles show that the active SML extends to 5 cm depth (Figure 50b). Below the SML, unsupported ^{210}Pb concentration decays exponentially to 22 cm depth. The ^{210}Pb SAR is 6.8 mm yr⁻¹. The ^{137}Cs concentration profile extends to 25 cm depth yielding a ^{137}Cs SAR of 4 mm yr⁻¹. Based on the burial rate and ^7Be data, the maximum residence time of sediment in the SML is six years.

Figure 50

Core SB-I1 (Shoal Bay intertidal): (a) x-radiograph; (b) dry bulk sediment density; (c) unsupported ^{210}Pb concentration profile with 95 per cent confidence intervals, time-averaged sediment accumulation rate (SAR) and coefficient of determination (r^2) derived from fit to data (red line), maximum ^7Be depth and maximum ^{137}Cs depth; (d) ^{137}Cs concentration profile with 95 per cent confidence intervals and time-averaged SAR. **Note:** the ^{137}Cs SAR is calculated after subtraction of ^7Be mixing depth.



4.3.3 Bioturbation

4.3.3.1 Comparison with bioturbation depths calculated using tracers

Depth of bioturbation and the bioturbation index (BI) were assessed for five intertidal sites (HN-I2, HN-I3, TA-I1, TA-I2 and WH-I2) and three subtidal sites (WT-S1, WT-S2, WT-S3) in the central harbour. Data for the subtidal sites were based on sampling conducted in 2002 (Lundquist et al. 2003).

Sediments at the five intertidal sites contain a range of bioturbating animals: crabs, shellfish (eg, *Austrovenus stutchburyi* and *Macomona liliana*), large polychaete worms (eg, Maldanidae tube worms, predatory Nereidae, deposit-feeding Orbinidae and *Scolecopides benhami*) and snails (*Zeacumantus lutulentus*) (Table 4). Crabs bioturbate in two ways: excavating burrows (for the species found here generally to 10 cm) and feeding on the sediment surface. *Austrovenus* also bioturbates in two ways: when not feeding it lives below the sediment surface and moves up to feed; it also moves over the sediment surface. *Macomona* live below the sediment surface (usually around 10 cm deep) and feed on the surface by means of a long siphon which is moved around and up and down. Maldanid tube worms feed with their heads down in the sediment (generally deeper than 10 cm) and defecate on the surface. *Orbinidae*

and *Nereidae* move throughout the sediment feeding. *Scolecopoides* feeds on the sediment surface and defacates at depth. *Zeacumantus* mainly bioturbates the surface by producing a track as it moves.

The three subtidal sites also had a range of bioturbating animals: crabs, shellfish (*Nucula hartvigiana*) and polychaete worms (*polydoridae* tube worms, predatory *Nereidae* and *Glyceridae*) (Table 5). Despite many of the taxa present in abundance being smaller than those from the intertidal sites, most taxa lived and moved throughout the sediment column.

Maximum depth of bioturbation varied from 5 cm to greater than 10 cm. Median depth of bioturbation varied from 2–5 cm to greater than 10 cm (Figure 51). The depth of bioturbation was determined by the relative abundances of bioturbating organisms and the depth range over which they actively bioturbate. The depth of bioturbation was also controlled by the presence (or absence) of a buried shell layer (eg, sites TA-I1 and TA-I2 had a shallow shell layer), which acts as a physical barrier to vertical movement of animals.

Figure 51

Histogram of bioturbation depths.

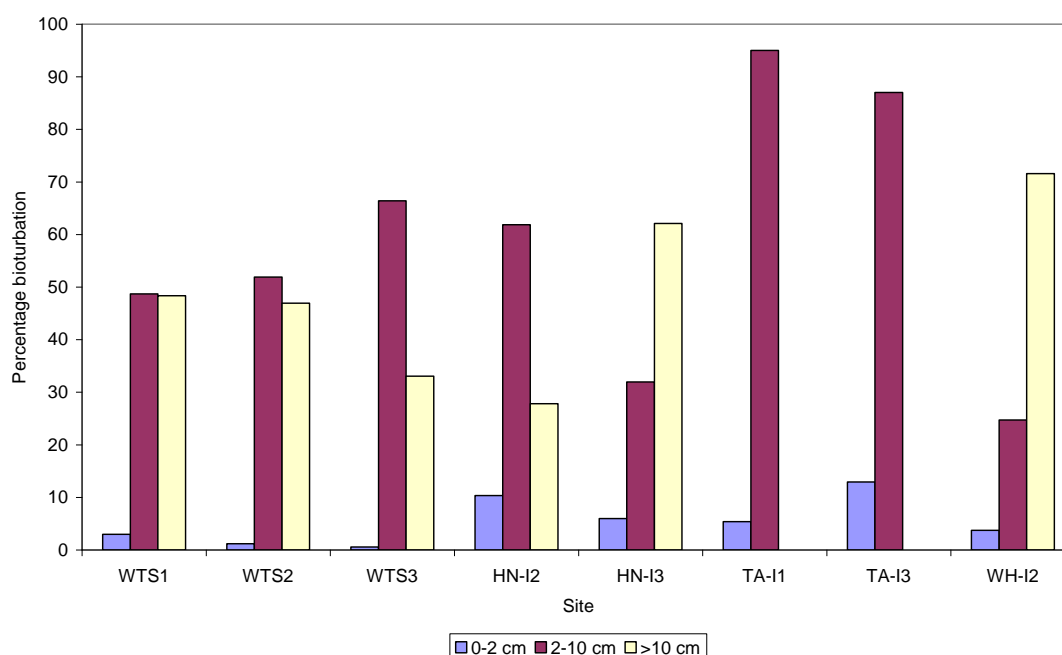


Table 4

Intertidal sites: site descriptions, bioturbation index and bioturbation depth.

	HN-I3	TA-I3	HN-I2	TA-I1	WH-I2
Main bioturbating taxa	<i>Macomona</i> and Maldanidae	Austrovenus dominated. <i>Macomona</i> , Nereidae and <i>Scolecopides</i> also occur	Medium- to low-density <i>Austrovenus</i> . <i>Macomona</i> , <i>Nemertea</i> and <i>Scolecopides</i> also occur	Polychaete dominated. mainly small species except for a few <i>Orbinidae</i> and <i>Nereidae</i> .	Polychaete dominated. mainly small species except for a few <i>Nereidae</i> . <i>Macomona</i> also occur.
Surface features	<i>Maldanid</i> patches and large sand ripples	Crab holes (one burrow every few metres, length 100–150 mm), <i>Zeacumantus</i> sp. and tracks, ray pits (1–2 per 15–20 m)	Crab holes (one burrow every few metres, length approx. 100–150 mm)	Crab holes (one burrow every one metres, length approx. 100–150 mm)	Shallow crab holes
Subsurface features				Dead cockle shell layer 4–5 cm deep	Dead cockle shell layer 5–6 cm deep.
X-ray evidence		Clear bioturbation to 6 cm by worms, probably to 11 cm on old crab burrow	Clear bioturbation only to 2.5 cm	Clear bioturbation by worms seen to 4–5cm, truncated by shell layer	Clear bioturbation by worms and <i>Macomona</i> seen 5–6.5 cm deep, truncated by shell layer
Bioturbation index	3248	5184	2352	3579	5603
Bioturbation depth maximum (cm)	>10	>10	>10	5	6

Table 5

Waitemata harbour subtidal sites: site descriptions, bioturbation index and bioturbation depth.

	WST1	WST2	WST3
Community type	Medium to low densities of the nut shell <i>Nucula hartvigiana</i> , low densities of tube building worms	Low densities of <i>Nucula hartvigiana</i> and large predatory worms	Low densities of <i>Nucula hartvigiana</i> , crabs and small worms
Likely surface features	Small holes from shrimps and brittle stars		Crab holes
X-ray evidence	No shell layer, bioturbation evident to 12 cm	No shell layer, bioturbation evident past 15 cm	No shell layer, bioturbation evident to 8 cm
Bioturbation index	971	533	1236
Bioturbation depth maximum (cm)	>10	>10	>10

4.3.3.2 Bioturbation index (BI)

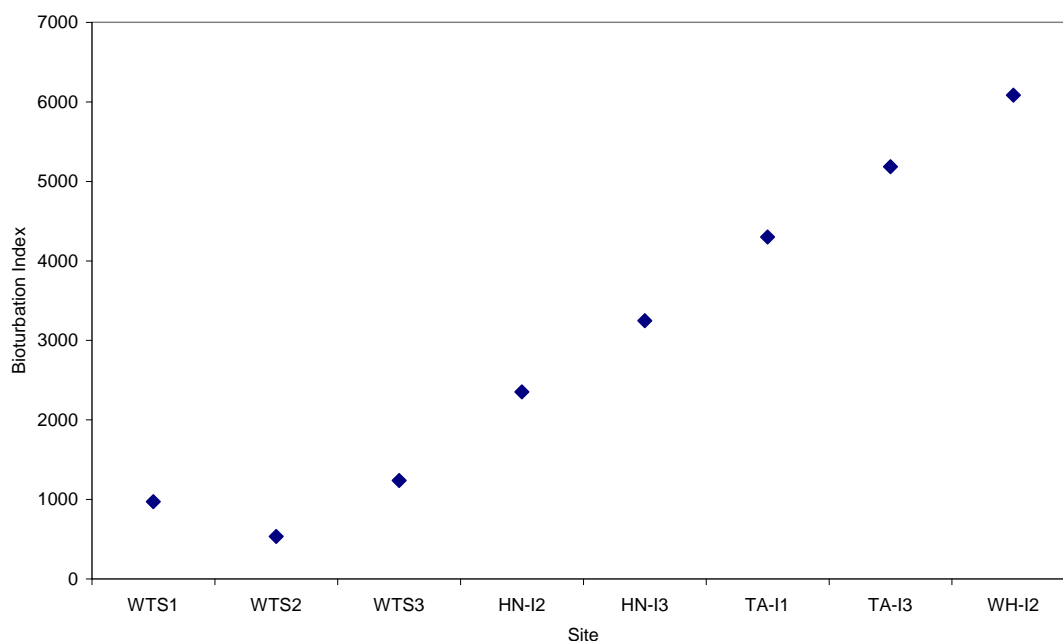
The BI provides a relative measure of the intensity of bioturbation by benthic animals.

At the intertidal sites, BI varied threefold, from lowest at site HN-I2 to highest at site WH-I2. Site WH-I2 had a high abundance of small animals that live and actively burrow or transport sediment to depth (eg, the polychaete *Heteromastus filiformis* and the shellfish *Nucula*). TA-I3 had the next highest BI, resulting from the presence of large animals such as crabs, adult *Austrovenus* and adult *Macomona*. The sites with lower BI (HN-I2, HN-I3 and TA-I1) either had more organisms that live on or just below the sediment surface (eg, the estuarine limpet *Notoacmea helmsii* or the polychaete *Aricidea* sp. respectively), or low densities of bioturbators. The subtidal sites generally had lower BI (533–1236) than intertidal sites, which reflected the lower densities and generally smaller sizes of animals at the subtidal sites.

There was an indication of increasing bioturbation from site HN-I2, close to Henderson Creek, along the western shore of the harbour to the Whau River entrance (Figure 52).

Figure 52

Bioturbation index, showing larger values for intertidal sites compared to subtidal sites.



4.3.3.3 Effect of season and year on bioturbation

Bioturbation depths and indices similar to those reported in Section 4.3.2 were determined for the ARC long-term benthic sites in the CWH and Shoal Bay that have been monitored since October 2001. These sites include Hobsonville (HBV), Henderson Ck (HC), Whau River (Whau), Meola Reef (Reef) and Shoal Bay (ShB) (Figure 53). Sites HBV and Whau have few burrowing animals that rework the sediment vertically. The majority of animals at these two sites move horizontally through the sediment or were surface bioturbators, such as cockles. At site HC, many bioturbators were mainly surface dwellers, and the median depth of bioturbation was 2–10 cm. All sites had animals that actively moved sediment down to at least 10 cm, but densities of deep bioturbating animals were highest at sites Reef and ShB (median depth of bioturbation >10 cm).

Seasonal cycles and multi-year variations in the densities of bioturbators are observed at these sites (Halliday et al. 2006) and are likely to affect both bioturbation rates and depths. Figure 54 shows an example of this temporal variability in animal density for the Whau site. Figure 55 confirms that the bioturbation depth shows temporal variations and between-site variations at the ARC monitoring sites (Figure 55). At site Reef, the depth of bioturbation has been increasing over the six-year period. By comparison, at Whau the average bioturbation depth has not changed.

Figure 53

Location of ARC long-term benthic-fauna monitoring sites in the CWH and Shoal Bay.

Figure 54

Density of sediment movers (rank 2 or above burrowing animals) at site Whau over time (from Halliday et al. 2006).

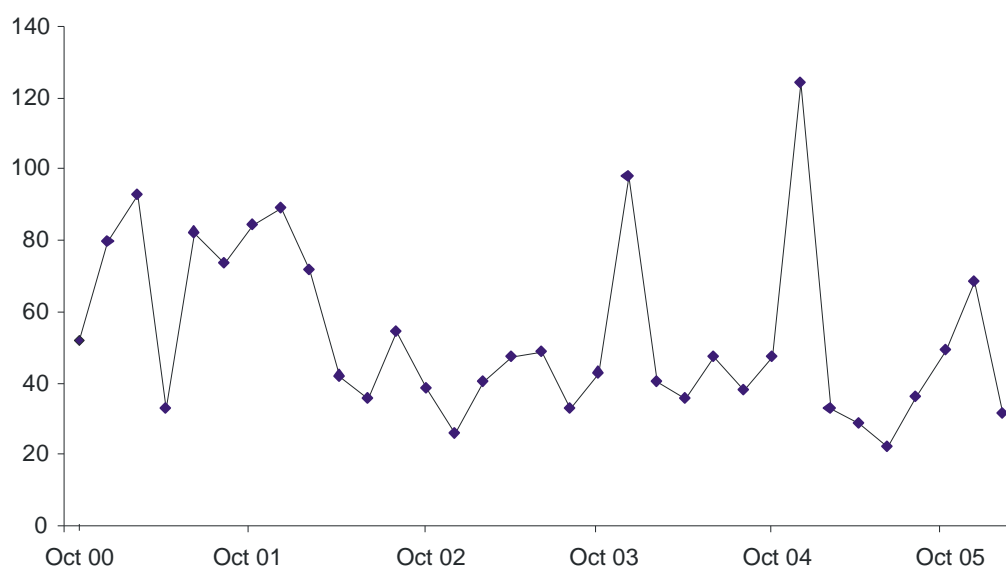
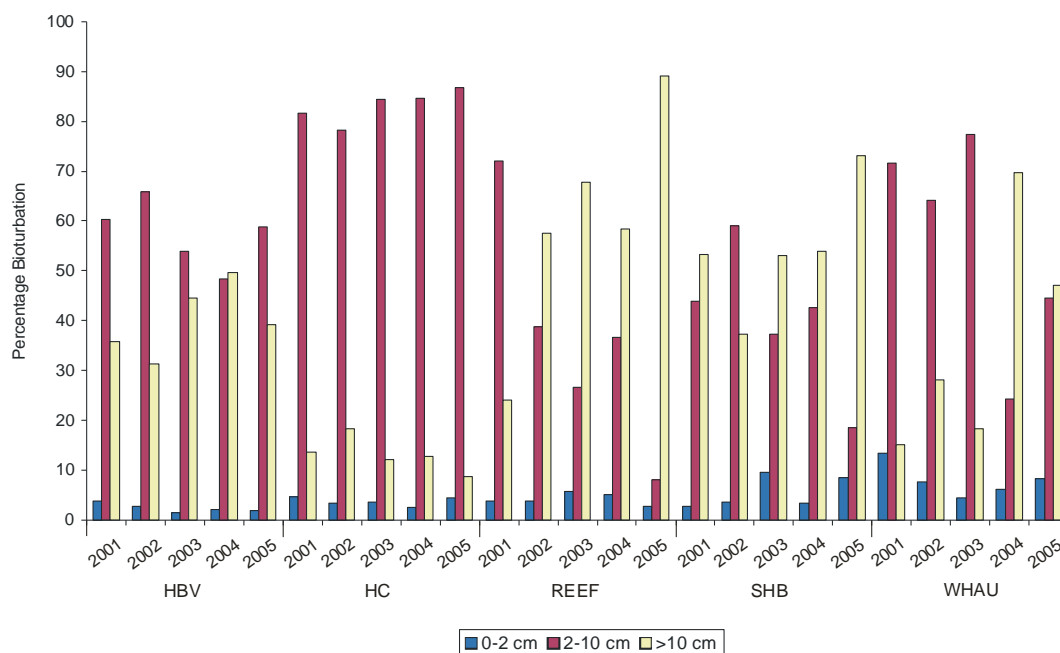


Figure 55

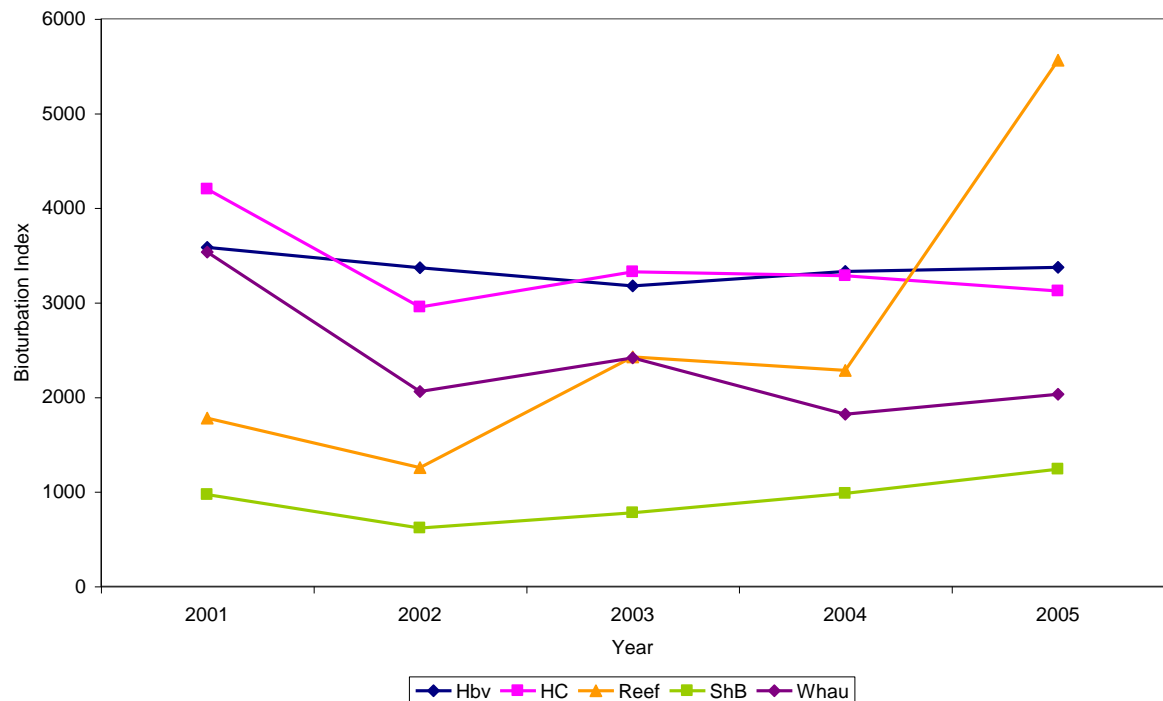
Temporal variation in bioturbation depth in the Central Waitemata Harbour over five years.



Bioturbation indices were calculated for each ARC long-term monitoring site in the CWH and Shoal Bay for every October (Figure 56). Sites HBV and ShB showed little change in BI over time. The Henderson Creek site (HC) had more variability and sites Whau and Reef showed decreasing and increasing trends, respectively, in BI.

Figure 56

Bioturbation index in October in the Central Waitemata Harbour over five years (2001–2005).



These changes largely match changes in the macrofaunal communities discussed by Halliday et al. (2006). Over time (2000–2006), distinct changes have been observed at site Reef due to the decline of *Nucula* and the increase of *Heteromastus*. As *Nucula* actively moves sediment in the upper 2 cm of the sediment column and *Heteromastus* can bioturbate the sediment column down to 10 cm, this significant change in the community structure has resulted in both a higher BI and a greater bioturbation depth.

Site Whau also had changes in community composition and trends in the abundance of a number of taxa that may account for variability in both the bioturbation rate and depth. At this site, densities of *Nucula* decreased, but the density of the deeply bioturbating Maldanidae (*Macrocliyenella stewartensis*) increased.

5 Synthesis: Recent Sedimentation and Mixing

5.1 Recent sedimentation in the Central Waitemata Harbour

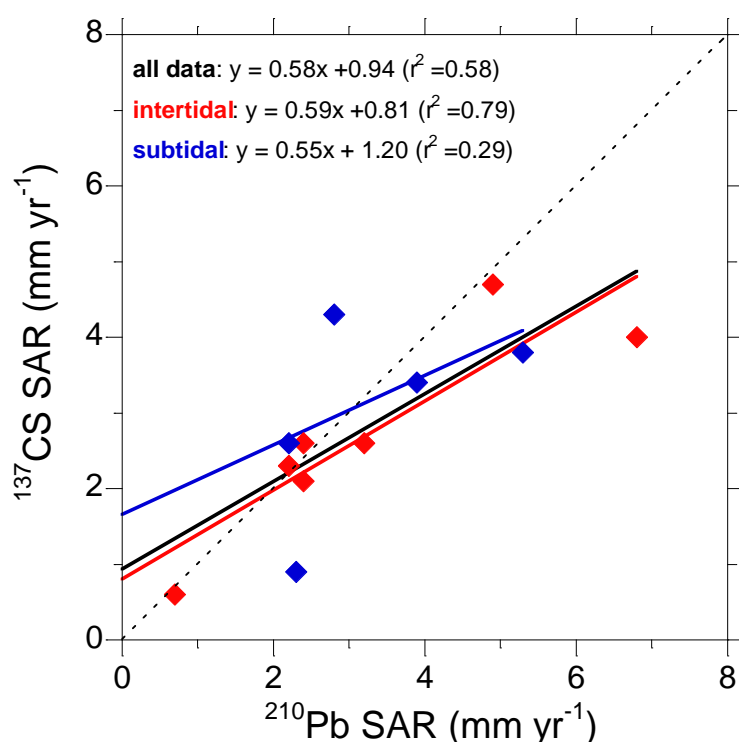
5.1.1 Comparison of ^{137}Cs and ^{210}Pb sediment accumulation rates

Figure 57 plots SAR estimated from the ^{210}Pb and ^{137}Cs dating. It can be seen that ^{210}Pb SARs are greater than ^{137}Cs SARs for most core sites, and there is a much closer agreement amongst SARs for the intertidal sites than for subtidal sites. A similar pattern was observed in the regional estuarine sedimentation study (Swales et al. 2002a). A possible explanation is that the ^{210}Pb profile samples a longer time period than ^{137}Cs . Another possibility is that ^{137}Cs is present deeper in the sediment column at concentrations below the minimum detectable concentration.

The ^{210}Pb SARs are likely to be more reliable than the ^{137}Cs SARs given that: (1) the ^{210}Pb SAR is based on a regression fitted to data rather than a maximum penetration depth as in the case of ^{137}Cs ; (2) the continuous input of ^{210}Pb from the atmosphere provides information on surface mixing; and (3) comparison of ^{210}Pb inventories and supply rates with other nearby cores, as well as with the measured atmospheric flux, provides information for validation of the ^{210}Pb SAR.

Figure 57

Comparison of ^{210}Pb and ^{137}Cs SARs.



5.1.2 ^{210}Pb and ^{137}Cs budgets and implications for fine sediment fate

^{210}Pb and ^{137}Cs are delivered to the Earth's surface as dry deposition or with rainfall. The latter appears to be more important (Matthews 1989). ^{210}Pb and ^{137}Cs are delivered to estuaries directly (by atmospheric deposition) and indirectly (attached to eroded soil particles). Once in the estuary, radioisotopes are scavenged by sediment particles suspended in the water column, which then may be deposited on the bed. ^{210}Pb and ^{137}Cs attached to soil particles will accumulate in tidal creeks close to catchment outlets (Swales et al. 2002b).

5.1.2.1 ^{210}Pb budget

The mean annual ^{210}Pb atmospheric flux (P_{atmos}) can be estimated from the inventory of unsupported ^{210}Pb in the sediment column, which is denoted by $A(o)$ (Bq cm^{-2}). This is estimated from the dry bulk density and unsupported ^{210}Pb concentration in sediment samples. The mean annual supply rate of unsupported ^{210}Pb (P , $\text{Bq cm}^{-2} \text{ yr}^{-1}$) is then calculated as $P = kA(o)$, where k is the ^{210}Pb decay constant. Note that unsupported ^{210}Pb is the atmospheric component of ^{210}Pb in sediments, as ^{210}Pb is also produced by in situ decay of parent radioisotopes present in sediments (Appendix 3).

The ^{210}Pb budget and P provide information about the movement of fine sediments. For example, $P > P_{\text{atmos}}$ indicates that fine sediment is preferentially being deposited at a site. By contrast, $P < P_{\text{atmos}}$ indicates that fine sediment is being winnowed. The ratio P/P_{atmos} is termed the concentration factor (C).

The atmospheric ^{210}Pb flux has been measured at monthly intervals by NIWA since June 2002 at a rainfall station in Howick. Monthly ^{210}Pb fluxes show substantial variability ($0.0001\text{--}0.002 \text{ Bq cm}^{-2} \text{ mo}^{-1}$, Figure 58), but annual-average fluxes are relatively constant at about $0.0052 \text{ Bq cm}^{-2} \text{ yr}^{-1}$. Constant ^{210}Pb supply at annual–decadal time scales is a key assumption of ^{210}Pb dating.

Figure 58

Monthly ^{210}Pb atmospheric flux (June 2002– January 2006) measured in rainwater samples at Howick, Auckland. Annual-average atmospheric ^{210}Pb flux is shown in brackets.

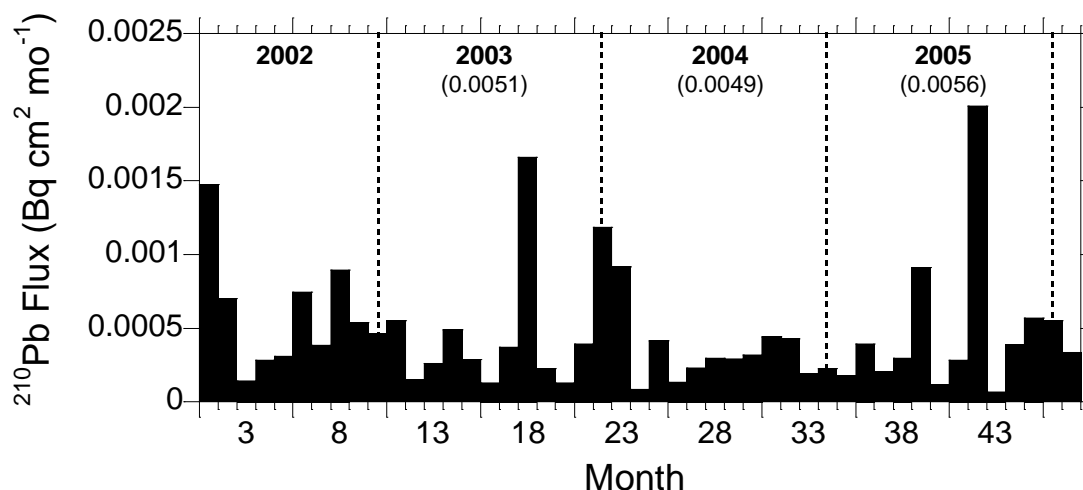


Figure 59 shows the vertical distribution of unsupported ^{210}Pb in CWH sediment cores. The core $A(0)$ value is calculated by integrating these profiles. Down-core variations in ^{210}Pb reflect several factors: (1) natural ^{210}Pb decay; (2) variations in sediment bulk density; (3) variations in mud content; and (4) depth and intensity of surface mixing. For example, the Henderson Creek cores were collected from intertidal flats composed of homogeneous muddy sands close to the catchment outlet. As a result, these cores have similar profiles and high unsupported ^{210}Pb concentrations (Figure 59a). By comparison, core HN-12, collected from wave exposed sand flats outside Henderson Creek, has substantially lower unsupported ^{210}Pb content (Figure 59d).

Figure 59

Profiles of unsupported ^{210}Pb concentration in sediment cores. The unsupported ^{210}Pb inventory, $A(o)$, and mean supply rate (P) are estimated from integration of these profiles.

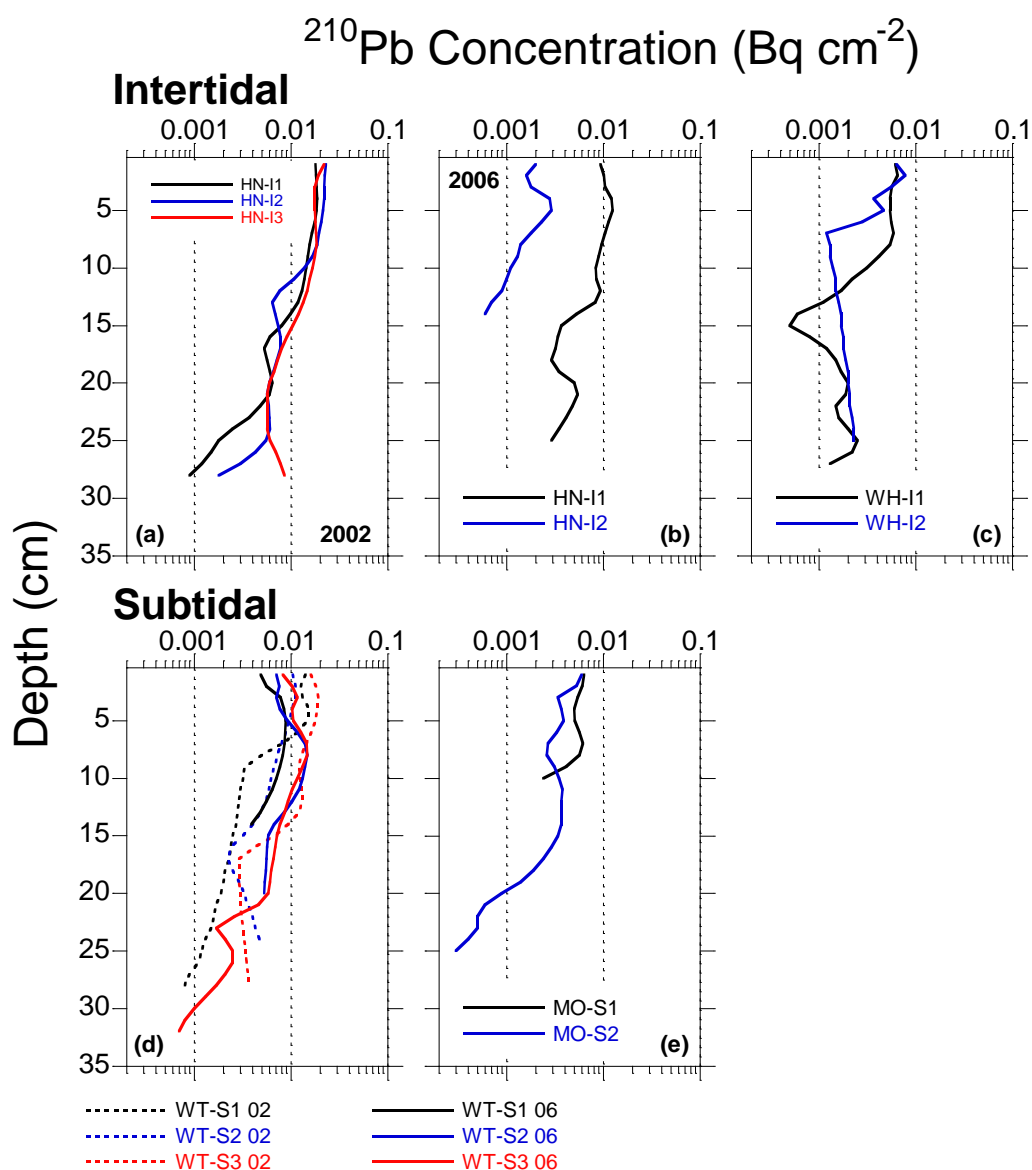


Table 6 summarises values for $A(o)$, P and C for the CWH and Shoal Bay sediment cores. Based on the assumption that bed sediments accumulate unsupported ^{210}Pb in proportion to P_{atmos} , these results suggest that tidal creeks, Shoal Bay and the central basin are long-term sinks for fine sediments. Intertidal flats and shallow subtidal flats provide temporary sinks for fine sediments.

Table 6

Unsupported ^{210}Pb inventories, $A(o)$ and mean supply rates (P) estimated from sediment cores. The concentration factor (C) is the ratio P/P_{atm} where P_{atm} (0.0052 Bq cm $^{-2}$ yr $^{-1}$) is the mean annual ^{210}Pb atmospheric flux.

Core site	$A(o)$ (Bq cm $^{-2}$)	P (Bq cm $^{-2}$ yr $^{-1}$)	C
Intertidal			
HN-I1 2002	0.279	0.0087	1.7
HN-I2 2002	0.313	0.0098	1.9
HN-I3 2002	0.339	0.0106	2.0
HN-I1 2006	0.170	0.0053	1.0
HN-I2 2006	0.029	0.0009	0.2
TA-I1	0.129	0.0040	0.8
TA-I2	0.128	0.0040	0.8
WH-I1	0.080	0.0025	0.5
WH-I2	0.065	0.0020	0.4
WH-I3	0.120	0.0037	0.7
SB-I1	0.322	0.0100	1.9
Subtidal			
WT-S1 2002	0.137	0.0043	0.8
WT-S2 2002	0.143	0.0045	0.9
WT-S3 2002	0.256	0.0800	1.5
WT-S1 2006	0.104	0.0032	0.6
WT-S2 2006	0.179	0.0056	1.1
WT-S3 2006	0.224	0.0070	1.3
MO-S1	0.048	0.0015	0.3
MO-S2	0.070	0.0022	0.4

5.1.2.2 ^{137}Cs budget

The ^{137}Cs inventory ($^{137}\text{Cs}_i$) can also be calculated and compared to the ^{137}Cs atmospheric flux ($^{137}\text{Cs}_{atmos}$). However, unlike ^{210}Pb , which is a natural product of uranium-238 decay, ^{137}Cs deposition resulted from atmospheric nuclear weapons tests. Deposition of ^{137}Cs occurred in New Zealand between 1953 and 1984.

The annual deposition rate of ^{137}Cs can be estimated from annual rainfall. In the present study, the annual rainfall record for Whenuapai (site A64761) was used to estimate annual ^{137}Cs atmospheric flux and the decay-corrected cumulative ^{137}Cs inventory (Figure 60). Peak ^{137}Cs deposition in 1964 (blue line) relates to large-scale nuclear weapons tests in the northern hemisphere and minor peaks in the early 1970s are from French weapons tests in the South Pacific. The cumulative ^{137}Cs deposition curve (red) shows that the total ^{137}Cs inventory has declined since the mid-1970s from 0.13 Bq cm $^{-2}$ to 0.029 Bq cm $^{-2}$ by January 2006, when the CWH sediment cores were collected. The decay-corrected ^{137}Cs inventory in 2002 was 0.034 Bq cm $^{-2}$, when sediment cores were first collected at the WT-S1, WT-S2 and WT-S3 sites.

Figure 60

^{137}Cs annual deposition and decay-corrected ^{137}Cs inventory estimated from Whenuapai rainfall.

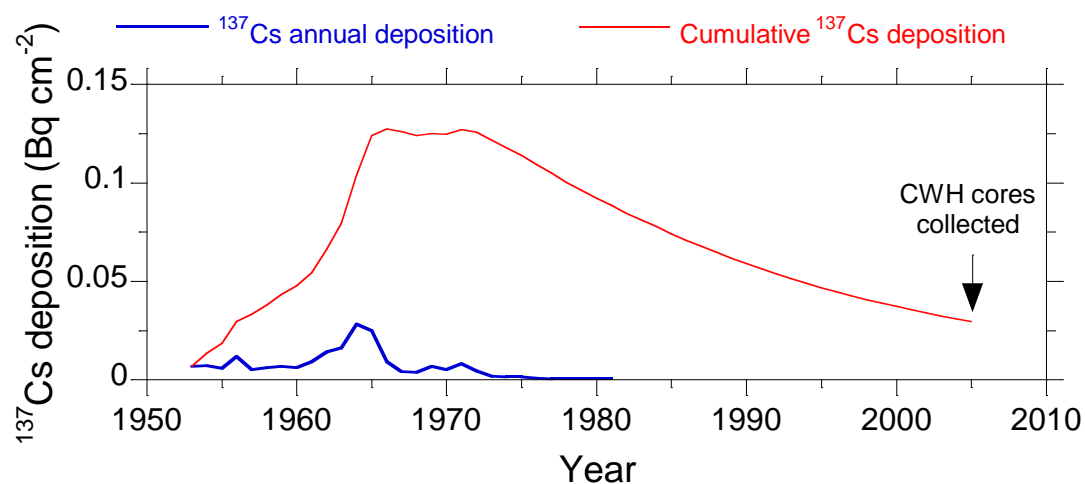


Table 7 presents the ^{137}Cs inventories for the CWH and Shoal Bay sediment cores. This shows that the ^{137}Cs inventories are substantially less than predicted by the decay-corrected cumulative ^{137}Cs flux. This may be due to the fact that ^{137}Cs concentrations are low and close to minimum detectable concentrations.

Table 7

Summary of ^{137}Cs inventories and concentration factor (C) calculated as the ratio $^{137}\text{Cs}_i / ^{137}\text{Cs}_{\text{cum}}$ where $^{137}\text{Cs}_{\text{cum}}$ is 0.03 Bq cm^{-2} for the 2006 cores and 0.034 Bq cm^{-2} for the 2002 cores.

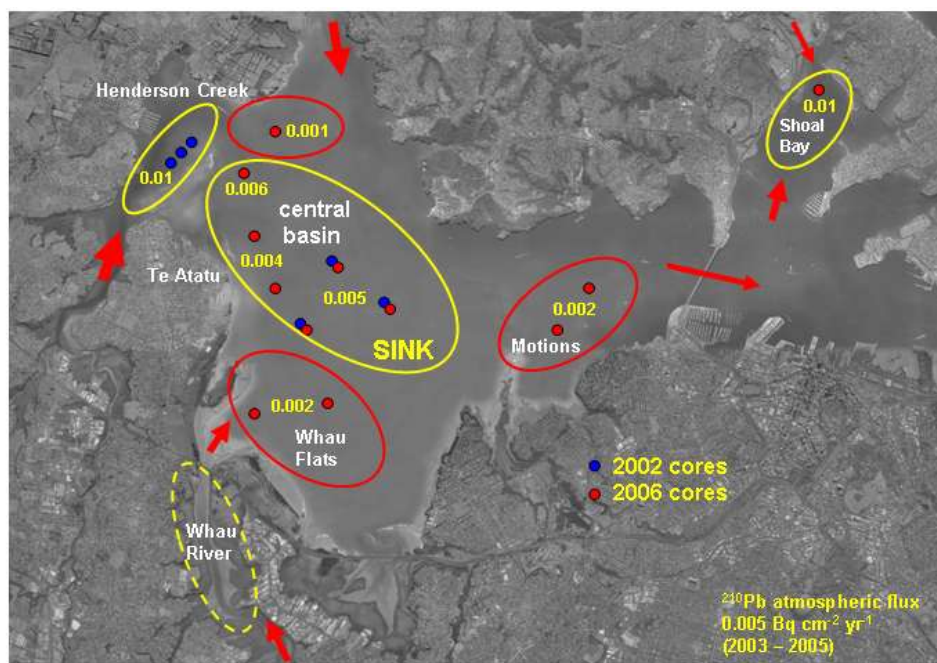
Core site	$^{137}\text{Cs}_i \text{ (Bq cm}^{-2}\text{)}$	C
Intertidal		
HN-I1 2002	0.012	0.34
HN-I2 2002	0.012	0.37
HN-I3 2002	0.024	0.72
HN-I1 2006	0.010	0.35
HN-I2 2006	0.004	0.15
TA-I1	0.089	0.30
TA-I2	0.016	0.54
WH-I1	0.006	0.20
WH-I2	0.002	0.08
SB-I1	0.025	0.86
Subtidal		
WT-S1 2002	0.008	0.24
WT-S2 2002	0.009	0.26
WT-S3 2002	0.009	0.26
WT-S1 2006	0.012	0.42
WT-S2 2006	0.010	0.33
WT-S3 2006	0.011	0.38
MO-S1	0.006	0.20
MO-S2	0.002	0.07

5.1.2.3 Fine sediment fate

Figure 61 presents a conceptual model of the dispersal and fate of fine sediment in the Central Waitemata Harbour over the last 50 years. Fine sediment is delivered to the tidal creeks fringing the CWH. The Whau River and Henderson Creek have substantially infilled with fine sediment. The sediment that does escape the tidal creeks is widely dispersed. Shoal Bay and the central basin of the Central Waitemata Harbour are long-term sinks for fine sediments. Intertidal flats and shallow subtidal flats provide temporary sinks for fine sediments.

Figure 61

Conceptual model of fine sediment fate in the Central Waitemata Harbour and Shoal Bay. Long-term sediment sinks are shown by yellow ellipses. Temporary sinks are shown by red ellipses. Red arrows represent the relative size of sediment inputs and transfers.



5.1.3 Comparison with previous studies

SARs determined in this study are similar at intertidal (3.2 mm yr^{-1} , range: $0.7\text{--}6.8 \text{ mm yr}^{-1}$) and subtidal sites (3.3 mm yr^{-1} , range: $2.2\text{--}5.3 \text{ mm yr}^{-1}$), although SAR is more variable at intertidal sites.

In a study of ten east-coast Auckland estuaries, Swales et al. (2002a) found that intertidal flats (4.7 mm yr^{-1}) are accumulating sediment more rapidly than subtidal areas (2.9 mm yr^{-1}). The size of these estuaries varied from 1.4 km^2 (Okura) to 80 km^2 (Waitemata), with most being less than 12 km^2 in area.

The higher SAR measured on intertidal flats in Auckland estuaries partly reflects the close proximity of these environments to catchment outlets, which discharge sediment to estuaries during storms. In the CWH, the ^{210}Pb inventory data (Figure 61) and sediment-transport modelling (Oldman et al. 2008b) indicate that mud ($< 63 \mu\text{m}$) deposited on the intertidal flats is being winnowed from the bed by waves, redistributed by currents and redeposited in the less energetic central basin, which represents a long-term mud sink. The sand fraction is substantially less mobile than the silt. Over time, redistribution of fine sediments by waves and currents removes differences in sedimentation rates between intertidal and subtidal environments in the CWH.

Fine sediments are also accumulating in the tidal creeks (Henderson Creek ^{210}Pb SAR $2.6\text{--}5.1 \text{ mm yr}^{-1}$, Swales et al. 2002a) and in mangrove habitats that fringe the CWH, as observed in other Auckland estuaries (eg, Craggs et al. 2001). Sedimentation rates of $20\text{--}30 \text{ mm yr}^{-1}$ over the last ~ 50 years are typical of Auckland's tidal creeks (Vant et al.

1993; Oldman and Swales, 1999; Swales et al. 1997; Swales et al. 2002b). It is likely that the sediment trapping in tidal creeks is now less effective than in the past because of reduced accommodation space.

5.2 Sediment mixing

The ^7Be and unsupported ^{210}Pb profiles preserved in cores show that surface sediments are well mixed to 1–5 cm depth and to ≥ 3 cm depth in 60 per cent of cases.

A feature of sediment mixing in the Waitemata Harbour is that the maximum ^7Be depth coincides with the surface mixed layer (SML) inferred from the unsupported ^{210}Pb profiles. The SML is characterised by uniform unsupported ^{210}Pb concentrations, which indicate complete mixing of the sediment. The significance of the ^7Be profile matching the ^{210}Pb SML is that this surface mixing is occurring over ≤ 100 days.

The maximum residence time of sediments within the SML typically varies between four and 14 years. For core WH-I2 (Whau intertidal) the estimated residence time of 29 years is longer than at other sites because of the low rate of sediment accumulation at this site. Sediments are eventually removed from the SML by burial. This sediment accumulation zone below the SML is indicated by the exponential reduction in ^{210}Pb concentration with depth.

The bioturbation index shows the potential for bioturbation to 10 cm depth or more at most sites. The bioturbation index was 120–970 at sites in the central basin and 2300–5600 at intertidal sites ringing the subtidal basin. The substantially lower values for the index in the subtidal sites reflect lower densities and sizes of animals, and suggests that sediment mixing is less intense than at intertidal sites. Of the intertidal sites, the maximum index occurred at site WH-I2 on the Whau intertidal flats. The SAR of 0.7 mm yr^{-1} at this site is substantially lower than measured elsewhere in the CWH (2.2 – 5.4 mm yr^{-1}). In general, the quantity of sediment mixed as a proportion of the total sediment volume will vary inversely with SAR.

X-radiographs typically do not preserve evidence of animal burrows or physical bedding below the ^7Be SML. Cores WT-S1, WH-I1 and WH-I2 preserve worm burrows infilled with mud, and cores WH-I2 and SB-I1 contain examples of millimetre-scale bedding.

In the present study, the maximum bioturbation depths of 10 cm+ inferred from the benthic-community data, x-radiographs and animal life-histories are substantially greater than the ≤ 5 cm SML depth determined from the ^7Be and unsupported ^{210}Pb profiles. Uniform concentrations of these radioisotopes to ≤ 5 cm depth within the SML indicate complete mixing of sediments. That homogenisation does not occur below the 5 cm deep SML does not preclude deeper mixing by animals, but does indicate that the rate of sediment mixing is low in sediments below 5 cm depth.

6 Acknowledgements

We thank Ms Emma Rush of the Department of Conservation Auckland Conservancy for expediting the permit to work within the Motu Manawa (Pollen Island) Marine Reserve. We are also grateful to the staff at NIWA Auckland who assisted with surface-sediment sampling, Marieke Vankooten and Margaret McMonagle (NIWA Hamilton) for preparing sediment samples for chemical analyses and Matt Lewis (NIWA Hamilton) for assistance with LISST field work. Dr Sam Bentley (Earth Sciences Department, Memorial University, New Foundland, Canada) provided x-ray images of the sediment cores during his sabbatical at NIWA, Hamilton.

7 References

- ABRAHIM, G.; PARKER, R., 2002. Heavy-metal contaminants in Tamaki estuary: impacts of city development and growth, Auckland, New Zealand. *Environmental Geology* 42: 883–890.
- AGRAWAL, Y.C.; POTTSMTIH, H.C., 2000. Instruments for particle size and settling velocity observations in sediment transport. *Marine Geology* 168: 89–114.
- AHRENS, M.; SWALES, A.; LEWIS, M.; HART, C., 2008. Central Waitemata Harbour Contaminant Study. Trace metals in harbour sediments. Prepared by NIWA Ltd for Auckland Regional Council. Auckland Regional Council Technical Report 2008/035
- ALEXANDER, C.R.; SMITH, R.G.; CALDER, F.D.; SCHROPP, S.J.; WINDOM, H.L., 1993. The historical record of metal enrichment in two Florida estuaries. *Estuaries* 16(3B): 627–637.
- ALLER, R.C., 1982. The effects of macrobenthos on chemical properties of marine sediment and overlying water, p 53–101. In: McCall, P.L. and Tevesz, M.J.S. Animal-sediment relations: the biogenic alteration of sediments, *Volume 2: Topics in Geobiology*. Plenum Press, New York, 336 p.
- BENOIT, G.; ROZAN, T.F.; PATTON, P.C.; ARNOLD, C.L., 1999. Trace metals and radionuclides reveal sediment sources and accumulation rates in Jordan Cove, Connecticut. *Estuaries* 22(1): 65–80.
- BROMLEY, R.G., 1996. *Trace fossils: biology, taphonomy and applications*, Second edition. Chapman and Hall, London, 361 p.
- CHAGUÉ-GOFF, C.; NICHOL, S.L.; JENKINSON, A.V.; HEIJNIS, H., 2000. Signatures of natural catastrophic events and anthropogenic impact in an estuarine environment, New Zealand. *Marine Geology* 167: 285–301.
- CRAGGS, R.; HOFSTRA, D.; ELLIS, J.; SCHWARZ, A.; SWALES, A.; NICHOLLS, P.; HEWITT, J.; OVENDEN, R.; PICKMERE, S., 2001. *Physiological responses of mangroves and saltmarsh to sedimentation*. NIWA Client Report ARC01268/1, 78 p.
- DENYER, K.; CUTTING, M.; CAMPBELL, G.; GREEN, C.; HILTON, M., 1993. *Waitakere Ecological District: Survey Report No. 15* for the Protected Natural Areas Programme, Auckland Regional Council.

- DYER, K.R., 1986. *Coastal and estuarine sediment dynamics*. John Wiley and Sons, Chichester. 342 p.
- FULLER, C.C.; VAN GEEN, A.; BASKARAN, M.; ANIMA, R., 1999. Sediment chronology in San Francisco Bay, California, defined by ^{210}Pb , ^{234}Th , ^{137}Cs and $^{239,240}\text{Pb}$. *Marine Chemistry* 64: 7–27.
- GOLDBERG, E.D.; KLODE, M., 1962. Geochronological studies of deep sea sediments by the ionium/thorium method. *Geochimica et Cosmochimica Acta* 26: 417–450.
- GREEN, M.O.; BLACK, K.P.; AMOS, C.L., 1997. Control of estuarine sediment dynamics by interactions between currents and waves at several scales. *Marine Geology* 144: 97–116.
- GUINASSO, N.L. JR.; SCHINK, D.R., 1975. Quantitative estimates of biological mixing rates in abyssal sediments. *Journal of Geophysical Research* 80: 3032–3043.
- HALLIDAY, J.; HEWITT, J.; LUNDQUIST, C., 2006. *Central Waitemata Harbour ecological monitoring: 2000-2006*. NIWA Client Report: HAM2006-007. Prepared for Auckland Regional Council, 101 p.
- HAYWOOD, B.W.; MORLEY, M.S.; STEPHENSON, A.B.; BLOM, W.M.; GRENFELL, H.R.; PRASAD, R.; ROGAN, D.; THOMPSON, F.; CHEETHAM, J.; WEBB, M., 1999. *Intertidal and subtidal biota and habitats of the central Waitemata harbour*. Auckland Regional Council, Technical Publication No. 127. 41 p.
- HILL, P.S.; SYVITSKI, J.P.; COWAN, E.A.; POWELL, R.D., 1998. In situ observations of flocc settling velocities in Glacier Bay, Alaska. *Marine Geology* 145: 85–94.
- KHELIFA, A. & HILL, P.S., 2006. Models for effective density and settling velocity of flocs. *Journal of Hydraulic Research* 44(3): 390–401.
- LUNDQUIST, C.; VOPEL, K.; THRUSH, S.F.; SWALES, A., 2003. *Evidence for the effects of catchment sediment run-off preserved in estuarine sediments: Phase III macrofaunal communities*. Auckland Regional Council Technical Publication 222. 48 p.
- MATTHEWS, K.M., 1989. *Radioactive fallout in the South Pacific a history. Part 1. Deposition in New Zealand*. Report NRL 1989/2. National Radiation Laboratory, Christchurch, New Zealand.
- OLDFIELD, F.; APPLEBY, P.G., 1984. Empirical testing of ^{210}Pb -dating models for lake sediments. In: *Lake sediments and environmental history*, Haworth and Lund (eds): pp 93–124.

- OLDMAN, J.W.; SWALES, A., 1999. *Maungamaungaroa estuary numerical modelling and sedimentation*. NIWA Client Report ARC70224 for Auckland Regional Council.
- OLDMAN, J.W.; HANCOCK, N.; LEWIS, M., 2008. *Central Waitemata Harbour Contaminant Study. Harbour Hydrodynamics and Sediment-Transport Fieldwork*. Prepared by NIWA Ltd for Auckland Regional Council. Auckland Regional Council Technical Report 2008/036
- OLDMAN, J.W.; GORMAN, R.; LEWIS, M., 2008b. *Central Waitemata Harbour Contaminant Study. Harbour hydrodynamics and sediment-model calibration and implementation*. Prepared by NIWA Ltd for Auckland Regional Council. Auckland Regional Council Technical Report 2008/037
- OLSEN, C.R.; SIMPSON, H.J.; PENG, T.-H.; BOPP, R.F.; TRIER, R.M., 1981. Sediment mixing and accumulation rate effects on radionuclide depth profiles in Hudson Estuary sediments. *Journal of Geophysical Research* 86 (C11): 11020–11028.
- PANNATIER, Y., 1996. VARIOWIN: Software for spatial data analysis in 2D. Statistics and Computing Series. Springer-Verlag, New York. 91 p.
- RITCHIE, J.C.; MCHENRY, J.R., 1989. *Application of radioactive fallout cesium-137 for measuring soil erosion and sediment accumulation rates and patterns: A review with bibliography*. Hydrology Laboratory, Agriculture Research Service, U.S. Department of Agriculture, Maryland.
- ROBBINS, J.A.; EDGINGTON, D.N., 1975. Determination of recent sedimentation rates in Lake Michigan using ^{210}Pb and ^{137}Cs . *Geochimica et Cosmochimica Acta* 39: 285–304.
- SHARMA, K.; GARDNER, L.R.; MOORE, W.S.; BOLLINGER, M.S., 1987. Sedimentation and bioturbation in a saltmarsh revealed by ^{210}Pb , ^{137}Cs , and ^7Be studies. *Limnology and Oceanography* 32(2): 313–326.
- SOMMERFIELD, C.K.; NITTROUER, C.A.; ALEXANDER, C.R., 1999. ^7Be as a tracer of flood sedimentation on the Northern California margin. *Continental Shelf Research* 19: 335–361.
- SWALES, A.; HUME, T.M.; OLDMAN, J.W.; GREEN, M.O., 1997. *Sedimentation history and recent human impacts*. NIWA Client Report ARC60201 for Auckland Regional Council, 90 p.
- SWALES, A.; HUME, T.M.; MCGLONE, M.S.; PILVIO, R.; OVENDEN, R.; ZVIGUINA, N.; HATTON, S.; NICHOLLS, P.; BUDD, R.; HEWITT, J.; PICKMERE, S.; COSTLEY, K., 2002a. *Evidence for the physical effects of catchment*

sediment run-off preserved in estuarine sediments: Phase II (field study).
NIWA Client Report HAM2002-067.

SWALES, A.; WILLIAMSON, R.B.; VAN DAM, L.F.; STROUD, M.J.; MCGLONE, M.S., 2002b. Reconstruction of urban stormwater contamination of an estuary using catchment history and sediment profile dating. *Estuaries* 25(1): 43–56.

SWALES, A.; BENTLEY, S.J.; MCGLONE, M.S.; OVENDEN, R.; HERMANSPAHN, N.; BUDD, R.; HILL, A.; PICKMERE, S.; HASKEW, R.; OKEY, M.J., 2005. *Pauatahanui Inlet: effects of historical catchment landcover changes on estuary sedimentation*. NIWA Client Report HAM2004-149 for Wellington Regional Council and Porirua City Council.

VALETTE-SILVER, N.J., 1993. The use of sediment cores to reconstruct historical trends in contamination of estuarine and coastal sediments. *Estuaries* 16(3B): 577-588.

VANT, W.N.; WILLIAMSON, R.B.; HUME, T.M.; DOLPHIN, T.J., 1993. *Effects of future urbanisation in the catchment of Upper Waitemata Harbour*. NIWA Consultancy Report No. ARC220.

WILLIAMSON, R.B.; MORRISEY, D.J., 2000. Stormwater contamination of urban estuaries. 1. Predicting the build up of heavy metals in sediments. *Estuaries* 23(1): 56–66.

WISE, S., 1977. *The use of radionuclides ^{210}Pb and ^{137}Cs in estimating denudation rates and in soil erosion measurement*. Occasional Paper No. 7 University of London, King's College, Department of Geography, London.

Personal Communication

PETCHY, F., 2007. Waikato University Radiocarbon Dating Laboratory.

8 Appendix 1: Location of Surface-sediment Samples and Dating Cores

Table 8

Location of surface sediment samples in the Central Waitemata Harbour. New Zealand Map Grid (NZMG) co-ordinates.

Sample site	Date sampled	NZMG Easting	NZMG Northing
1	19 January 2006	2660208.9	6487336.6
3	19 January 2006	2659514.9	6487131.5
4	19 January 2006	2660341.9	6487065.4
5	19 January 2006	2658637.5	6486759.0
6	19 January 2006	2659342.0	6486733.1
7	19 January 2006	2660184.7	6486693.3
8	19 January 2006	2660394.3	6486642.5
9	19 January 2006	2659053.2	6486474.5
10	19 January 2006	2659435.4	6486217.3
11	19 January 2006	2658781.0	6486108.0
12	19 January 2006	2659668.3	6486167.3
13	19 January 2006	2660038.9	6486132.3
14	19 January 2006	2660558.3	6486220.9
15	19 January 2006	2659318.3	6485928.8
16	19 January 2006	2660693.3	6486054.0
17	19 January 2006	2659789.0	6485719.8
20	19 January 2006	2658714.7	6485450.0
24	19 January 2006	2659602.3	6485209.6
27	19 January 2006	2658714.1	6484867.2
29	19 January 2006	2660086.6	6484878.2
30	19 January 2006	2660571.5	6484803.2
32	19 January 2006	2659669.7	6484545.6
34	19 January 2006	2658747.0	6484038.6
35	19 January 2006	2659406.2	6484029.1
36	19 January 2006	2660037.4	6484004.5
37	19 January 2006	2660578.0	6483998.4
38	19 January 2006	2661210.3	6483984.8
39	19 January 2006	2661914.8	6484147.4
41	19 January 2006	2662544.3	6484172.6
43	20 March 2006	2663171.8	6484136.8
44	19 January 2006	2663426.8	6484219.4
45	19 January 2006	2664127.1	6484347.5
48	19 January 2006	2663773.8	6484123.7
49	20 March 2006	2664398.8	6484145.5
50	19 January 2006	2664577.8	6484265.1

Sample site	Date sampled	NZMG Easting	NZMG Northing
51	19 January 2006	2664970.0	6484152.9
52	19 January 2006	2665614.3	6483806.9
57	19 January 2006	2662942.4	6483777.3
59	19 January 2006	2658706.3	6483548.8
60	19 January 2006	2659387.5	6483527.7
61	19 January 2006	2660027.7	6483507.5
62	19 January 2006	2660575.2	6483492.3
63	19 January 2006	2661219.9	6483520.7
64	19 January 2006	2661848.6	6483508.2
65	19 January 2006	2662538.1	6483497.9
66	19 January 2006	2663177.3	6483477.4
67	19 January 2006	2663862.7	6483440.4
68	19 January 2006	2664483.3	6483423.5
74	20 January 2006	2663427.1	6483119.4
75	20 January 2006	2664796.7	6483168.5
76	20 January 2006	2665274.8	6483296.5
77	20 January 2006	2658762.2	6482938.3
78	20 January 2006	2659387.5	6482933.9
79	20 January 2006	2660042.5	6482943.3
80	20 January 2006	2660564.2	6482933.1
81	20 March 2006	2661218.6	6482915.8
82	20 January 2006	2661855.3	6482902.1
83	20 January 2006	2662468.1	6482897.7
84	20 January 2006	2662969.6	6482856.6
85	20 January 2006	2663797.1	6482840.1
86	20 January 2006	2664407.1	6482873.4
87	20 January 2006	2658699.8	6482295.8
88	20 January 2006	2659304.8	6482444.9
89	20 January 2006	2660444.9	6482535.8
90	20 January 2006	2660909.2	6482557.8
91	20 March 2006	2662310.1	6482486.8
92	20 January 2006	2662709.0	6482494.4
93	20 January 2006	2663174.0	6482549.5
94	20 January 2006	2663506.6	6482500.7
95	20 January 2006	2664089.5	6482519.0
96	20 January 2006	2659950.3	6482335.8
100	20 January 2006	2662436.5	6482246.8
101	20 January 2006	2663078.2	6482221.8
102	20 January 2006	2663773.7	6482203.4
103	20 January 2006	2638567.2	6481899.9
104	20 January 2006	2660385.9	6481851.0
105	20 March 2006	2660979.3	6482088.0
106	20 January 2006	2662180.6	6481941.1
108	20 January 2006	2663241.6	6481915.5
109	20 January 2006	2664038.9	6482087.1
110	20 January 2006	2658562.1	6481635.8
111	20 January 2006	2659266.8	6481636.5

Sample site	Date sampled	NZMG Easting	NZMG Northing
112	20 January 2006	2659712.4	6481620.1
113	20 March 2006	2660722.4	6481725.7
114	20 January 2006	2661211.6	6481655.0
115	20 January 2006	2661800.4	6481657.8
116	20 January 2006	2663014.6	6481713.6
117	20 January 2006	2658237.2	6481318.3
119	20 January 2006	2660902.6	6481361.4
120	20 January 2006	2661704.1	6481299.0
121	20 January 2006	2661972.4	6481335.8
122	20 January 2006	2659237.7	6481062.1
123	20 January 2006	2659835.1	6481053.8
124	20 January 2006	2660521.6	6481035.9
125	20 January 2006	2661163.6	6481031.0
126	20 January 2006	2661840.9	6481001.0
127	20 January 2006	2661202.4	6480735.0
128	20 January 2006	2661674.7	6480713.5
129	20 March 2006	2659430.2	6482242.7
133	20 January 2006	2658447.1	6485823.4

Table 9

Location and details of surface sediment samples collected in Shoal Bay. New Zealand Map Grid (NZMG) co-ordinates.

Sample site	Date sampled	NZMG Easting	NZMG Northing
SB-1	19 January 2006	2667971.0	6487694.8
SB-2	19 January 2006	2667762.2	6487611.4
SB-5	19 January 2006	2668270.3	6487144.8
SB-6	19 January 2006	2667565.1	6486618.7
SB-7	19 January 2006	2668259.3	6486607.8
SB-9	19 January 2006	2667087.9	6486325.4
SB-11	19 January 2006	2668537.5	6486161.4
SB-12	19 January 2006	2667013.8	6485886.3
SB-13	19 January 2006	2667516.6	6485902.6
SB-14	19 January 2006	2668118.4	6485917.0
SB-15	19 January 2006	2666822.6	6485526.1
SB-19	19 January 2006	2666848.1	6485288.1
SB-20	19 January 2006	2667569.0	6485281.1
SB-29	19 January 2006	2667613.8	6484681.9
SB-30	19 January 2006	2668172.2	6484628.3
SB-32	19 January 2006	2666544.8	6484505.1
SB-34	21 March 2006	2668063.5	6484546.2

Table 10

Location and sampling details of sediment-dating cores collected in the Central Waitemata Harbour and Shoal Bay. New Zealand Map Grid (NZMG) co-ordinates.

Core site	Date	Time (NZST)	Water depth (m)	NZMG Northing	NZMG Easting
Intertidal					
HN-I1	8-Feb-2006	1437	2.2	6486038	2658904
HN-I2	8-Feb-2006	1631	1.9	6486767	2659597
HN-I3	8-Feb-2006	1732	2.5	6486358	2660242
TA-I1	9-Feb-2006	1618	2.5	6484836	2658998
TA-I2	9-Feb-2006	1516	2.3	6483971	2659311
TA-I3	9-Feb-2006	1440	1.2	6483300	2659096
WH-I1	9-Feb-2006	1410	1.2	6481975	2659061
WH-I2	9-Feb-2006	1326	1.5	6482187	2660338
WH-I3	9-Feb-2006	0810	1.2	6481341	2659888
SB-I1	20-Mar-2006	1135	2.0	6487042	2667910
SB-I2	20-Mar-2006	1225	1.5	6486460	2668421
SB-I3	20-Mar-2006	1252	1.8	6486467	2667481
Subtidal					
WT-S1	9-Feb-2006	0943	1.6	6484166	2660433
WT-S2	9-Feb-2006	0905	3.0	6483673	2661318
WT-S3	9-Feb-2006	1115	1.8	6483344	2659995
ME-S1	9-Feb-2006	1215	2.0	6482661	2661886
ME-S2	9-Feb-2006	1145	2.6	6483605	2662132
ME-S3	9-Feb-2006	1244	2.3	6483015	2662791
MO-S1	10-Feb-2006	0831	2.2	6483505	2663916
MO-S2	10-Feb-2006	0910	3.2	6484115	2664316
MO-S3	10-Feb-2006	0751	3.9	6483374	2664814

9 Appendix 2: Spatial Distribution of Sediments – Geostatistics

Experimental variograms were constructed using data from 112 sample sites and modelled using the Variowin 2.2 software (Pannatier 1996). The presence of well-defined “sills” in the variograms indicated that the data were stationary and did not require de-trending. The variogram models are continuous mathematical functions that provide information about the spatial continuity of any spatially varying parameter at un-sampled locations. The fitted models were used to customise the kriging algorithm, which is a commonly used spatial-estimation technique. We employed the ordinary kriging (OK) method. An example variogram-model fit for the percentage $\leq 250 \mu\text{m}$ size fraction in the central harbour sediments is presented in Figure 62. The tidal channels and Meola (Te Tokaroa) Reef were excluded from the kriging process using a blanking file. The channel sediments are a coarse shell/gravel lag deposit that differs markedly from sediments in intertidal and subtidal areas.

The goodness-of-fit of the OK interpolations for each sediment parameter was assessed by cross-validation. Cross-validation (CV) involves temporarily discarding samples one at a time and estimating the parameter using nearby samples and the customised kriging procedure. This process generates estimates that can be compared to measurements. The results of a CV exercise can be misleading if the data are highly clustered and/or there are large gaps in the sampled area. In the present study samples were collected on a semi-regular grid so that CV provides a reasonable assessment of the OK errors. Table 11 provides details of the experimental and model variogram fits and cross-validation results for the ordinary-kriging interpolations.

Figure 62

Variogram-model fit to the experimental (sample) variogram data for the percentage $\leq 250 \mu\text{m}$ size fraction, CWH sediments. The fitted model: spherical, range=784 m, sill (semi-variance) = 120, anisotropy = 1. The dashed horizontal line represents the sample variance.

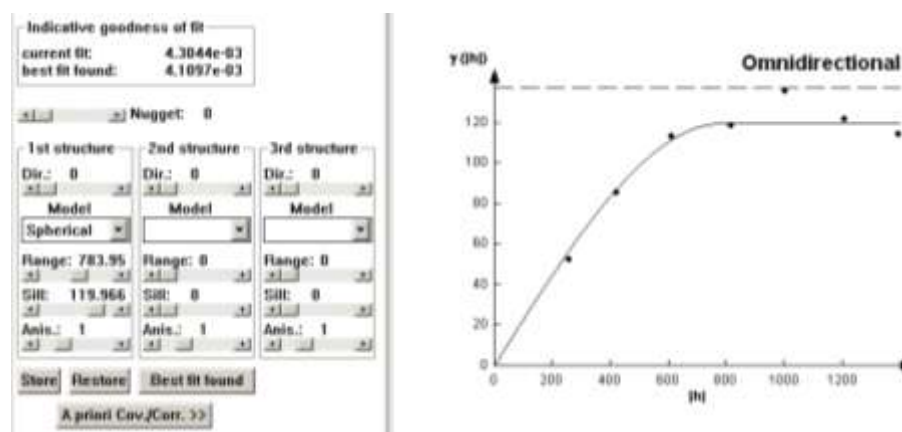


Table 11

Central Waitemata Harbour surface-sediment particle size parameters: experimental and model semi-variogram attributes and cross-validation results for the ordinary-kriging spatial interpolations. Note: CV results are for the standard mean and root-mean-squared standard mean errors. Sample standard deviation (*s*).

Parameter	Experimental variogram		Variogram model			Cross validation errors	
	Lag (m)	Lag Tolerance (m)	Type	Sill	Range (m)	Std mean	RMS Std
Mean	250	150	Spherical	1510	840	0.009	1.04
Median	500	250	Exponential	780	720	0.020	0.99
s	350	200	Spherical	700	960	-0.035	1.02
s %	400	250	Spherical	83	872	-0.062	1.14
<62.5 μ m	450	250	Gaussian	40	490	-0.0005	1.21
<25 μ m	300	300	Gaussian	19	490	-0.0017	1.26

Spatial estimation or interpolation using ordinary kriging was implemented using the ESRI ArcGIS Geostatistical Analyst. The modelled semi-variogram range, sill, lag-size and number of lags were used to customise the OK procedure. A circular search area was used based on the omni-directional semi-variograms with a minimum of three and a maximum of seven neighbours used.

The cross-validation analysis provides various estimation-error measures. In the present study we have adopted the standard mean error and the RMS standard error. The mean standard error should be as small as possible and the RMS standardised error should be close to one. Table 11 shows that the OK estimates of mean and median particle size are more accurate than the estimates for the mud and less than 25 μ m fractions.

10 Appendix 3: Dating of Estuarine Sediments

Sediment cores were dated using beryllium-7 (^7Be , $\frac{1}{2}$ -life 53 days), caesium-137 (^{137}Cs , $\frac{1}{2}$ -life 30 years) and lead-210 (^{210}Pb , $\frac{1}{2}$ -life 22.3 years) concentration profiles in sediment cores. Radioisotope (activity) concentrations are expressed in Becquerels (Bq), which is the S.I. unit of radioactivity. The Bq is equivalent to one radioactive disintegration per second.

10.1 ^{137}Cs dating

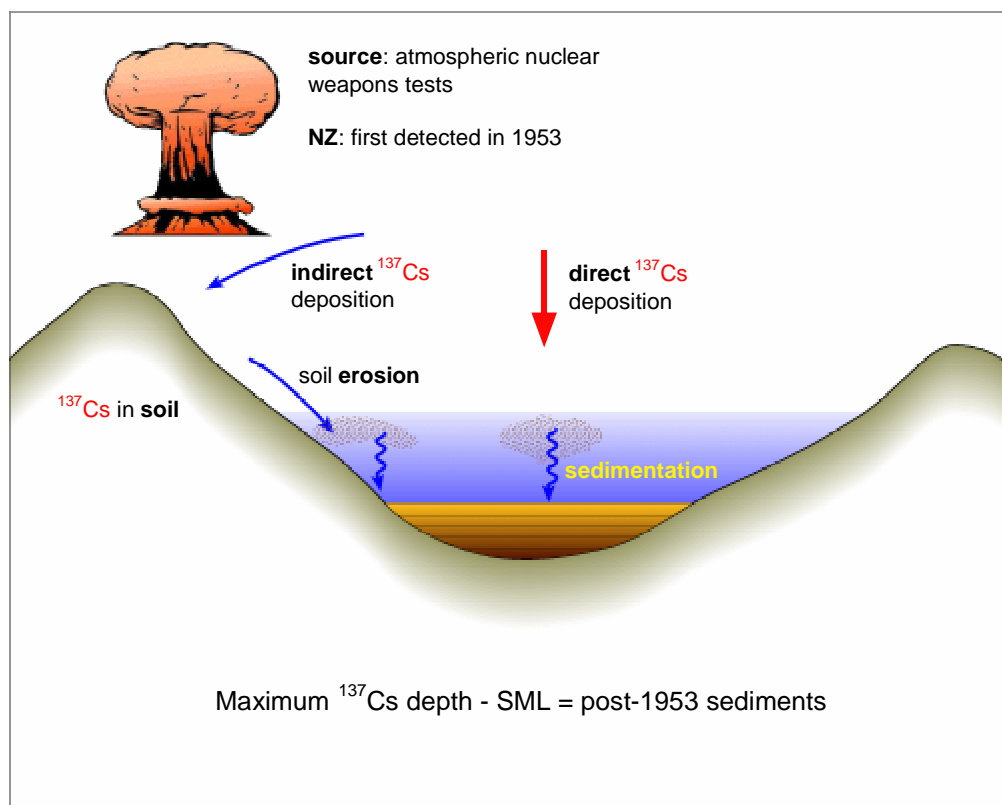
^{137}Cs was introduced to the environment by atmospheric nuclear weapons tests in 1953, 1955–1956 and 1963–1964. A minor ^{137}Cs deposition peak was also detected in New Zealand as a result of French nuclear-weapons tests in the South Pacific during the early 1970s. Peaks in annual ^{137}Cs deposition corresponding to these dates are the usual basis for dating sediments (Wise 1977, Ritchie and McHenry, 1989). Although direct atmospheric deposition of ^{137}Cs into estuaries is likely to have occurred, ^{137}Cs is also incorporated into catchment soils, which are subsequently eroded and deposited in estuaries (Figure 63). In New Zealand, ^{137}Cs deposition was first detected in 1953 and its annual deposition was measured at several locations until 1985. Annual ^{137}Cs deposition can be estimated from rainfall using known linear relationships between rainfall and Strontium-90 (^{90}Sr) and measured $^{137}\text{Cs}/^{90}\text{Sr}$ deposition ratios (Matthews 1989). Experience shows that ^{137}Cs profiles measured in estuarine sediments bear no relation to the record of annual ^{137}Cs deposition (ie, 1955–1956 and 1963–1964 ^{137}Cs -deposition peaks absent), but rather preserve a record of direct and indirect (ie, soil erosion) atmospheric deposition since 1953 (Swales et al. 2002a). The maximum depth of ^{137}Cs occurrence in sediment cores, corrected for sediment mixing is taken to coincide with the year 1953, when ^{137}Cs deposition was first detected in New Zealand. We assume that there is a negligible delay in initial atmospheric deposition of ^{137}Cs in estuarine sediments (eg, ^{137}Cs scavenging by suspended particles), whereas there is likely to have been a small time-lag (ie, less than 1 yr) in ^{137}Cs inputs to estuaries from topsoil erosion, which would coincide with the occurrence of floods.

If a surface mixed layer (SML) is evident in a core, as shown by an x-ray image and/or a tracer profile (eg, ^7Be , ^{210}Pb) then ^{137}Cs is likely to have been rapidly mixed through the SML. Therefore to calculate time-averaged sedimentation rates, the maximum depth of ^{137}Cs occurrence is reduced by the maximum depth of the SML.

Uncertainty in the maximum depth of ^{137}Cs ($^{137}\text{Cs}_{\text{max}}$) results from the depth interval between sediment samples and the minimum detectable concentration of ^{137}Cs , which is mainly determined by sample mass and counting time. The 1963–1964 ^{137}Cs deposition peak was about five times greater than the deposition plateau that occurred between 1953 and 1972. Thus, depending on the sample size, there is uncertainty in the age of $^{137}\text{Cs}_{\text{max}}$ (ie, 1953–1963). To reduce this uncertainty, we have maximised the sample mass that is analysed.

Figure 63

^{137}Cs pathways to estuarine sediments.



10.2 ^{210}Pb dating

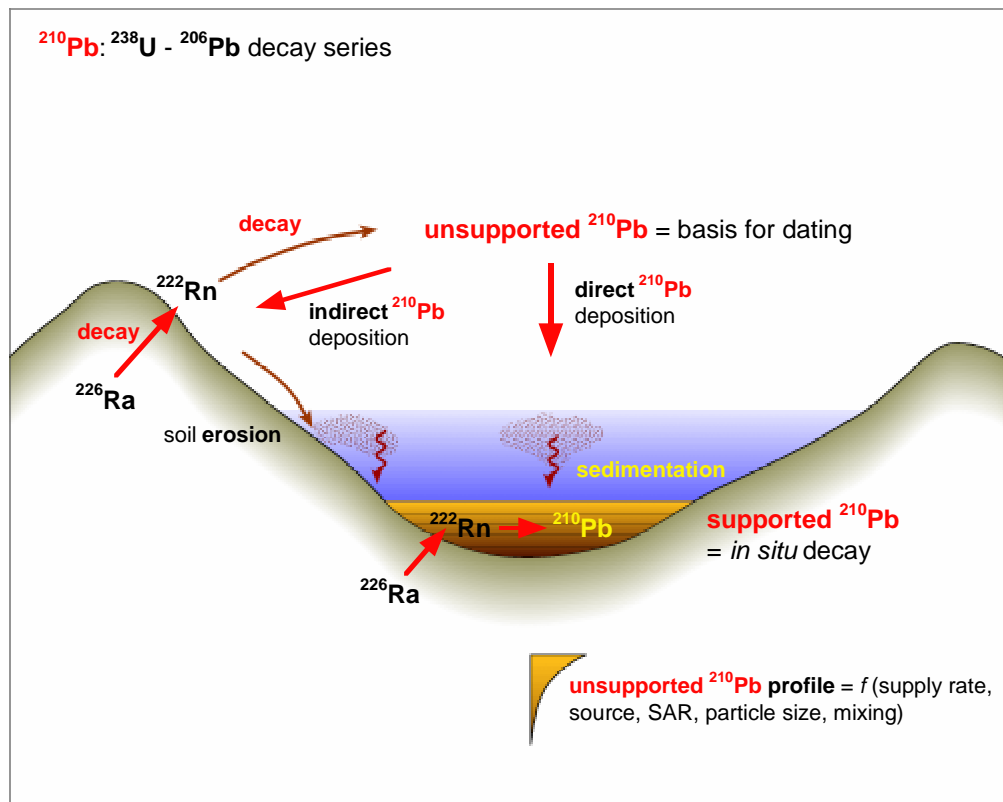
^{210}Pb (half-life 22.3 yr) is a naturally occurring radioisotope that has been widely applied to dating recent sedimentation (ie, last 150 yr) in lakes, estuaries and the sea (Figure 64). ^{210}Pb is an intermediate decay product in the uranium-238 (^{238}U) decay series and has a radioactive decay constant (k) of 0.03114 yr^{-1} . The intermediate parent radioisotope radium-226 (^{226}Ra , half-life 1622 years) yields the inert gas radon-222 (^{222}Rn , half-life 3.83 days), which decays through several short-lived radioisotopes to produce ^{210}Pb . A proportion of the ^{222}Rn gas formed by ^{226}Ra decay in catchment soils diffuses into the atmosphere where it decays to form ^{210}Pb . This atmospheric ^{210}Pb is deposited at the earth's surface by dry deposition or rainfall. The ^{210}Pb in estuarine sediments has two components: supported ^{210}Pb derived from in situ ^{222}Rn decay (ie, within the sediment column) and an unsupported ^{210}Pb component derived from atmospheric fallout. This unsupported ^{210}Pb component of the total ^{210}Pb concentration in excess of the supported ^{210}Pb value is estimated from the ^{226}Ra assay (see below). Some of this atmospheric unsupported ^{210}Pb component is also incorporated into catchment soils and is subsequently eroded and deposited in estuaries. Both the direct and indirect (ie, soil inputs) atmospheric ^{210}Pb input to receiving environments, such as estuaries, is termed the unsupported or excess ^{210}Pb .

The concentration profile of unsupported ^{210}Pb in sediments is the basis for ^{210}Pb dating (Oldfield & Appleby, 1984). In the absence of atmospheric (unsupported) ^{210}Pb fallout, the ^{226}Ra and ^{210}Pb in estuary sediments would be in radioactive equilibrium,

which results from the substantially longer ^{226}Ra half-life. Thus, the ^{210}Pb concentration profile would be uniform with depth. However, what is typically observed is a reduction in ^{210}Pb concentration with depth in the sediment column. This is due to the addition of unsupported ^{210}Pb directly or indirectly from the atmosphere that is deposited with fine sediment particles on the bed.

Figure 64

^{210}Pb pathways to estuaries.



A substantial proportion of the radioisotope concentration is associated with the clay-fraction. This unsupported ^{210}Pb component decays with age ($k = 0.03114 \text{ yr}^{-1}$) as it is buried through sedimentation. In the absence of sediment mixing (see below) the unsupported ^{210}Pb concentration displays an exponential decay profile with depth in the sediment column. Thus, the age of the sediment increases as the concentration of unsupported ^{210}Pb decreases with increasing depth in the sediment column. The validity of the ^{210}Pb dating rests on how accurately the ^{210}Pb delivery processes to the estuary are modelled, and in particular the rates of ^{210}Pb and sediment inputs (ie, constant versus time variable).

10.3 Sediment accumulation rates (SAR)

Sedimentation rates calculated from cores are *net average* sediment accumulation rates (SAR), which are usually expressed in units of mm yr^{-1} . These SAR are net values because cores integrate the effects of all the processes, which influence sedimentation at a given location, usually over years, decades or centuries. However,

at short time scales (ie, seconds–months), sediment may be deposited and then subsequently resuspended by tidal currents and/or waves. Thus, over the long-term, sedimentation rates derived from cores represent the net or cumulative effect of potentially many cycles of sediment deposition and re-suspension. Less disrupted sedimentation histories are found where sediment mixing is limited. The effects of bioturbation on sediment profiles and dating resolution reduce as SAR increase (Valette-Silver 1993). Net sedimentation rates statistics also mask the fact that estuary sedimentation is an episodic process, which largely occurs during catchment floods, rather than the continuous gradual process that is implied.

Although sedimentation rates are usually expressed as a sediment thickness deposited per unit time (ie, mm yr⁻¹) this statistic does not account for changes in dry sediment mass with depth in the sediment column due to compaction. Typically, sediment density ($\rho = \text{g cm}^{-3}$) increases with depth and therefore some workers prefer to calculate dry mass accumulation rates per unit area per unit time (g cm⁻² yr⁻¹). These data can be used to estimate the total mass of sedimentation in an estuary (tonnes yr⁻¹) (eg, Swales et al. 1997). However, in our experience of estuarine cores (up to 4 m long) the effects of compaction are often offset by changes in bulk sediment density reflecting layering of low-density mud (ie, dry density (ρ_d) < 1 g cm⁻³) and higher density (ie, ρ_d > 1 g cm⁻³) sand deposits. Furthermore, the significance of a SAR expressed as mm yr⁻¹ is more readily grasped than a dry-mass sedimentation rate in g cm⁻³ yr⁻¹. For example, the rate of estuary aging due to sedimentation (mm yr⁻¹) can be directly compared with the potential mitigating effect of local sea level rise (mm yr⁻¹).

10.4 SAR derived from ²¹⁰Pb dating

In this study, we calculate an average sediment accumulation rate for the zone of exponential ²¹⁰Pb concentration decrease. The rate of ²¹⁰Pb concentration decrease with depth can be used to calculate a net sediment accumulation rate. Given an initial unsupported ²¹⁰Pb concentration (C_0), the value of C (Bq kg⁻²) will decline exponentially with age (t):

$$C_t = C_0 e^{-kt} \quad \text{Eq. 1}$$

Assuming that within a finite time period, sedimentation (S) or SAR is constant, then $t = z/S$ can be substituted into Eq. 1 and by re-arrangement:

$$\frac{\ln \left[\frac{C_t}{C_0} \right]}{z} = -k / S \quad \text{Eq. 2}$$

For an exponential decay model, a depth profile of natural log(C) should yield a straight line of slope $b = -k/S$. We fitted a linear regression model to natural-log transformed ²¹⁰Pb concentration data to calculate b . The sedimentation rate over the depth of the fitted data is given by:

$$S = -(k)/b \quad \text{Eq. 3}$$

An advantage of this method is that the sedimentation rate is based on the entire ²¹⁰Pb profile rather than a single layer, as is the case for ¹³⁷Cs. Furthermore, if the pollen or ¹³⁷Cs tracer is present at the bottom of the core then the estimated SAR is a minimum

value. The SAR found by the ^{210}Pb method can also be used to estimate the residence time (R) of sediment particles in the surface mixed layer (SML) before they are removed by burial. For example, given an SML (L) depth of 40 mm and S of 2 mm yr⁻¹ then $R = L/S = 20$ years. Although this greatly simplifies the process (ie, the likelihood of particle mixing reduces with depth in the SML), this approach provides a useful measure of the relative effect of sediment mixing between cores, sub-environments and estuaries.

11 Appendix 4: Dating of Estuarine Sediments

11.1 Usefulness of the Haywood et al. (1999) CWH habitat map

If a match could be found between the habitats described by Haywood et al. (1999), the area over which relative bioturbation rates could be estimated would be extended to the whole of the CWH. Given that the habitat map gave information only on the dominant animals, comparisons were made with it and the communities observed in this study and the influence of those dominant animals on the bioturbation potential and depth.

11.1.1 Comparison with Haywood et al. (1999) habitat mapping

Haywood et al. (1999) mapped the dominant macrofauna and habitat types in the Waitemata Harbour and, by comparing our macrofaunal community data with the habitat map, it was possible to extend our knowledge of relative bioturbation rates to other sites. In addition, sites HN (I2 & I3) and WH-I2 of this study are close to ARC monitored sites HC and Whau, respectively, so spatial comparison between sites is viable.

The macro-invertebrate information (in the form of dominant species) reported by Haywood et al. (1999) is generally consistent with the macro-invertebrate communities sampled for this project and by the ARC (Halliday et al. 2006). However, in some areas dominance seemed to have changed. For example, *Zeacumantus* was not abundant in the area of site TA-I2 as suggested by Haywood et al. (1999). According to Halliday et al. (2006), densities of *Zeacumantus* have been declining in the inner Waitemata Harbour (near sites HN and TA) since 2001. Moreover, abundant *Austrovenus* reported by Haywood et al. (1999) were not always observed in this study. Also, Haywood et al. (1999) did not include *Nucula* as a dominant organism, although in the present study they were frequently more abundant than *Austrovenus*.

Furthermore, the dominant species (Haywood et al. 1999) did not necessarily contribute significantly to bioturbation rates for each site. For example, the contribution of *Austrovenus* to bioturbation was not overly significant. The high densities of *Nucula* observed in our study meant it frequently had a similar or even greater contribution to bioturbation rates than *Austrovenus* (Figure 65). Spionid polychaetes (eg, *Prionospio aucklandica*), also mentioned by Haywood et al. (1999) as a dominant macrofauna in some areas of the harbour, did not contribute significantly to bioturbation and *Macomona* contributed to bioturbation more consistently than adult *Austrovenus*. These problems meant that the information contained in Haywood et al. (1999) could not be used to extend our estimates of bioturbation.

Figure 65

Relative contribution of dominant taxa (as observed by Haywood et al.(1999) to the bioturbation index at sites HN (Henderson), WH (Whau River) and TA (Te Atatu). Large, medium and small *A. stutchburyi* and *M. liliiana* refer to those bivalves in the size classes < 5 cm, 5–20 cm and > 20 cm, respectively and for *N. hartvigiana* <2cm, 2–5 cm and > 5 cm, respectively.

